AD-A056 644 ENVIRONMENTAL RESEARCH AND TECHNOLOGY INC CONCORD MASS F/G 1/3
CONCORDE AIR QUALITY MONITORING AND ANALYSIS PROGRAM AT DULLES --ETC(U)
DEC 77 D G SMITH, R J YAMARTINO, C BENKLEY DOT-FA76WA-3816
UNCLASSIFIED ERT-P-2495-VOL-1 FAA-AEQ-77-14-VOL-1 NL

1 OF 2
AD
A056644

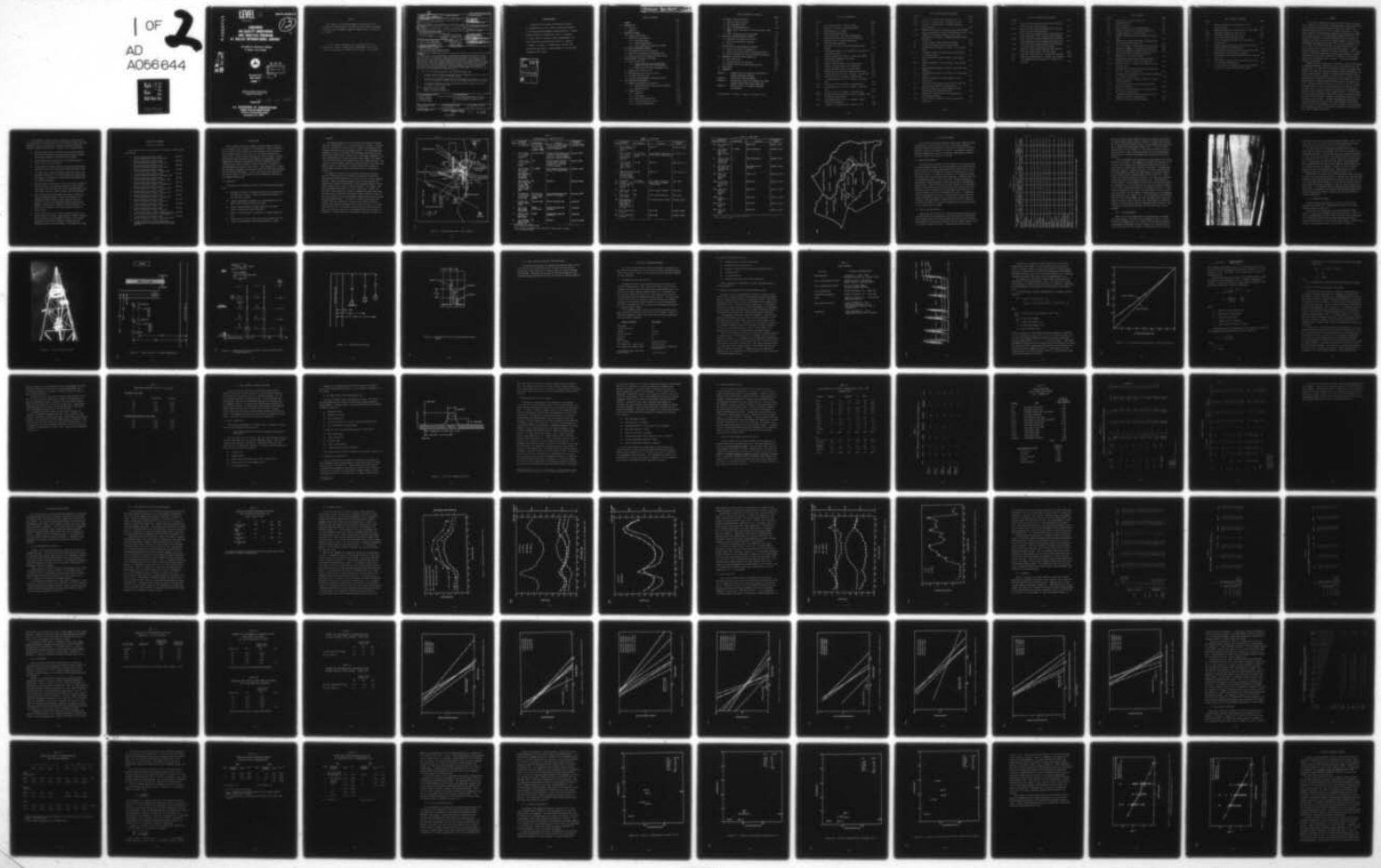

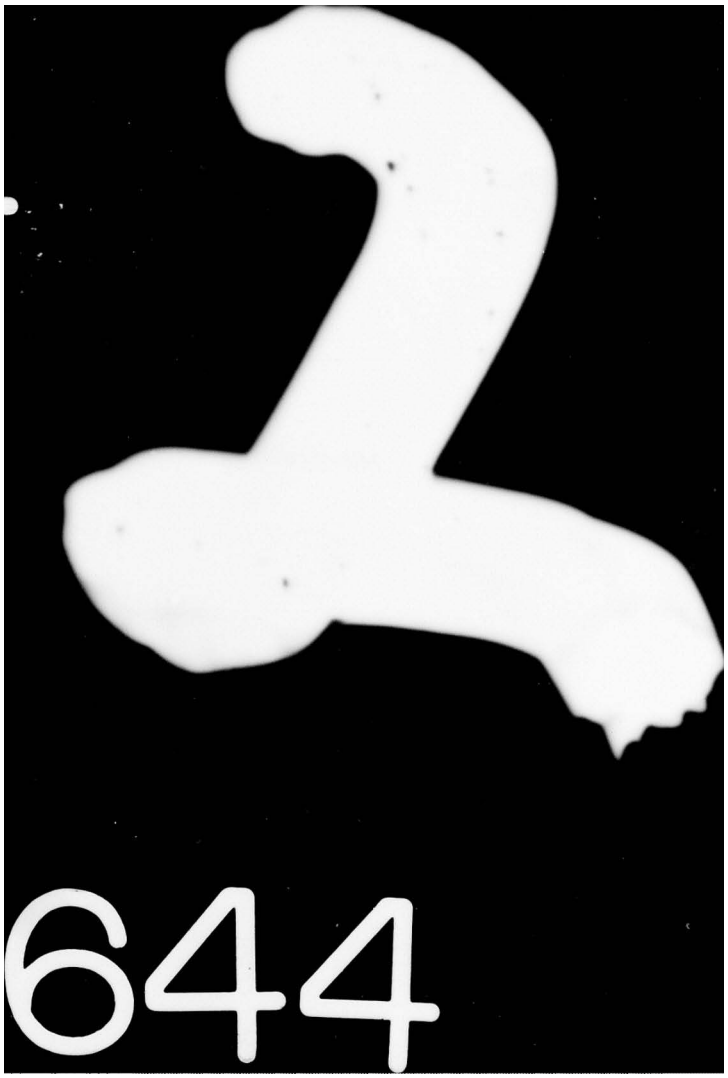
644

LEVEL III

A056506

AD A056644

AD No.
DDC FILE COPY

Report No. FAA-AEQ-77-14

12

CONCORDE AIR QUALITY MONITORING AND ANALYSIS PROGRAM AT DULLES INTERNATIONAL AIRPORT

D.G. Smith, R.J. Yamartino, C. Benkley
R. Isaacs, J. Lee, D. Chang

DDC
RECEIVED
JUL 21 1978
E

December 1977
FINAL REPORT
VOLUME I

Document is available to the public through
the National Technical Information Service
Springfield, Virginia 22161

78 07 14 048

Prepared for

U.S. DEPARTMENT OF TRANSPORTATION
FEDERAL AVIATION ADMINISTRATION
Office of Environmental Quality
Washington, D.C. 20591

NOTICE

This document is disseminated under the sponsorship of the Department of Transportation in the interest of information exchange. The United States Government assumes no liability for its contents or use thereof.

The United States Government does not endorse products or manufacturers. Trade or manufacturer's names appear herein solely because they are considered essential to the object of this report.

Technical Report Documentation Page

1. Report No. FAA-AEQ-77-14 VOL-1	2. Government Accession No.	3. Recipient's Catalog No.
4. Title and Subtitle Concorde Air Quality Monitoring and Analysis Program at Dulles International Airport Volume I		5. Report Date December 1977
		6. Performing Organization Code
7. Author(s) D. G. Smith, R. J. Yamartino,* C. Benkley, R. Isaacs, J. Lee, D. Chang		8. Performing Organization Report No. P-2495
9. Performing Organization Name and Address Environmental Research & Technology, Inc. 696 Virginia Road Concord, Massachusetts 01742		10. Work Unit No. (TRAIS)
		11. Contract or Grant No. DOT-FA76WA-3816
12. Sponsoring Agency Name and Address U.S. Dept. of Transportation Federal Aviation Administration Office of Environmental Quality Washington, D.C. 20591		13. Type of Report and Period Covered Final Report June 1976 - December 1977
		14. Sponsoring Agency Code FAA-AEQ-10

ERT-P-2495-VOL-1

168p.

15. Supplementary Notes *Affiliated with:
Argonne National Laboratory
Energy and Environmental Systems Division
9700 South Cass Avenue, Argonne, Illinois

16. Abstract

On February 4, 1976, the Secretary of Transportation ordered the FAA to monitor Concorde emissions at Dulles International Airport during its initial 16 month trial period. To comply with this order, it was necessary to measure the ambient pollution levels (background) in and around Dulles Airport and to trace the dispersion of emissions from a single Concorde aircraft. While the more conventional background measurements could be easily performed, there was no known case where the vertical and horizontal profile of the emission plume from a single aircraft had been identified. Special instruments were required to measure the discrete, non-steady nature of the dispersion of the aircraft plume. The final measurement system, which consisted of continuously recording electro-chemical sensors coupled with high-speed chart recorders, successfully detected CO emissions from a single aircraft.

Results of this measurement program on and around Dulles Airport show:

- Concorde CO emissions from taxiing aircraft dilute to background levels within 2,000 ft and do not reach the terminal in measurable amounts.
- Emissions from the airport property could not be detected at Sterling Park, or several more distant communities, even when the winds were blowing toward them from the airport.
- Actual Concorde operations were less polluting than had been indicated in the Final Environmental Impact Statement (FEIS).

NOTE: THIS REPORT IS IN TWO VOLUMES
VOLUME I - Main body of report.
VOLUME II - Appendixes (FAA-AEQ-14A)

17. Key Words (Suggested by Author(s))	18. Distribution Statement
Aircraft Emissions Airport Air Pollution Diffusion Modeling Concorde Aircraft Monitoring Program	This document is available to the public through the National Technical Information Service, Springfield, Virginia 22151

19. Security Classif. (of this report)	20. Security Classif. (of this page)	21. No. of Pages	22. Price
Unclassified	Unclassified	176	

Form DOT F 1700.7 (8-72) Reproduction of completed page authorized.

78 07 14 048

391776

ACKNOWLEDGEMENT

In addition to the large contributions of authors R.J. Yamartino and J. Lee, those of several other members of the Energy and Environmental Systems Division of Argonne National Laboratory, including D.M. Rote, L.E. Wangen, I.T. Wang, and L.A. Conley are hereby acknowledged. The data collection and documentation skills of D. Muldoon, T. Thomson, R. Deteso, J. Lindonen and S. Doucette have contributed importantly to the development of the data base described in this report.

ACCESSION for
NTIS White Section ☒
DDC Buff Section ☐
UNANNOUNCED ☐
JUSTIFICATION.....
BY.....
DISTRIBUTION/AVAILABILITY CODES
Dist. AVAIL. and/or SPECIAL
A

Preceding Page Blank - Not Filmed

TABLE OF CONTENTS

		Page
1.	SUMMARY	1-1
2.	INTRODUCTION	2-1
	2.1 Objectives	2-1
	2.2 Approach	2-2
3.	MONITORING PROGRAM	3-1
	3.1 Regional Measurements	3-1
	3.2 Single Event Measurements	3-1
	3.2.1 Taxi Measurements	3-3
	3.2.2 Takeoff Measurements	3-5
	3.2.3 Other Landing and Takeoff Cycle Modes	3-11
4.	AIR QUALITY MEASUREMENT METHODS	4-1
	4.1 Instrumentation and Site Selection	4-1
	4.2 Analysis of Calibration and Response Times	4-2
	4.3 Limits of Precision, Sensitivity and Accuracy	4-8
5.	DULLES AIRPORT AIR QUALITY DATA BASE	5-1
	5.1 Dulles Airport Data	5-1
	5.1.1 Dulles South Ramp and Sterling Park Background Concentration Measurements	5-1
	5.1.2 Single Event Pollution Measurement Data	5-2
	5.2 Regional Air Pollution Data	5-2
	5.3 Meteorological Data for the Airport	5-4
	5.4 Aircraft Activities Data	5-6
	5.5 Aircraft Design Geometry and Emission Rates	5-6
6.	DATA REDUCTION AND ANALYSIS	6-1
	6.1 Regional Background Data Analysis	6-1
	6.1.1 Stratification by Wind Direction and Speed	6-2
	6.1.2 Diurnal Analyses	6-4
	6.2 Single Event Data	6-8
	6.2.1 Summaries	6-11
	6.2.2 Correlations	6-15
	6.2.3 Multilinear Regressions	6-27
	6.2.4 Dose Versus Emission Index	6-33
	6.2.5 Turbulence Measurements	6-34

TABLE OF CONTENTS (Continued)

		Page
7.	AIR QUALITY MODELING APPROACH	7-1
	7.1 Regional Modeling Methods	7-5
	7.2 Multi-parameter Models	7-7
	7.3 Quasi-Instantaneous Models	7-10
	7.4 ALSM, A Quasi-Continuous Line Source Gaussian Plume Model	7-5
	7.5 AVAP, A Continuous Line Source Model	7-17
8.	RESULTS OF REGIONAL MODELING ANALYSIS	8-1
	8.1 Regression and Correlation Analyses	8-2
	8.2 Wind Direction-Specific Analysis	8-8
	8.3 Summary	8-14
9.	RESULTS OF SINGLE EVENT MODELING ANALYSIS	9-1
	9.1 Plume Rise and Multi-Parameter Fit	9-1
	9.2 Results Obtained with Quasi-Instantaneous Models	9-9
	9.3 Results of ALSM Quasi-Continuous Model Application	9-17
10.	COMPARISON OF RESULTS WITH ORIGINAL EIS	10-1
	10.1 AVAP Comparisons	10-2
	10.2 Single Event Area of Influence	10-13
	10.3 Aircraft Emission and Wake Characteristics	10-14
11.	CONCLUSIONS	11-1
12.	REFERENCES	12-1

* APPENDIX A DOCUMENTATION OF AIR QUALITY DATA BASE FOR CONCORDE MONITORING PROGRAM

* APPENDIX B SINGLE EVENT MODELING METHODS

* APPENDIX C SUPPLEMENTARY STATISTICAL SUMMARIES AND CROSS VARIABLE ANALYSES FOR SINGLE EVENT DATA

* APPENDIX D COMPLETE RESULTS OF REGIONAL BACKGROUND DATA ANALYSES

*APPENDIXES ARE IN VOLUME II (Report No. FAA-AEQ-77-14A)

LIST OF ILLUSTRATIONS

Figure		Page
2-1	Air Monitoring Sites - Dulles Airport	2-6
2-2	Regional Air Quality Monitoring Stations	2-7
3-1	Monitoring Sites - Taxiway	3-4
3-2	Pollution Monitoring Tower	3-6
3-3	Station Locations - Two Tower Demonstration	3-7
3-4	Characteristic Strip Chart Plots of Wind and Pollution (CO) Two Tower Demonstration	3-8
3-5	Takeoff Station Locations	3-9
3-6	Characteristic Plot of NO_x Concentration During Takeoff	3-10
4-1	Instrument Response to CO Calibration Gas Pulses of Diffusion Durations	4-4
4-2	Ecolyzer Output Pulse Width Vs. Input Pulse Width	4-6
5-1	Concentration Parameter Definition	5-3
6-1	Diurnal Wind Analysis	6-5
6-2	Diurnal Pollution Analysis for Sterling Park	6-6
6-3	Diurnal Pollutant Analysis for Lewinsville	6-7
6-4	Diurnal Pollutant Analysis for South Ramp	6-9
6-5	Diurnal Analysis of Dulles Airport Activity Data	6-10
6-6a	CO Concentration (14 ft) Vs. Distance: Infield Data	6-19
6-6b	CO Dose (14 ft) Vs. Distance: Infield Data	6-20
6-7a	CO Concentration (14 ft) Vs. Distance: One-Tower Data	6-21
6-7b	CO Dose (14 ft) Vs. Distance: One-Tower Data	6-22
6-8a	CO Concentration (14 ft) Vs. Distance: Two-Tower Data	6-23
6-8b	CO Dose (14 ft) Vs. Distance: Two-Tower Data	6-24
6-9a	NO_x Measured Concentration (14 ft) Vs. Distance: End of Runway During Takeoff	6-25
6-9b	NO_x Measured Dose (14 ft) Vs. Distance: End of Runway During Takeoff	6-26
6-10	CO Dose Vs. Emission Rate, 1st Tower at 14 ft	6-35

LIST OF ILLUSTRATIONS (Continued)

Figure		Page
6-11	CO Dose Vs. Emission Rate, 2nd Tower at 14 ft	6-36
6-12	CO Dose Vs. Emission Rate, Last Sensor at 14 ft	6-37
6-13	CO Dose Vs. Emission Rate, 1st Tower, Composite of all Heights	6-38
6-14	Comparison of Observed 3-Minute σ_θ with 1-Hour Average Value, Stratified by Pasquill-Turner Stability Class	6-40
6-15	Comparison of Observed 3-Minute σ_θ with 1-Hour Average Value, Stratified by Modified Pasquill-Turner Stability Class	6-41
7-1	Aircraft Exhaust Plume Dispersion Geometry	7-13
7-2	Geometry of Concorde and Its Exhaust Plume	7-15
9-1	Distribution of Plume Rise at Tower 1, All Aircraft Types	9-3
9-2	Incremental Plume Rise Between Tower 1 and Tower 2, All Aircraft Types	9-4
9-3	Vertical Spread of Plume at Tower 1, All Aircraft Types	9-5
9-4	Along Wind Spread of Plume at Tower 1, All Aircraft Types	9-6
9-5	Multiparameter Estimate of Peak CO Vs. Distance from Taxiway	9-7
9-6	Multiparameter Estimate of CO Dose Vs. Distance from Taxiway	9-8
9-7	Effect of Plume Rise on Model Comparison with Observations	9-10
9-8	Effect of Initial Plume Size and Rate of Dispersion on Comparison of Model with Observations	9-11
9-9	Effect of Plume Rise on Model Comparison with Observations for Concorde Aircraft	9-13
9-10	Comparison of Model Variants with Observations for Concorde Aircraft	9-14
9-11	Area of Concorde Influence for CO at Dulles for South Wind	9-15

LIST OF ILLUSTRATIONS (Continued)

Figure		Page
10-1a	Dulles 1978 with Concorde Original AVAP Prediction (EIS) CO 1-Hour, Wind from South	10-4
10-1b	Dulles 1978 with Concorde Modified AVAP Prediction (EIS) CO 1-Hour, Wind from South	10-5
10-2a	Dulles 1978 with Concorde Original AVAP Prediction (EIS) Hydrocarbon 1-Hour Average, Wind from South	10-6
10-2b	Dulles 1978 with Concorde Modified AVAP Prediction (EIS) Hydrocarbon 1-Hour Average, Wind from South	10-7
10-3a	Dulles 1978 with Concorde Original AVAP Prediction (EIS) NO_x 1-Hour Average Wind from South	10-8
10-3b	Dulles 1978 with Concorde Modified AVAP Prediction (EIS) NO_x 1-Hour Average, Wind from South	10-9
10-4	Hourly CO Concentration Vs. Distance with Concorde	10-10
10-5	Hourly NO_x Concentration Vs. Distance with Concorde	10-11
10-6	Total Hydrocarbon Concentration Vs. Distance with Concorde	10-12

LIST OF TABLES

Table		Page
2-1	Characteristics of Monitoring Sites	2-3
3-1	Background Stations	3-2
4-1	Sensor Equipment	4-3
5-1	Dulles Airport Daily Aircraft Operations	5-7
5-2	Observed Distribution of Concorde Operations	5-8
5-3	Aircraft Operations - Dulles Airport	5-9
5-4	Aircraft Design Dimensions and Pollutant Emission Rates	5-10
6-1	Direction of Maximum Concentration of Species for all Wind Speeds and Stabilities	6-3
6-2	Statistical Summary of One Tower CO Tests for SST	6-12
6-3	Statistical Summary of Infield CO Tests for SST	6-13
6-4	Statistical Summary of Takeoff NO_x Tests for SST	6-14
6-5	Averaged THC Peak Concentrations and Doses Measured at 14 ft on First Tower	6-15
6-6a	Concorde Peak Instantaneous CO Concentration Vs. Height and Distance: One and Two Tower Data	6-17
6-6b	Concorde CO Dose Vs. Height and Distance: One and Two Tower Data	6-17
6-7	Concorde Peak Instantaneous CO Concentrations and Dose Vs. Distance: Infield Data	6-18
6-8	Concorde Peak Instantaneous NO_x Concentration and Dose Vs. Distance: Takeoff Data	6-18
6-9	Results of Linear Correlations Analysis for Single Event Measurements	6-28
6-10	Correlations Between CO Concentration and Wind Speed and Turbulence	6-29
6-11	Stepwise Multilinear Regression Screening Results for Peak CO Concentrations	6-31
6-12	Stepwise Multilinear Regression Results for the Logarithm of Peak CO Concentrations	6-32
7-1	Airport Air Pollution Diffusion Models	7-2

LIST OF TABLES (Continued)

Table		Page
7-2	Plume Rise Estimates Derived from Two Tower Tests at Dulles	7-12
8-1	Regression Results for Sterling Park Vs. South Ramp	8-3
8-2a	Correlation Coefficients NO_2, O_3, WS	8-4
8-2b	Correlation Coefficients NO_2, O_3, WS	8-5
8-3	Correlation Coefficient NO_2 Vs. O_3	8-7
8-4	CO Vs. NO_x Regression Results for South Ramp Vs. Sterling Park	8-7
8-5	Regional Data Wind Direction Selection Criteria for Airport Upwind of Monitoring Site	8-9
8-6	Wind-Specific Correlation Coefficients Between South Ramp and Other Sites for NO_2, CO and O_3	8-10
8-7	Wind-Specific Correlation Coefficients CO Vs. NO_2 and NO_2 Vs. O_3	8-12
8-8	Correlation Coefficients for Aircraft Activity Data Vs. Pollutant Concentrations	8-13
9-1	Distance from the Taxiway Where the CO Concentration Falls to 0.25 ppm for Three Aircraft Types	9-17

1. SUMMARY

The air quality monitoring program at Dulles Airport was carried out in response to the Secretary of Transportation's order of February 4, 1976 to monitor both pollutant emissions and noise levels of the Concorde aircraft during its initial 16-month trial period. The air quality aspects of the monitoring program are described in this report. The principal objective of the measurement program at Dulles was to identify the influence of Concorde operations on the air quality in populated areas both on and off the airport property. While the more conventional background measurements could be easily performed, there was no known case where the vertical and along wind profile of the emission plume from a single aircraft had been measured. A mobile monitoring program was therefore initiated to determine if the emission plume of a taxiing or taking off aircraft could be detected. Special instruments were required to measure the dispersion of the aircraft plumes which is nonsteady state in nature. A long term measurement program was then begun.

Concorde effects on pollution at the airport itself were determined by operating monitoring stations very close to the aircraft taxi and takeoff paths. The data have been analyzed in detail to provide information on jet plume rise, actual atmospheric dispersion parameters, and vertical and horizontal "profiles" of exhaust-plume pollutant concentrations for individual aircraft in actual service. Analysis of these measurements has succeeded in identifying the contribution of specific aircraft types to hourly-average pollution levels on the airport property. Pollution estimates previously given in the FEIS were compared with measurements by rerunning the diffusion model originally used in the FEIS, but with earlier assumptions of plume rise and atmospheric dispersion rates adjusted to reflect measured values. The measurement data show that the pollutant dispersion for single Concordes (as well as for several other aircraft) is greater than previously estimated; concentrations are thus lower. Pollutant concentrations attributable to single Concordes were diluted to less than background levels within 2,000 ft of the aircraft movement path and, therefore, could not measurably influence air quality at the airport terminal or at Sterling Park (the closest community monitored).

In the community, measured values of ambient air pollution data were statistically analyzed along with data obtained at Dulles and other regional locations to determine the possible influence of aircraft emissions on nearby Sterling Park. Analysis of all these data show:

- Emissions from aircraft activities on the airport property could not be detected at Sterling Park, even when the winds were blowing toward Sterling Park from the airport.
- Concorde emissions at Dulles dilute to background levels within 2,000 ft of the aircraft.
- Actual Concorde operations were less polluting than had been indicated in the Final Environmental Impact Statement (FEIS).
- The small area of Concorde influence predicted with the computational method used in the FEIS becomes even smaller when the analysis is improved by incorporating data obtained from this monitoring program.
- Based on engine emission rates listed in the FEIS, Concorde CO emissions for the taxi mode are expected to be up to three times higher than B707 emissions, but actual measurements near the taxiway show nearly equal CO impact from both aircraft.
- Engine emission rate measurements alone may not reflect aircraft environmental impact. Factors contributing to this difference between published engine emission rates and measured air quality concentration include airplane engine geometry, engine exhaust temperature and wake dynamics. The Concorde is considerably different from other aircraft in these respects.
- The most direct measure of aircraft emissions impact is the actual ambient air quality change measured at nearby receptors. Thus, the ambient air measurements obtained in the current program are an important supplement to engine emission measurements made in the environment of the engine test stand.

DOCUMENTATION SUMMARY

(Concorde Monitoring)

This report provides data and analyses relating to the following publications:

1)	Concorde Monitoring Monthly Report Dulles International Airport - May 1976	DOT-FAA
2)	Concorde Monitoring Monthly Report Dulles International Airport - June 1976	DOT-FAA
3)	Concorde Monitoring Monthly Report Dulles International Airport - July 1976	DOT-FAA
4)	Concorde Monitoring Monthly Report Dulles International Airport - August 1976	DOT-FAA
5)	Concorde Monitoring Monthly Report Dulles International Airport - September 1976	DOT-FAA
6)	Concorde Monitoring Monthly Report Dulles International Airport - October 1976	DOT-FAA
7)	Concorde Monitoring Monthly Report Dulles International Airport - November 1976	DOT-FAA
8)	Concorde Monitoring Monthly Report Dulles International Airport - December 1976	DOT-FAA
9)	Concorde Monitoring Monthly Report Dulles International Airport - January 1977	DOT-FAA
10)	Concorde Monitoring Monthly Report Dulles International Airport - February 1977	DOT-FAA
11)	Concorde Monitoring Monthly Report Dulles International Airport - March 1977	DOT-FAA
12)	Concorde Monitoring Monthly Report Dulles International Airport - April 1977	DOT-FAA
13)	Concorde Monitoring Monthly Report Dulles International Airport - May 1977	DOT-FAA
14)	Concorde Monitoring Six Months Summary Report Dulles International Airport - May-November 1976	DOT-FAA
15)	Concorde Monitoring Summary Report Dulles International Airport - May 1976-May 1977	DOT-FAA
16)	H. Segal, Monitoring Concorde Emissions, Journal of the Air Pollution Control Association - July 1977	

2. INTRODUCTION

The air quality monitoring program at Dulles Airport was carried out in response to the Secretary of Transportation's order of February 4, 1976, to monitor both pollutant emissions and noise levels associated with Concorde aircraft at that facility. This report describes the scope of the air quality monitoring program at Dulles airport, the data base that has been derived from that program, the measurement results, comparisons of ambient concentrations with those predicted from published emission indices and model estimates of areas of influence of Concorde operations based on these results. Also discussed are a number of preliminary refinements for prediction models that have been developed from the current measurements. Finally, the results are compared with the previous analysis of the impact of Concorde operations presented in the original Concorde FEIS.

2.1 Objectives

The objectives of the Dulles Airport air quality monitoring program were:

- determine the effect of Concorde emissions on air quality and, in particular, on the air quality at populated locations at and near Dulles Airport;
- compare measurements of ambient air concentrations with estimates based upon published emission rates;
- analyze local turbulence, buoyant plume rise, and other factors affecting the plume dispersion;
- define the expected area of influence of Concorde operations and
- compare the air quality predictions in the Concorde FEIS with those of improved models based on measurements at Dulles.

2.2 Approach

A two-phase program was used to determine the effect of Concorde emissions on populated areas at and near the Dulles Airport. The first phase was concerned with establishing the impact of the airport (and Concorde) emissions on the surrounding vicinity. The second phase was designed to detect the emissions from individual aircraft before they were diluted sufficiently to become lost in the ambient background. Air quality measurements at two main populated areas, namely, the airport itself and the Sterling Park Community were given highest priority. The locations of the principal long-term monitoring sites at the airport are shown in Figure 2-1 and Table 2-1, and the proximity to Dulles of Sterling Park and other regional monitoring sites is illustrated in Figure 2-2.

The impact of the airport (and Concorde) emissions on the air quality at Sterling Park was determined by measuring the pollution background upwind and downwind of the airport as well as other regional stations. Hourly average measurements were considered adequate for comparisons of ambient concentrations between regional monitors off the airport property and a central reference monitor at the airport. However, preliminary measurements at Dulles showed that, to obtain the sensitivity and selectivity necessary to separate emissions from single aircraft from the background, measurement locations had to be close to the source operations and the measurements themselves had to be recorded with high speed recorders. The impact of Concorde emissions on the airport itself was determined by measuring the change in pollutant concentrations caused by emissions from a single aircraft as it started, taxied and took off. The distance from the taxiing aircraft source at which these emissions blend into the background outlines the "area of influence" of Concorde emissions (conceptually indicated in Figure 2-1).

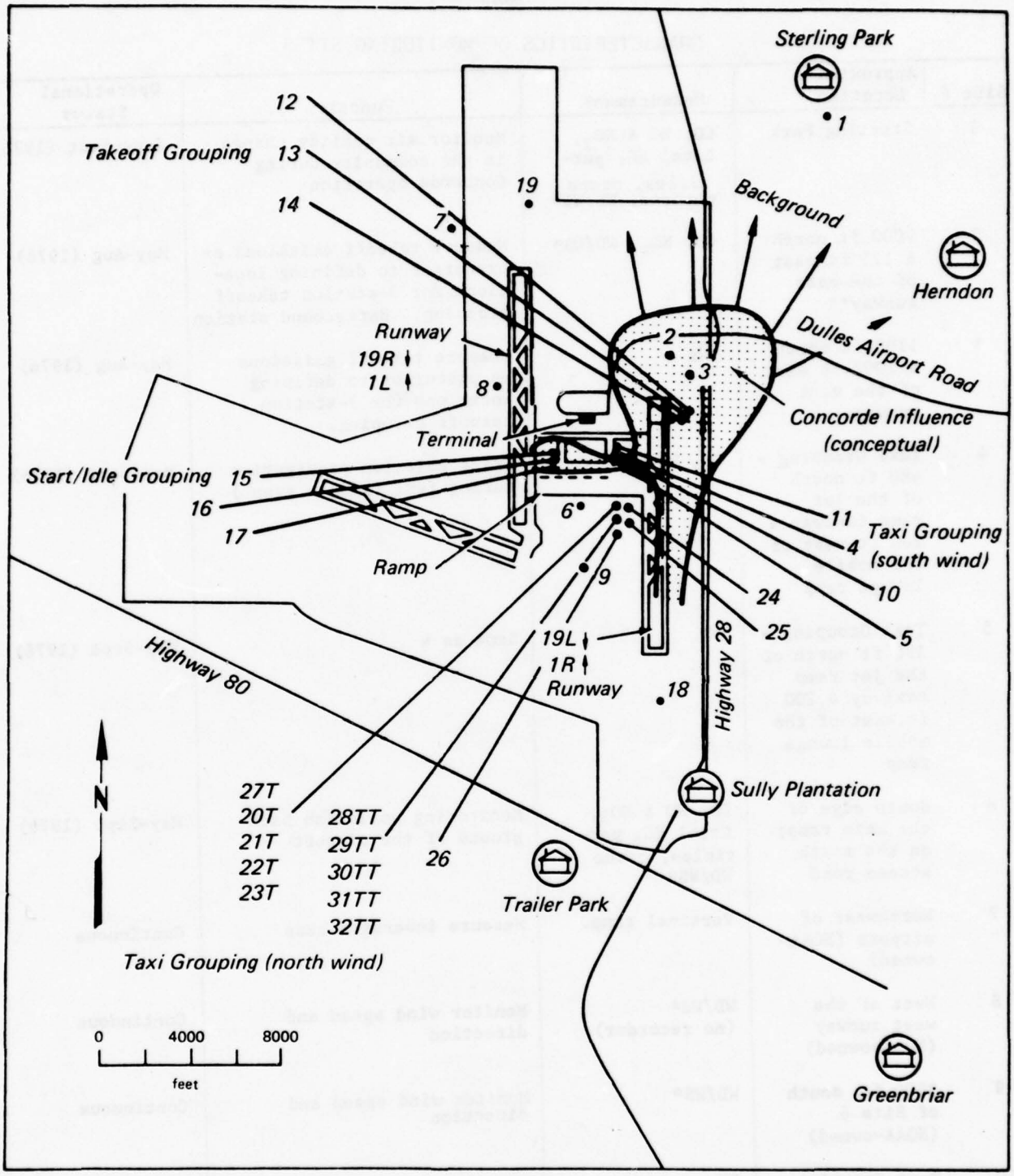

712070 A

Figure 2-1 Air Monitoring Sites - Dulles Airport

TABLE 2-1

CHARACTERISTICS OF MONITORING SITES

Site #	Approximate Location	Measurement	Function	Operational Status
1	Sterling Park	CO, NO & NO_2, total HC, particles, ozone methane, WD/WS*	Monitor air quality change in the community during Concorde operation	June-Sept (1976)
2	2000 ft. north & 125 ft. east of the east runway**	CO, NO_x, WD/WS*	Measure takeoff emissions as precursor to defining locations for 3-station takeoff grouping. Background station	May-Aug (1976)
3	1100 ft. north & 1000 ft east of the east runway	NO_x	Measure takeoff emissions as precursor to defining locations for 3-station takeoff grouping.	May-Aug (1976)
4	Taxi Grouping - 480 ft. north of the jet ramp taxiway & 200 ft. east of the mobile lounge ramp	CO, WD/WS*	Trace emission propagation during taxi (single event)	May-Sept (1976)
5	Taxi Grouping - 190 ft. north of the jet ramp taxiway & 200 ft. east of the mobile lounge ramp	CO	Same as 4	May-Sept (1976)
6	South edge of the main ramp; on the south access road	CO, NO & NO_2, total HC, particles, ozone WD/WS*	Monitoring pollution background of the airport	May-Sept (1976)
7	Northwest of airport (NOAA-owned)	Vertical temp.	Measure inversion base	Continuous
8	West of the west runway (NOAA-owned)	WD/WS* (no recorder)	Monitor wind speed and direction	Continuous
9	3000 ft. south of Site 6 (NOAA-owned)	WD/WS*	Monitor wind speed and direction	Continuous
10	Taxi Grouping - midway between Sites 4 & 5	CO	Same as 4	June-July (1976)

*WD/WS-Wind direction/Wind speed

**All dimensions are measured from centerline of ramp, runway or taxiway unless otherwise needed.

TABLE 2-1 (Continued)

Site #	Approximate Location	Measurement	Function	Operational Status
11	Taxi Grouping - 200 ft. north of Site 4	CO	Same as 4	July-Sept (1976)
12	Takeoff Grouping - 285 ft east and 100 ft. north of Site 13	CO, NO & NO_2, total HC, ozone, WD/WS*	Trace emission propagation during takeoff (single event)	Oct 76-May 1976
13	Takeoff Grouping - 185 ft. east & 140 ft. north of Site 14	CO, NO_x	Same as 12	Sept 76-May 1976
14	Takeoff Grouping 450 ft. east of the east runway & 1040 ft. south of its north end	CO, NO_x	Same as 12	Sept 76-May 1976
15 16 17	Start/idle Grouping - north of the west & of the jet ramp taxiway	CO, WD/WS*, (at one site)	Trace emission propagation during engine start/idle (single event)	Spot check
18	South of the east runway	NO_x	Monitor takeoff emissions	Spot check
19	North of the west runway	NO_x	Monitor landing emissions	Spot check
20T	South edge of main ramp 1700 ft*** west of Runway 19L, 56-ft. elevation on tower	-	Air intake position (tower)	November (1976)
21T	41-ft. elevation on tower	-	Same as 20T	November (1976)
22T	26-ft. elevation on tower	-	Same as 20T	November (1976)

TABLE 2-1 (Continued)

Site #	Approximate Location	Measurement	Function	Operational Status
23T	14-ft. elevation on tower	-	Same as 20T	November (1976)
24	South edge of main ramp ** 1665 ft*** west of Runway 19L	CO, WS/WD*	Tower measurements	November (1976)
25	1665 ft*** west of Runway 19L 164 ft south of Site 24	CO	Tower measurements	November (1976)
26	1700 ft*** west of Runway 19L 164 ft. south of Site 25	-	Air intake position (Surface)	November (1976)
27T	Same as 20T 80-ft. elevation on tower	-	Same as 20T	Feb-March (1977)
28TT	164 ft. south of 20T. 80-ft. elevation on tower	-	Same as 20T	Feb-April (1977)
29TT	Same as 28TT 56-ft. elevation on tower	-	Same as 20T	Feb-April (1977)
30TT	41-ft. elevation on tower	-	Same as 20T	Feb-April (1977)
31TT	26-ft. elevation on tower	-	Same as 20T	Feb-April (1977)
32TT	14-ft. elevation on tower	-	Same as 20T	Feb-April (1977)

***215 ft. south of south jet ramp centerline
****South end centerline

706089

Figure 2-2 Regional Air Quality Monitoring Stations

3. MONITORING PROGRAM

The air quality monitoring program at Dulles had a number of impact assessment goals that required a variety of measurement approaches. Different techniques were required to measure the influence of Concorde emissions on local and regional air quality. A measurement program to develop a comprehensive air quality data base containing both regional and local (single event) data was initiated.

3.1 Regional Measurements

To assess regional effects of Dulles operations, the initial phase of the measurement program employed conventional air quality monitoring stations located at a point approximately 200 ft south of the jet taxi ramp, as well as in the community of Sterling Park three miles to the NNE of the airport. At these two stations all of the major pollutants associated with aircraft emissions were measured: carbon monoxide (CO), total hydrocarbons (THC), nitric oxide (NO), nitrogen dioxide (NO_2), photochemical oxidant measured as ozone (O_3) and total suspended particulates (TSP). Regional monitoring stations (Figure 2-2) at Bethesda, Maryland (the National Institute of Health) and at Lewinsville, Massey and Seven Corners, Virginia provided comparable hourly data logs for these pollutants for the May to September 1976 period. An additional station was temporarily set up as a takeoff monitor near the airport property boundary to measure CO, NO_x (NO and NO_2) and wind speed and direction. The other regional stations shown in Figure 2-2 collected only TSP data (Table 3-1), and were therefore not of principal interest in the current analysis studies.

3.2 Single Event Measurements

Between May 1976 and July 1977, the air quality monitoring systems recorded the pollution background on and off the airport and emissions from aircraft single events during engine start/idle, taxi and takeoff. Major emphasis was placed upon monitoring the jet exhaust emissions from a taxiing or taking off aircraft. Carbon monoxide was the tracer

TABLE 3-1

BACKGROUND STATIONS

STATION \ PARAMETER	Wind Direction WD	Wind Speed WS	Carbon Monoxide CO	Nitrogen Dioxide NO_2	Nitric Oxide NO	Ozone O_2	Total Hydrocarbons THC	Methane CH_4	Total Suspended Particulates TSP*	Sulphur Dioxide
Station #1 Sterling Park	✓	✓	✓	✓	✓	✓	✓	✓	✓	
Station #6 South Ramp	✓	✓	✓	✓	✓	✓	✓	✓	✓	
Massey			✓	✓	✓	✓			✓	
Lewinsville			✓	✓	✓	✓			✓	
Seven Corners			✓	✓	✓	✓	✓			
NIH Bethesda			✓	✓	✓	✓			✓	✓
Herndon									✓	
Cub Run									✓	
Douglas Elem. School									✓	
Xerox Training School									✓	
Burning Tree									✓	
Gaithersburg H.S.									✓	
Poolesville Elem. School									✓	
Rockville									✓	

*TSP values are not reported on an hourly basis but are reported as daily (24) hour values.

pollutant measured during start/idle and taxi operations, while NO_x was the tracer measured during takeoff. Different "tracers" were selected for the taxi and takeoff modes because CO is predominant during taxi and NO_x is predominant during takeoff (Segal, 1973). A list of the monitoring sites is given in Table 2-1. The locations of these sites are shown in Figure 2-1 and a detailed discussion of the instrumentation, site selection, calibration procedures and sensitivities is given in Section 4.

A major consideration for monitoring site selection was the traffic pattern at the airport. Most commercial aircraft do not operate in the vicinity of the terminal, but rather position themselves at the jet ramp, which is located 2,300 ft south of the terminal. Airplanes move around this ramp in a clockwise direction. For south-wind operations, which are predominant during the summer months, the airplanes usually proceed from the ramp to takeoff runway 19-left (Figure 2-1), which ensures the shortest possible taxi distance. For north-wind operation, airplanes proceed from the ramp to runway 1-left. Considering this traffic pattern, the most effective location for taxi monitoring during the summer months is at the turf area just off the northeastern edge of the taxi ramp. Monitoring started at two locations (4 and 5). A third location was added, first at site 10 and then moved to site 11 to provide three points in a line normal to the taxiway to aid in determining plume dispersion rates (Figure 3-1). As the predominant wind shifted to the north in the winter months, the three taxi monitoring stations were moved to the other side of the taxi ramp. Measurements to record the vertical pollution profile were also performed at this location. Power for all taxi monitoring was provided by an FAA 15KW diesel electric generator.

3.2.1 Taxi Measurements

Three sets of taxiing mode emission measurements were recorded during the program. The first set was recorded at sites 4, 5 and 11 from May to September 1976. The second set of taxi mode measurements incorporated tower-mounted CO sensors (Figure 3-2), allowing the vertical distribution of the jet plume to be examined for the first time.

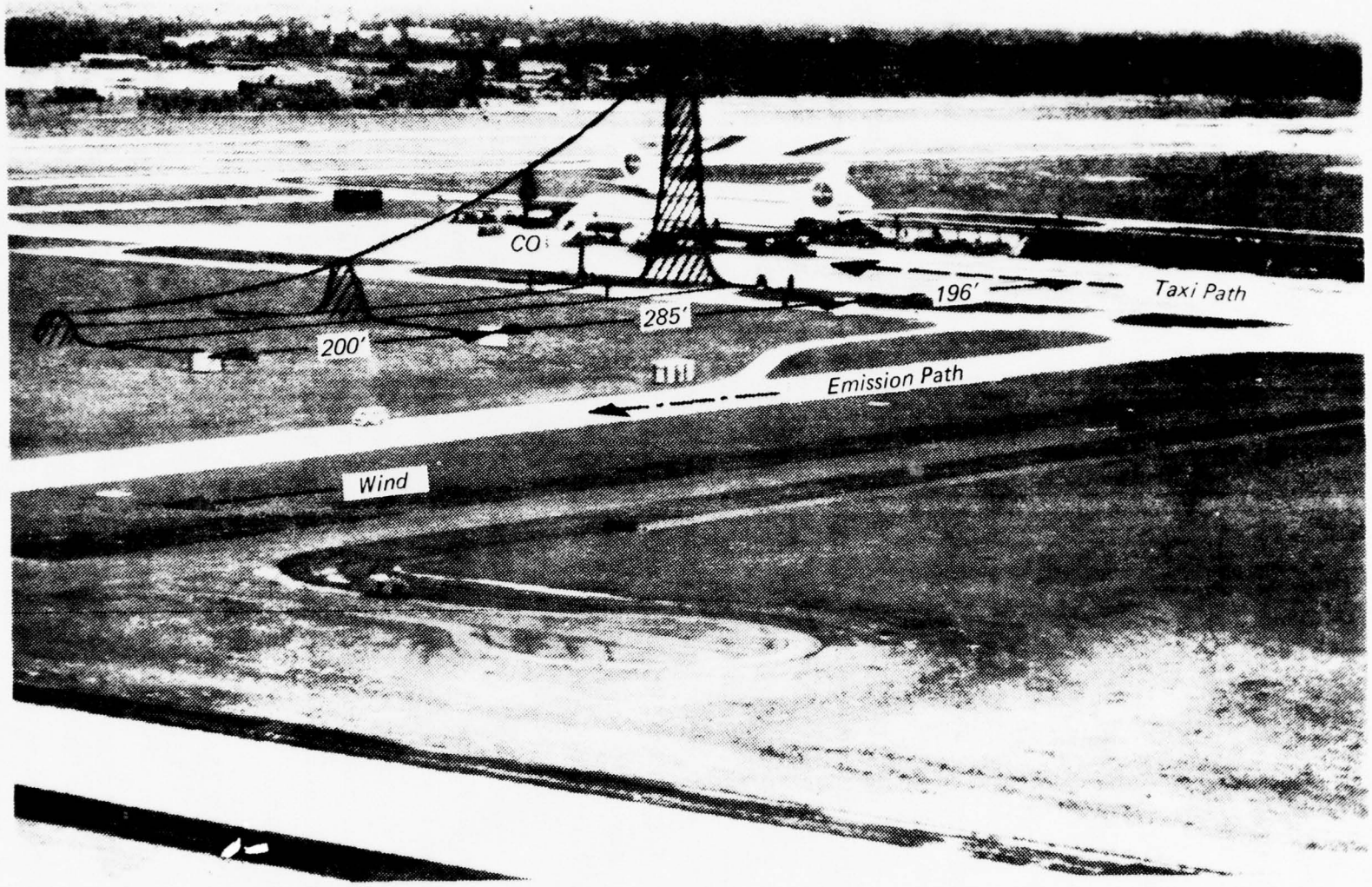

Figure 3-1 Monitoring Sites - Taxiway

These single-tower tests were performed between November 1 and 15, 1976 using a 58 ft tower at 215 ft from the taxiway centerline with four vertical pollution intake positions (14, 26, 41 and 56 ft).

To refine plume rise estimates and determine rate of rise, a second tower was added at the original 379 ft (115 m) distance of the second downwind sensor. The two-tower tests were started on February 20, 1977 for a five-week time period. The height of the first 58 ft tower was increased to 82 ft, so that each 82 ft tower had five intake positions. Each sampling port on both towers had its own sampling pump, which transmitted the air sample via an identical length sampling line to a separate Ecolyzer (CO monitor). Figures 3-3 and 3-4 show the geometry of the two tower installation. Characteristic CO pulse measurements from this array are illustrated in Figure 3-4.

Observations were made on the days when northerly winds transported emissions over the monitoring locations. Aircraft type, time of passage and mode of operation were recorded by the observer in a data log. The use of high speed chart recorders for wind speed and direction allowed wind turbulence intensity parameters σ_θ and σ_u/u to be derived for the tower tests. It was expected that this added information would improve the accuracy of dispersion rate estimates and would help determine the relative importance of ambient turbulence and jet wake turbulence as dispersion mechanisms.

3.2.2 Takeoff Measurements

Takeoff emissions were measured at sites 12, 13 and 14 from November 1976 to April 1977. Measurements were taken at the three downwind locations (Figure 3-5).

Locations of these monitoring sites were determined through analysis of precursor measurements taken at sites 2 and 3. Sites 12, 13 and 14 are approximately 1,000 ft south of the north end of the runway. This location was selected because plume concentrations could be measured effectively and electrical power was available. Characteristic traces of NO_x measurement versus time are shown in Figure 3-6.

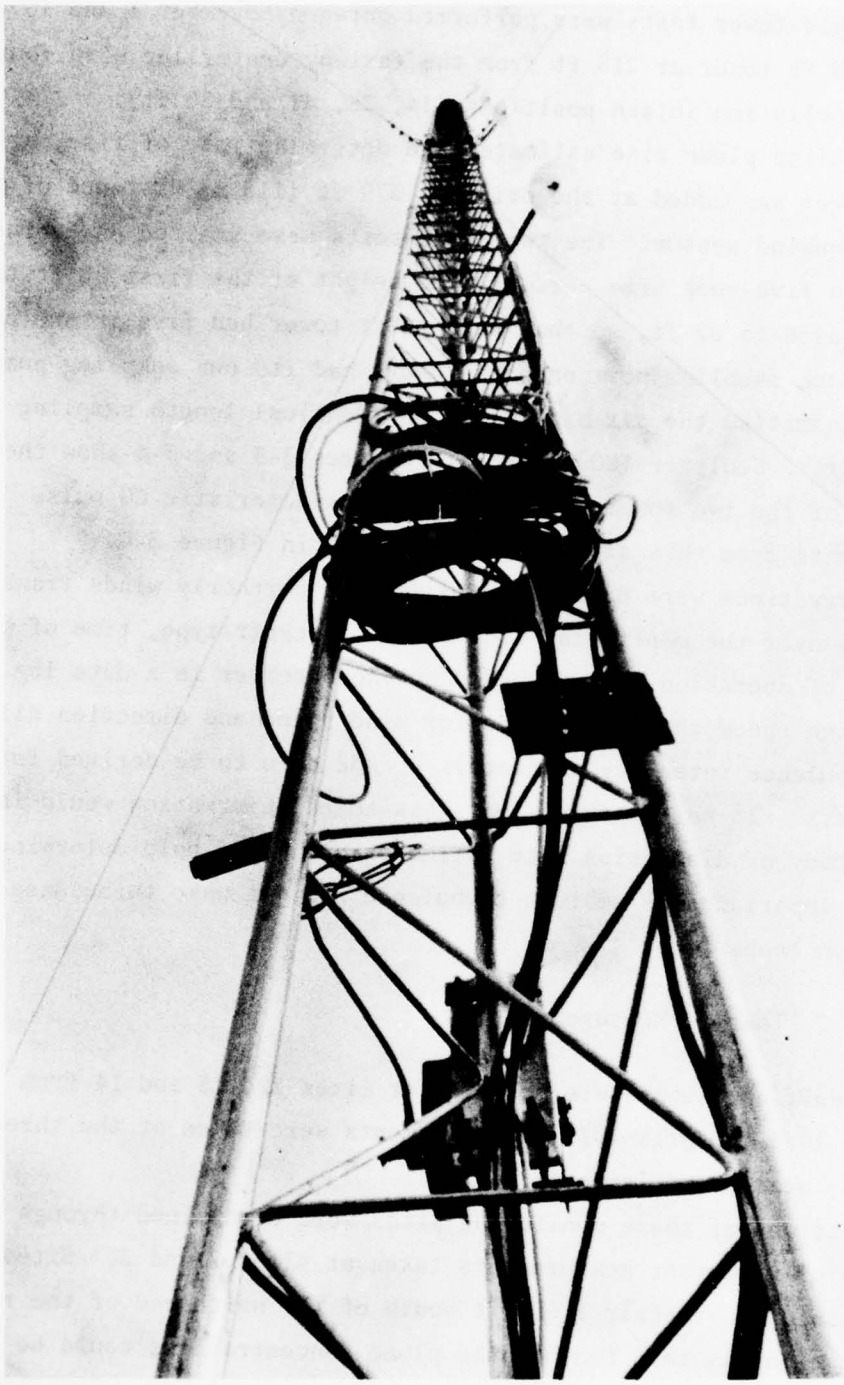

Figure 3-2 Pollution Monitoring Tower

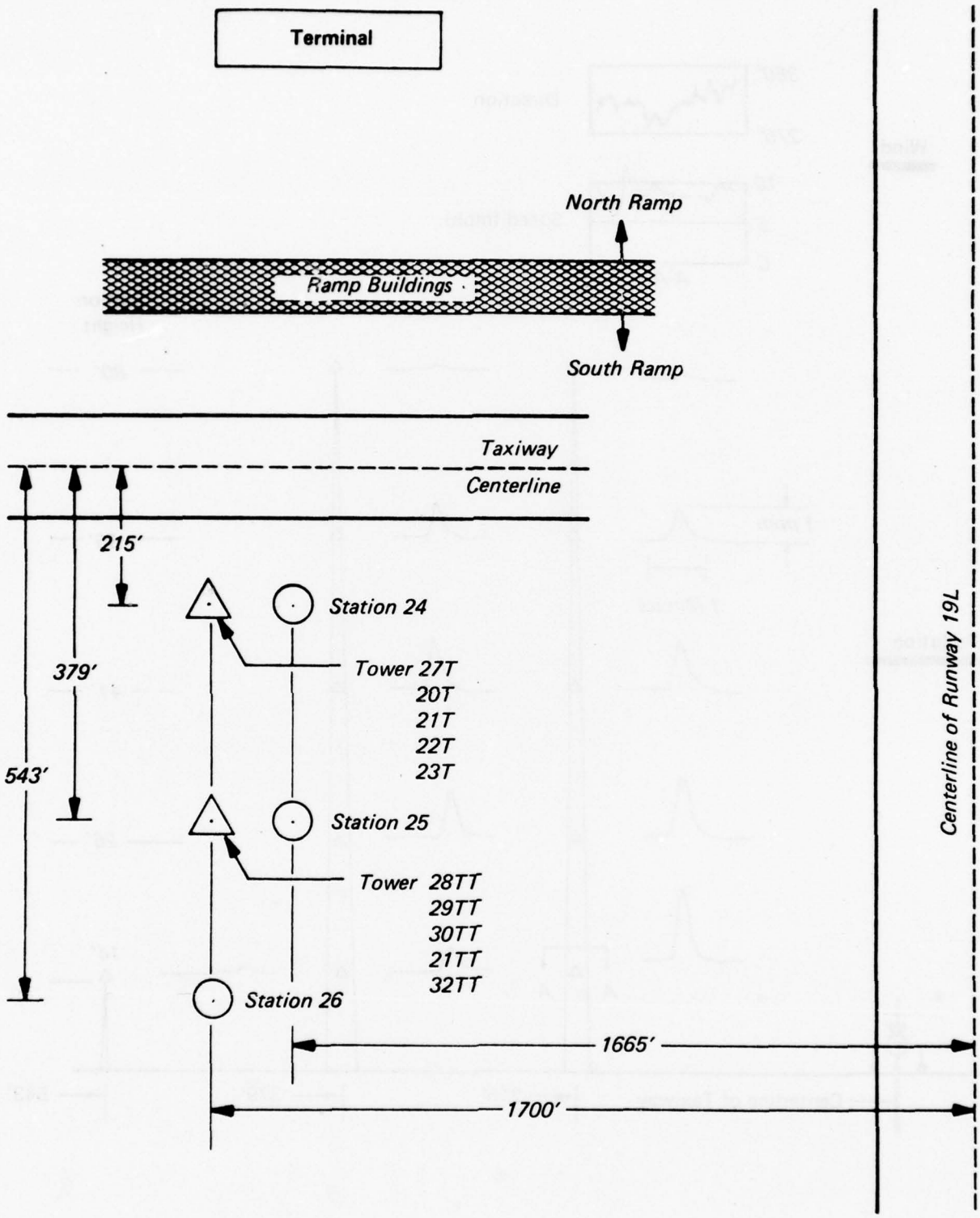

Figure 3-3 Station Locations - Two Tower Demonstration

712068

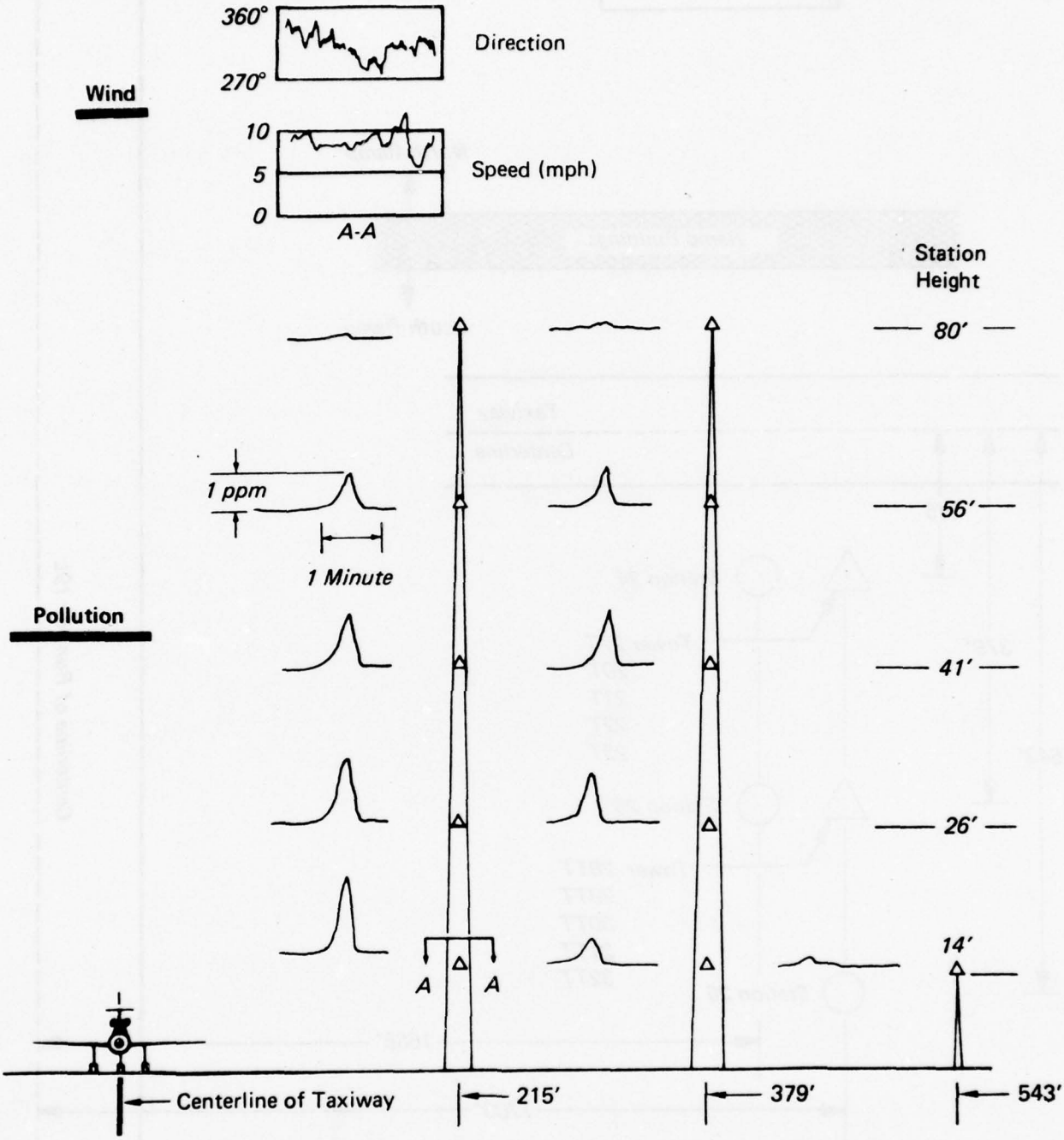

712069

Figure 3-4 Characteristic Strip Chart Plots of Wind and Pollution (CO) Two Tower Demonstration

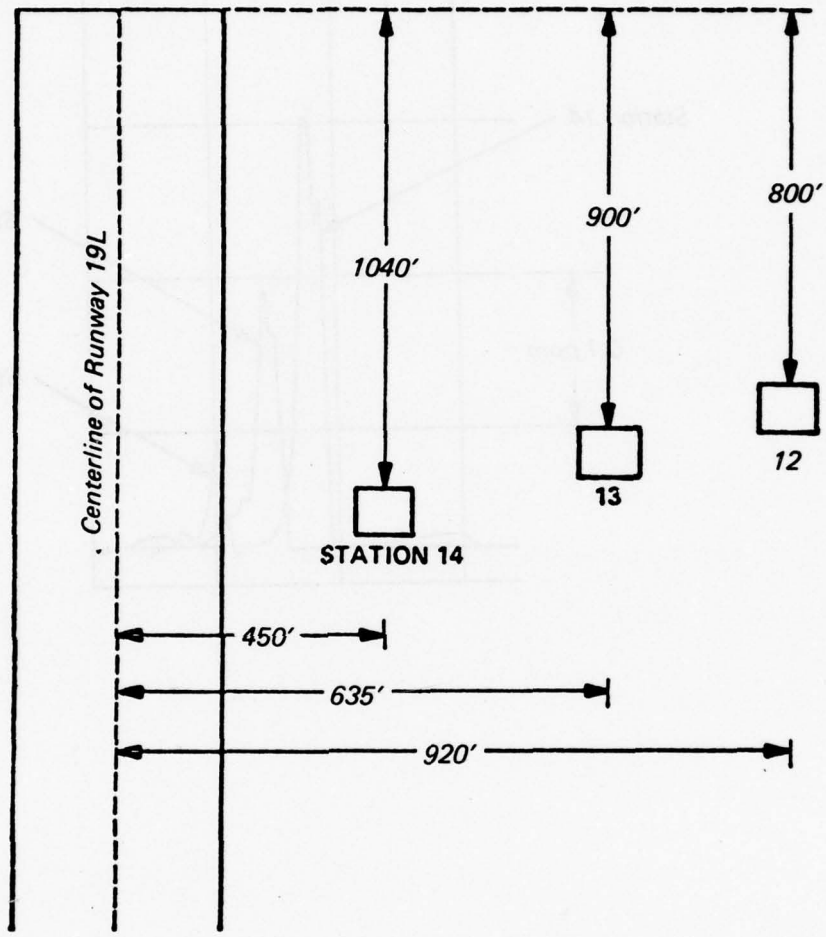

Figure 3-5 Takeoff Station Locations

712077

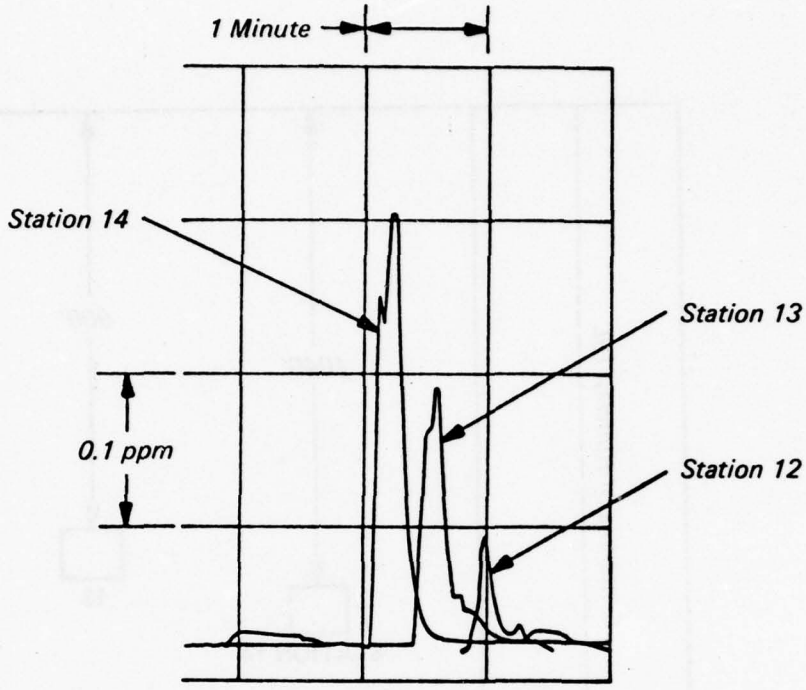

Figure 3-6 Characteristic Plot of NO_x Concentration During Takeoff

712076

3.2.3 Other Landing and Takeoff (LTO) Cycle Modes

Concentrations associated with approach and climb out phases of the LTO cycle were not analyzed because of the small data base and the uncertainties associated with jet exhaust plume rise and wake downwash during flight. Monitoring for queuing was initially planned but then cancelled because queuing did not occur at the time of Concorde departure.

4. AIR QUALITY MEASUREMENT METHODS

This section identifies the pollution measurement instrumentation and calibration methods used in the Dulles air quality monitoring programs. Limits of precision, sensitivity and accuracy for each pollutant measured are also identified.

4.1 Instrumentation and Site Selection

Instrument selection was influenced by the unique nature of the aircraft pollution source. Many non-aircraft sources are relatively continuous in nature and may be sampled over long averaging times. The emission plume from a moving aircraft, however, is a nonsteady-state puff and each sensor must respond to a wide concentration excursion as the plume passes over the downwind monitoring station. This event which usually takes less than two minutes, requires continuously recording instruments and high-speed chart recorders for precise documentation. This type of equipment was used to record the short-duration passage of the Concorde emission plume.

Six instrumented trailers plus mobile pollution monitoring equipment were moved at different times at the 32 sites shown in Figure 2-1. Monitoring equipment at these sites measured the following operational modes and weather parameters:

Purpose of Monitor	Site Number
Background	1,6
Takeoff (precursor)	2,3
Takeoff	12,13,14
Engine Start/Idle	15,16,17
Climb out	18
Approach	19
Taxi (surface)	4,5,10,11,24,25,26
Taxi (plume rise--single tower)	20T,21T,22T,23T
Taxi (plume rise--double tower)	27T,20T,21T,22T,23T,28TT,29TT, 20TT,31TT,32TT
Meteorological data (wind speed and direction)	7,8,9,6,10,12,24

Site selection considerations were:

- probable success in detecting an event;
- freedom from spurious emissions;
- frequency at which aircraft passed the monitoring sites;
- available power;
- wind direction and
- noninterference with other airport operations.

Sensor equipment for background and single event monitoring are listed in Table 4-1.

4.2 Analysis of Instrument Calibration and Response Times

Response of the CO instrumentation to pulses of constant concentrations, but of varying duration, was analyzed to quantify the dependence of system output on different concentration values. Strip charts examined were from 1 March, 2 March, and 26 April with calibration gas concentrations of 7.6, 18.0 and 7.6 ppm, respectively. No systematic variation of response characteristics with concentration of calibration gases was noted. The correction factors discussed below were derived for modeling instantaneous peak concentrations and pulse durations.

An independent calibration system was designed to insure that the monitoring instrumentation would record the true concentration of the gas sample during the short time it takes the emission plume to pass over the monitoring station. Calibration gas was released in pulses of five different durations from 10 to 60 seconds to simulate expected variations in emission plume passage times. Equal lengths of air sampling tubing were used to insure uniform instrument response.

Figure 4-1 illustrates the fraction of full scale response obtained for input CO pulses of varying duration (in seconds) during a typical calibration sequence. It is apparent that the modeling of instantaneous concentrations for comparison with measurements must incorporate corrections for the CO monitor's response time. Such corrections would not be very significant at the sensor distances if the source emissions were steady for more than one minute. Comparison tests with THC sensor indicated that its response time was about one-half the period required for the CO measurement system.

TABLE 4-1

SENSOR EQUIPMENT

Pollutant	Instrument and Manufacturer
Carbon monoxide	Intertech Co. - URAS2 - NDIR Energetic Sciences, Inc., Ecolyzer 2600E
Nitric oxide/nitrogen dioxide	Thermo Electron Co. 14B Analyzer Monitor Labs Inc., 8500 Calibrator
Total suspended particulates	BGI-IIA Hi Volume Sampler BGI-HCII Standard Calibrator
Total hydrocarbons	Beckman Instruments Inc. - Model 400
Nonmethane hydrocarbons	Beckman Instruments Inc. - Model 6800
Ozone	McMillan Electronics Co. - 1100 Analyzer, 1020 Ozone Generator
Wind speed and direction	Climet Instruments Co.-011-1 Wind Speed Transmitter, 012-10 Wind Direction Transmitter, 060-10 Transmitter
Temperature	Climet Instrument Co. - 015-3 Temperature Sensor, 060-10 Translator

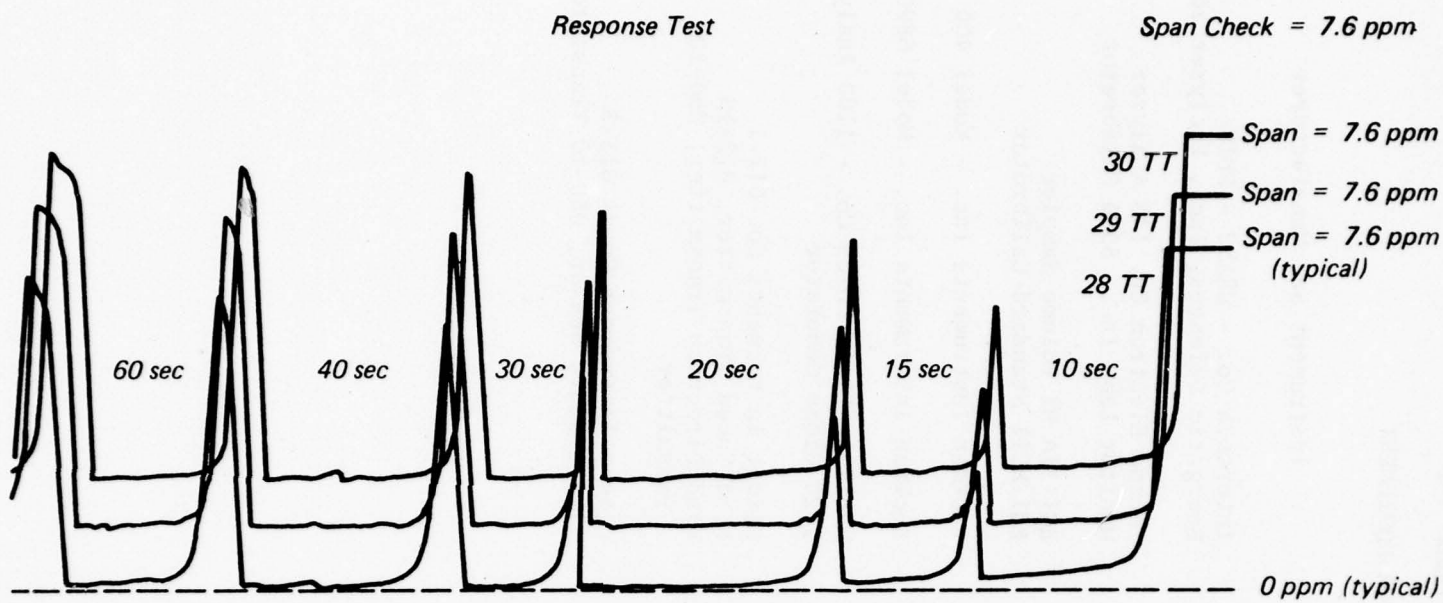

Figure 4-1 Instrument Response to CO Calibration Gas Pulses of Different Durations

In Figure 4-2 the average recorded CO pulse full width at half maximum peak height (FWHM) is plotted against input pulse duration. There is a linear response for longer pulses while for shorter pulses (<20 sec) the output pulse is artificially broadened by the instrument. Extrapolation of the lower end of the "actual" response curve, indicates a minimum discernible output pulse width of approximately 15 sec.

An examination of the product of peak heights and durations has shown that, to a first approximation, dose is conserved by the system. The widening of the FWHM at short pulse inputs is primarily a consequence of slowed response to the amplitude of the incoming CO concentration pulse.

To describe what is observed mathematically, the response function adopted is:

$$S(\Gamma) = S_{max} [1 - \exp(-\Gamma/\Gamma_r)] \quad \Gamma \leq \Gamma_p$$

$$= S_{max} [1 - \exp(-\Gamma_p/\Gamma_r)] \exp[-(\Gamma - \Gamma_p)/\Gamma_f] \text{ for } \Gamma > \Gamma_p$$

where

$\frac{S(\Gamma)}{S_{max}}$ is percent full scale response at time Γ (sec)

S_{max} is full scale response

Γ_r is rise time constant (sec)

Γ_f is decay time constant (sec)

Γ_p is pulse duration (sec)

Plotted in Figure 4-1 is the percent full scale response as a function of time in seconds for pulses of 10, 15, 20, 30, 40 and 60 seconds. The rise and decay response times were adopted from measured strip charts and the average values of $\Gamma_r = \Gamma_f = 12.0$ sec were used. Peak heights and FWHM were compared with those plotted from the calibration strip charts. The analysis using the adopted functional form of correction factor confirmed that dose was adequately conserved. Additionally, since the measured pulses reach their maximum at time Γ_p, the measured peak height and the true maximum are related by:

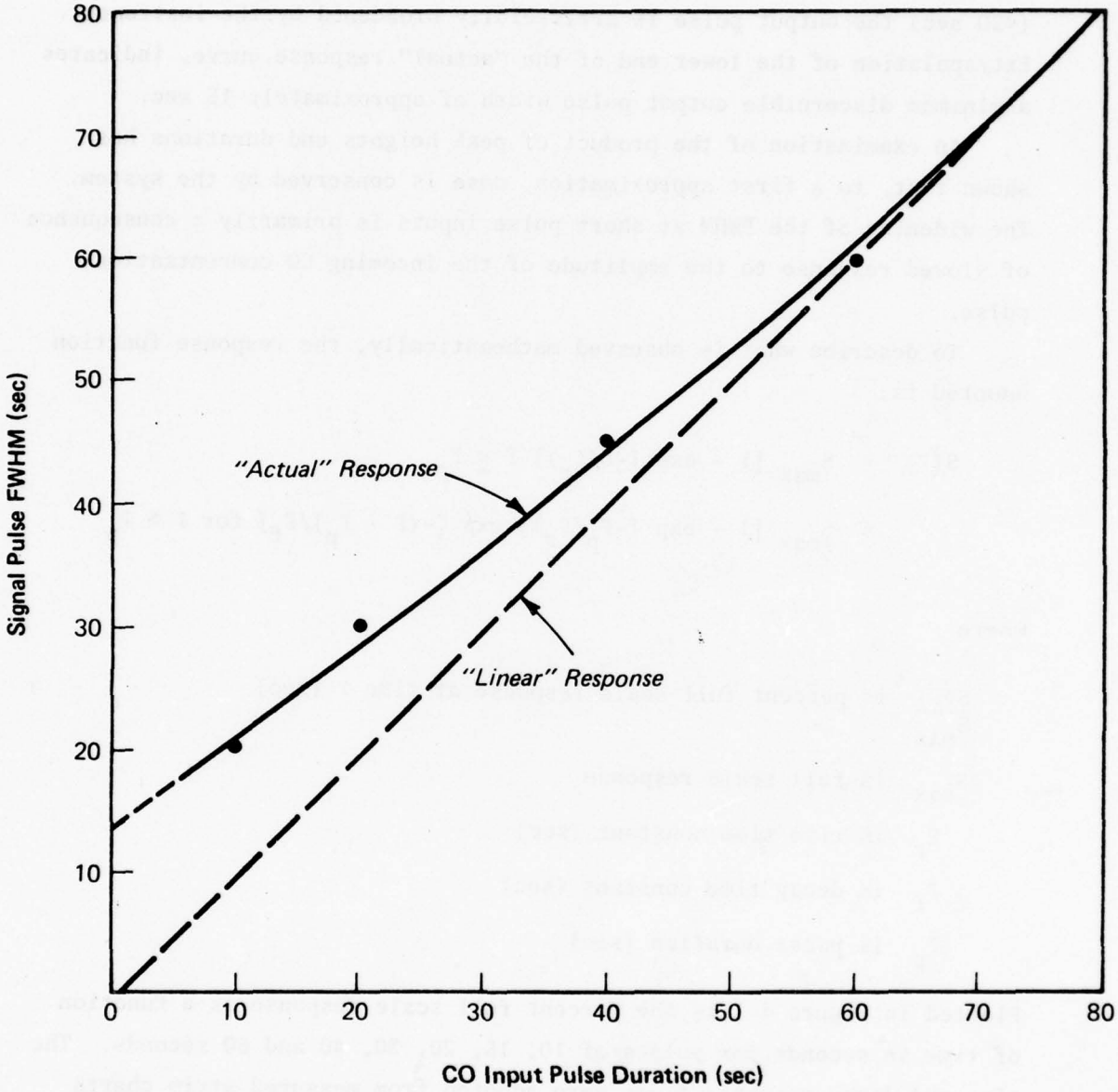

Figure 4-2 Ecolyzer Output Pulse Duration Vs. Input Pulse Duration

710169

$$S(\text{true max}) = \frac{S(\text{measured peak})}{1-\exp(-\Gamma_p/\Gamma_r)}$$

Thus, measured peak height responses are representative of the true event only for pulse durations longer than the instrument's rise time constant (12 sec). For example a 40 sec event yields a response of approximately 90%.

The previous discussion has dealt with the modification of square wave inputs by the instrumental system. A modified formulation is required to correct peak heights for input signals (responses to concentrations) which have a Gaussian distribution:

$$\chi_t = \chi_m \sqrt{\pi}/2 \left(\frac{\sigma_x}{\tau}\right) e^{(\sigma_x/2\tau^2)} \cdot e^{-(t/\tau)} \cdot$$

$$\left[1 + \operatorname{erf}\left(\frac{1}{\sqrt{2}\,\frac{t}{\sigma_x}} - \frac{\sigma_x}{\tau}\right)\right]$$

where

χ_t = theoretical peak concentration

χ_m = measured peak concentration

σ_x = plume width along wind

τ = response time of instrument

t = travel time with respect to sensor

An adequately precise approximation to this expression (solved for the expected measured concentration) has been found to be:

$$\chi_m = \frac{\chi_t}{1 + b(\tau/\Gamma_t)^p}$$

where

p = 1.2

b = 0.789

Γ_t = theoretical pulse duration (full width of half peak height) found from:

$$\Gamma_{tm} = \Gamma_t + \tau \ln 2/[1 + b(\Gamma_t/\tau)^p]$$

$$p = 1.4$$

$$b = 0.0912$$

where

Γ_{tm} is measured pulse width based upon the theoretical response.

4.3 Limits of Precision, Sensitivity and Accuracy

The precision of an instrument is a measure of reproducibility of its results (sometimes expressed as the complement, the variability of response to a known concentration). An understanding of the measurement system capabilities requires information concerning its precision, its sensitivity and its accuracy. The most critical of these quantities is usually the precision. Precision usually improves at concentrations well above an instruments limit of sensitivity. Instrument sensitivity refers to the minimum threshold concentration value for a measurable response to be noted and is dependent upon precision at the lowest end of the instrument response scale. In contrast, accuracy is a quantity describing the mean instrument response to a known calibration concentration and is therefore a measure of the signal-to-noise ratio of the instrument under a constant input signal at intermediate or higher scale deflections.

The precision of the difference between measurements on two instruments must take into account systematic errors in calibration as well as the rms sum of the errors in each measurement due to instrument noise or recorder chart errors. The precision of an instrument's measurement, or even that of the difference between two instrument measurements, may be characterized by a smaller error figure than the absolute accuracy of either instrument. The absolute accuracy must include the accuracy of the calibration standard. Only the relative accuracy contributes to the precision of a difference measurement. Careful adjustment of all instruments to the same standard minimizes the contribution of the

relative accuracy to overall uncertainties in the experiments at Dulles. The total uncertainty in both single instrument measurements and in difference measurements is dominated in these tests by the limits of chart recorder precision.

For both the CO and THC sensors sensitivity and accuracy are 0.5% and ±1.0% of full scale, respectively. However, the sensitivity in the total measurement system is reduced by the strip chart recorders which limit the sensitivity to 1.0% of the chart scale. These figures yield sensitivities of 0.1 and 0.25 ppm for THC and CO, respectively, while corresponding accuracies are ±0.2 and ±0.50 ppm.

It should be noted that these are conservative estimates and represent instrumental characteristics only. Since additional information is available in assessing strip chart traces (such as the time of an event), it is possible to extract higher degrees of sensitivity from the trace noise level by effectively using this correlative data. It is estimated that this factor increases the effective sensitivity of each instrument to approximately 0.5% full scale. This point is illustrated by Table 4-2.

TABLE 4-2

MONITORING INSTRUMENT SENSITIVITY AND ACCURACY

Instrument Alone (ppm)

	Sensitivity	Accuracy
CO	0.25	0.50
THC	0.10	0.20
NO_x	0.005	0.01
O_3	0.005	0.01

Instrument and Correlative Data (ppm)

CO	0.125	0.50
THC	0.05	0.20
NO_x	0.002	0.01
O_3	0.002	0.01

5. DULLES AIRPORT AIR QUALITY DATA BASE

A data base has been developed for the Dulles Airport area to support both current and future analyses of air quality and air pollution transport at the airport and in its surrounding region. The four types of data included in this data base are: (1) air pollutant and meteorological data from the measurement programs at the airport and in its immediate vicinity; (2) similar data from regional state-operated air pollution stations; (3) meteorological data from the nearby National Weather Service Station; and (4) airport activity data, including aircraft operations records and other operations-related source data for Dulles. The computerized data base utilized for the current data analysis tasks is described briefly below and in detail in Appendix A.

5.1 Dulles Airport Data

The following measurements at the airport and its immediate vicinity have been incorporated into the data base.

5.1.1 Dulles South Ramp and Sterling Park Background Concentration Measurements

Data from these two sites (CO, NO_x, THC, O_3, wind speed and direction) have been reduced and put into computer compatible format. After visual inspection and appropriate annotations, the original strip-chart data were digitized to yield hourly averages. Each data point was appropriately labelled with the following information:

- station name;
- parameter name;
- month, date of the month, hour (local standard time);
- hourly averages of the parameters; and
- the engineering units.

Examples of the information content of this data set have been given in the Concorde Monthly Reports, and are included in Appendix A to this report.

5.1.2 Single Event Pollution Measurement Data

Two types of single "event" measurements were made. They were CO emission dispersion for taxiing aircraft and NO_x emission dispersion during takeoff. A typical "event" can be characterized by the following parameters (Figure 5-1):

- background level;
- duration of "event";
- peak concentration;
- half width times of the "event" (indicating skewness) and
- dose or exposure (area under peak).

In addition, each of the measurement points is labelled by:

- date (month, day);
- time of day (LST);
- aircraft type;
- mode of operation and
- "dispersion meteorology" parameters

The "dispersion meteorology" parameters are explained in Section 5.3.

5.2 Regional Air Pollution Data

The Air Pollution Control Authority of the State of Virginia has made background pollution measurements of certain pollutants at several sites (Figure 2-2 and Table 3-1). These can be used in the overall evaluation of the background concentrations in the vicinity of Dulles. The data were originally on coding forms in SAROAD* format. ERT has incorporated these data in the data base in a format consistent with

---

*See Appendix A.

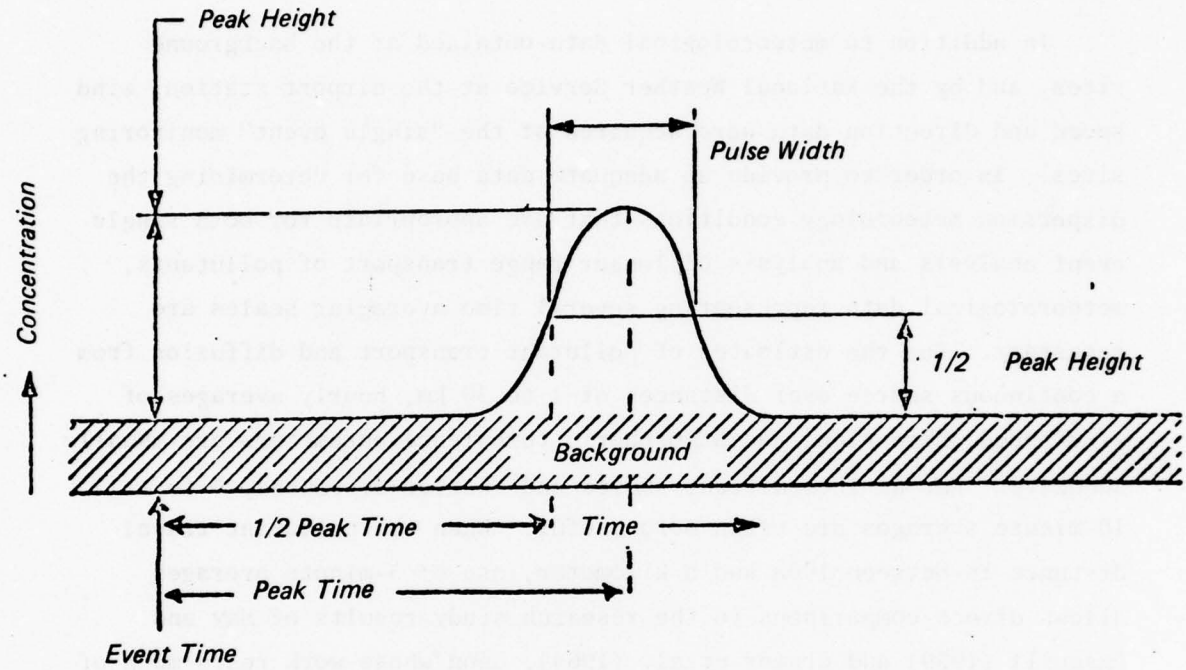

Figure 5-1 Pollution Parameter Definition

that used for the Sterling Park and South Ramp pollution measurement data. The regional air quality influence of Dulles Airport operations and Concorde operations has been evaluated by comparing these measurements with similar data obtained from the Dulles South Ramp and Sterling Park Stations.

5.3 Meteorological Data for the Airport

In addition to meteorological data obtained at the background sites, and by the National Weather Service at the airport station, wind speed and direction data were acquired at the "single event" monitoring sites. In order to provide an adequate data base for determining the dispersion meteorology conditions that are appropriate for both single event analysis and analysis of longer range transport of pollutants, meteorological data representing several time averaging scales are necessary. For the estimates of pollutant transport and diffusion from a continuous source over distances of 1 to 30 km, hourly averages of wind speed, direction, and atmospheric turbulence parameters are usually adequate. For an intermittent source and shorter distances, 3 to 10-minute averages are often more useful. When the pollutant travel distance is between 100m and a kilometer, use of 3-minute averages allows direct comparisons to the research study results of Hay and Pasquill (1959) and Cramer et al. (1964), upon whose work rests much of the empirical validation of Gaussian plume dispersion models. The fundamental relationships between dispersion of pollutants for any plume travel distances, the appropriate averaging times for wind turbulence statistics, and sampling times for concentration measurements have been discussed in detail by Pasquill (1974) and Gifford (1968). The important result for the present study plan is the determination of the appropriate averaging times for wind and turbulence parameters as indicated by the detailed discussion given in Appendix B; a 6-second averaging time and a 3-minute sampling time for turbulence parameter calculations best utilized the available data (when high speed charts are employed).*

---

*When only slow speed charts were available, a simpler method of turbulence intensity calculation based upon range measurements was used.

In the present analyses, the 3-minute sampling time serves as the averaging time for the calculation of a mean wind characterizing short range pollutant transport. For longer distance transport predictions, an hourly average wind speed has been employed. For the latest series of measurements temperature gradients (ΔT) between two levels on the closest tower have been recorded. These ΔT measurements can be used to identify atmospheric stability, and thereby estimate plume rise and dispersion potential. When both ΔT and lateral turbulence measurements are available, the latter generally take precedence for estimates of lateral dispersion parameters, and the former maybe used to estimate vertical dispersion parameters. Therefore, the complete set of data made available to FAA from the ERT-operated meteorological instruments at the runway site includes:

- mean wind speed (1 hour)
- mean wind speed (3 minutes)
- standard deviation of wind speed (6 sec, 3 minutes)
- mean wind direction (1 hour)
- mean wind direction (3 minutes)
- standard deviation of wind direction (6 sec, 3 minutes)
- vertical temperature gradient (1 hour)
- vertical temperature gradient (3 minutes)

In the initial monitoring program reports, the wind data were reported simply in terms of hourly averaged wind speeds and direction. These have been augmented for the two tower test series to include all of the parameters identified above. These parameters are useful as a description of the small scale diffusion properties of the air and have been utilized in the model analyses described in Section 7.

5.4 Aircraft Activities Data

It was essential to the analyses of the pollution data on a regional scale to have a measure of the level of aircraft activity at times corresponding to those of the measurements. Summary listings of Official Airline Guide (OAG) schedules of arrivals and departures are generally available from the FAA. However, these schedules do not include general aviation or military operation data. An onsite survey was therefore necessary to assess variations in these other activities on a weekly, daily and hourly basis. Table 5-1 presents a summary of the data collected on May 6 and 7, 1977 (a Friday and Saturday) to define weekday-weekend variations. On both days military traffic was insignificant, while general aviation accounted for 53% of all operations (i.e., either takeoffs or landings). The main difference between weekdays and weekends are the reduced numbers of commercial air carriers and near elimination of air taxis on the weekend. The numbers of commercial operations agreed well with the available OAG data. A complete log of all Concorde operations from May to November 1976 is reported in Table 5-2, while Table 5-3 summarizes the total of Dulles Airport activities over a 6-month period.

5.5 Aircraft Design Geometry and Emission Rates

Table 5-4 summarizes a variety of useful aircraft type-specific design dimensions and pollutant emissions. All design dimensions are from Janes, All the World's Aircraft. Emission data (except those for the Concorde) are from the U. S. EPA's Document AP-42. This emissions inventory by aircraft type is essentially the same as that used by the authors of Concorde Supersonic Transport Aircraft, Final FEIS (September 1975) in deriving an average emission rate during an LTO (Landing-Taxi-Takeoff) cycle. The Concorde emissions data are estimates supplied by the Federal Aviation Administration. All LTO emission rates utilized in this project are listed in Table 5-4.

TABLE 5-1

DULLES AIRPORT DAILY AIRCRAFT OPERATIONS (May 6 and 7, 1976)

SUMMARY TABLE

Aircraft	Weekday	%	Weekend	%	Total	%
B737	5	2.6	6	3.9	11	3.2
DC-9	25	13.2	21	13.8	46	13.4
YS-11	3	1.6	-	-	3	0.9
B-727	47	24.7	49	32.0	96	28.0
DC-8	25	13.2	17	11.1	42	12.2
B-707	39	20.5	33	21.6	72	21.0
IL-62	-	-	-	-	-	-
DC-10	18	9.5	14	9.1	32	9.3
L-1011	6	3.2	2	1.3	8	2.3
B-747	19	10.0	6	3.9	25	7.3
VC-10	-	-	2	1.3	2	0.6
Concorde	3	1.5	3	2.0	6	1.8
Total	190	100.0	153	100.0	343	100.0
Type						
Air Carrier	190	36.1	153	44.3	343	39.3
Air Taxi	39	7.4	3	0.9	42	4.8
General Aviation	279	52.9	185	53.6	464	53.2
Military	19	3.6	4	1.2	23	2.7
Total	527	100.0	345	100.0	872	100.0

TABLE 5-2

OBSERVED DISTRIBUTION OF CONCORDE OPERATIONS (MAY TO NOVEMBER 1976)

	MAY	JUNE	JULY	AUGUST	SEPTEMBER	OCTOBER	NOVEMBER	TOTAL
North Arrivals	4	9	12	11	14	14	12	76
South Arrivals	2	14	12	10	8	10	11	67
North Departures	1	11	17	14	14	18	14	89
South Departures	5	11	6	9	8	9	11	59
Runway 30 Arrivals	0	0	0	0	1	3	2	6

TABLE 5-3

AIRCRAFT OPERATIONS

DULLES INTERNATIONAL AIRPORT

JUNE - NOVEMBER 1976

Aircraft	Type	Scheduled Air Carrier 6 Mos. Operation
B-737	Two-engine narrow body	728
DC-9	Two-engine narrow body	2,134
DC-9S	Two-engine narrow body (stretched)	1,456
YS-11	Two-engine turboprop	364
B-727	Three-engine narrow body	5,096
B-727s	Three-engine narrow body (stretched)	3,276
DC-8	Four-engine narrow body	2,910
B-707	Four-engine narrow body	6,508
1L-62	Four-engine narrow body	60
DC-10	Three-engine jumbo	2,180
L-1101	Three-engine jumbo	364
B-747	Four-engine jumbo	1,636
Concorde	Four-engine supersonic	280
	TOTAL	26,992

Actual Operations by Type	Total for 6 Mos.
Air Carrier	28,624
Air Taxi	6,786
General Aviation	36,163
Military	2,715
Total Operations	74,288

TABLE 5-4

AIRCRAFT DESIGN DIMENSIONS AND POLLUTANT EMISSION RATES

AIRCRAFT	ENGINES: Engine Type	ENGINES: Number of Engines	ENGINES: Engine Locations	Fuel Rate (lb/hr)	Mode	EMISSIONS: CO lb/hr-eng	EMISSIONS: HC lb/hr-eng	EMISSIONS: NO_x lb/hr-eng	EMISSIONS: TSP lb/hr-eng
B707	JT-3D	4	2/wing72	872	T-I	109.0	98.6	1.4	0.45
				10,835	T-O	12.3	4.65	148.0	8.25
				8,956	C	15.3	4.92	96.2	8.5
				4,138	A	39.7	7.84	21.8	8.0
				4,432	LTO (lb)***	207.5	175.3	29.3	4.55
B727	JT-8D	3	3 tail	959	T-I	33.4	6.99	2.9	0.36
				8,755	T-O	7.49	0.778	198.0	3.7
				7,337	C	8.89	0.921	131.0	2.6
				3,409	A	18.2	1.75	30.9	1.5
				3,042	LTO (lb)	48.3	9.5	31.2	1.18
B737	JT-8D	2	1/wing	959	T-I	33.4	6.99	2.9	0.36
				8,755	T-O	7.49	0.778	198.0	3.7
				7,337	C	8.89	0.921	131.0	2.6
				3,409	A	18.2	1.75	30.9	1.5
				2,028	LTO (lb)	32.2	6.4	20.8	0.79
B747	JT-9D	4	2/wing	1,738	T-I	102.0	27.3	6.06	2.2
				17,052	T-O	8.29	2.95	720.0	3.75
				14,317	C	11.7	2.65	459.0	4.0
				5,204	A	37.6	3.00	54.1	2.3
				7,500	LTO (lb)	192.0	59.3	125.9	5.19
DC8	JT-3D	4	2/wing	872	T-I	109.0	98.6	1.4	0.45
				10,835	T-O	12.3	4.65	148.0	8.25
				8,956	C	15.3	4.92	96.2	8.5
				4,138	A	39.7	7.84	21.8	8.0
				4,432	LTO (lb)	207.5	175.3	29.3	4.55
DC9	JT-8D	2	2 tail	959	T-I	33.4	6.99	2.9	0.36
				8,755	T-O	7.49	0.778	198.0	3.7
				7,337	C	8.89	0.921	131.0	2.6
				3,409	A	18.2	1.75	30.9	1.5
				2,028	LTO (lb)	32.2	6.4	20.8	0.79
DC10	JT-9D	3	1/wing 1 tail	1,738	T-I	102.0	27.3	6.06	2.2
				17,052	T-O	8.29	2.95	720.0	3.75
				14,317	C	11.7	2.65	459.0	4.0
				5,204	A	32.6	3.00	54.1	2.3
				5,475	LTO (lb)	144.0	44.46	94.4	3.89
Concorde	Rolls Royce Olympus 593	4	2/wing	2,500	T-I	295.0	90.0	6.0	
				50,000	T-O	1,450.0	145.0	625.0	
				20,000	C	400.0	30.0	250.0	
				5,200	A-I	426.0	114.0	21.0	
				10,000	A-F	550.0	85.0	65.0	
				12,982	LTO (lb)	800.0	194.0	106.0	2.40

T-I = Taxi-idle
T-O = Take-off
C = Climbout
A = Approach
A-I = Intermediate
A-F = Final
*** = LTO units are: total pounds per aircraft cycle.

TABLE 5-4 (Continued)

		AIRCRAFT DIMENSIONS				EXHAUST LOCATIONS AND DIMENSIONS				
Aircraft	Series #	Height (m)	Length (m)	Wingspan (m)	Wing Area (m)	Engine #	Height (m)	Distance from fuelage center (m)	Distance forward from tail (m)	Exhaust Diameter (m)
B707		12.93	46.61	44.42	283.4	1	2.48	15.63	24.32	0.88
						2	1.91	9.91	17.92	0.88
						3	1.91	-9.91	17.92	0.88
						4	2.48	-15.63	24.32	0.88
B727		10.36	46.69	32.92	157.9	1	3.90	2.92	9.45	0.75
						2	6.24	0		0.75
						3	3.90	-2.92	9.45	0.75
B737		11.28	30.48	28.35	91.05	1	1.51	5.15	11.93	0.85
						2	1.51	-5.15	11.93	0.85
B747	Reg*	20.80	70.51	59.64	511.0	1*	2.60	16.74	31.81	1.08
						2	2.13	9.42	20.73	1.08
	SP	19.94	56.31	59.64	511.0	3	2.13	-9.42	20.73	1.08
						4	2.60	-16.74	31.81	1.08
DC8	61**	12.92	57.12	43.41	267.9	1**	3.25	14.14	38.59	1.35
	62	12.92	47.98	45.23	271.9	2	2.66	9.73	35.64	1.35
	63	12.92	57.12	45.23	271.9	3	2.66	-9.73	35.64	1.35
						4	3.25	-14.14	38.59	1.35
DC9	10	8.38	31.82	27.25	86.77					
	20	8.38	31.82	28.47	92.97					
	30	8.38	36.37	28.47	92.97	1	3.41	2.95	8.84	1.05
	40	8.53	38.28	28.47	92.97	2	3.41	-2.95	8.84	1.05
	50†	8.53	40.72	28.47	92.97					
DC10	10	17.70	55.30	47.34	358.7	1††	2.67	8.20	28.09	1.15
	30††	17.70	55.30	50.41	367.7	2	9.43	0	0.41	1.15
	40	17.70	55.30	50.41	367.7	3	2.67	-8.20	28.09	1.15
CONCORDE		12.19	62.10	25.56	358.25	1	3.1	5.27	14.42	0.93
						2	3.1	4.34	14.42	0.93
						3	3.1	-4.34	14.42	0.93
						4	3.1	-5.27	14.42	0.93

*Data given for Req. Series

**Data given for 61 Series

†Data given for 50 Series

††Data given for 30 Series

For many of the aircraft types, there is more than one manufacturer's series number. In these cases, dimensions are listed for the different series numbers. The exhaust locations and dimensions listed are, however, specific to the series number indicated. Each engine of an aircraft is arbitrarily assigned a number in the table, and the coordinate of each corresponding engine exhaust orifice is measured from an origin (0,0) on the fuselage centerline at the aft tip of the aircraft tail.

6. DATA REDUCTION AND ANALYSIS

The first analyses of the measurement data obtained in the Concorde monitoring program consisted of examination and reduction of the data into formats that could be analyzed on the computer by standard statistical methods. Both regional background measurements and single event measurements were included in this computerized data base in consistent units as outlined in Section 5. This section discusses the fundamental methods used to investigate simple relationships between measured variables and presents some sample results that led to important conclusions. Complete statistical summary results for all experiments involving single aircraft are given in Appendix C. Supportive tables and figures for regional background data analyses are contained in Appendix D.

6.1 Regional Background Data Analysis

A number of statistical techniques have been used to analyze the regional data base. The most basic was the stratification of the data by wind direction and speed characteristics and by atmospheric stability. This process helped identify where particular pollutants appeared to come from for each of the monitoring sites. This method was especially useful for determining whether or not the airport is identifiable as a predominant source in the region.

Another technique involved stratification according to time of day to discover patterns of diurnal variation. This procedure aided in identifying effects of photochemical mechanisms and potential sources whose maximum contributions to regional air quality levels peak at specific times of the day (such as automobile traffic).

To determine the strength of the relationships indicated by stratification, a correlation analysis was carried out. This was followed by linear and multilinear regression analyses. Because these latter quantitative results are most useful when discussed in terms of a model, they are presented separately in Section 8.

6.1.1 Stratification by Wind Direction and Speed

To examine upwind-downwind relationships between Dulles Airport and the various regional monitoring sites, a wind frequency distribution analysis by speed category and atmospheric stability class was performed. Results are presented in Appendix D in Tables D1.1-D1.7. The Dulles wind frequency distribution, or wind "rose," for all stability classes is summarized in Table D1.8. Winds are generally from the south and west-northwest directions. Similar tables are presented for Sterling Park (D1.9) and South Ramp (D1.10) and show similar distribution characteristics. Figures D1.11 and D1.12 reproduce these tables as wind rose plots and demonstrate the predominant winds for June to September 1976.

Using these wind data for the June to August 1976 period, pollution concentration values of O_3, CO and NO_2 were stratified by wind speed and direction and stability (stable, unstable and neutral) for Sterling Park, South Ramp, Massey, Lewinsville, Seven Corners and NIH Bethesda. (O_3-Tables D1.13-D1.17; CO-D1.18-D1.22; NO_2-D1.23-1.28) Additionally, one set of hydrocarbon data was available from Seven Corners (D1.29). Corresponding pollution rose plots are presented (Figures D1.13-D1.28). In no location does the direction of the maximum pollutant contribution (the most significant direction in the pollution rose plot) correspond to the relative direction of the airport. There is a moderate variability of this maximum direction with stability class and wind speed category; however, it is adequately summarized by the "all" wind speed and stabilities cases. Table 6-1 presents this result for each monitoring site. Beneath each site is the relative direction of Dulles in parentheses. None of the predominant source directions are towards the airport. A major roadway can be identified as a nearby source for Lewinsville based on the CO data. Additionally, the opposite directions identified for Massey and Seven Corners indicate a source between them that is probably Interstate 495. A comparison of the results of Table 6-1 and the wind rose plot for Sterling Park (Figure D1.11) indicates that the pollution source directions occupy quadrants of characteristically low wind speed, suggesting the predominance of nearby sources.

TABLE 6-1

DIRECTION OF MAXIMUM CONCENTRATION OF SPECIES
FOR ALL WIND SPEEDS AND STABILITIES
(June to August 1976)

(I):	O_3	THC	CO	NO_2
Sterling Park (SSW)*	SSE		ENE	ENE
Massey (NNW)	NE		ENE	E
Lewinsville (NW)	NE		SE	SSE
Seven Corners (NW)	NE	SE	WSW	SE
NIH (Bethesda) (W)				ESE

*( ) indicates primary wind directions for which airport sources could contribute to pollutant concentrations.

6.1.2 Diurnal Analyses

Since hourly data were available from the regional data base, stratification by hour of the day was performed to provide an insight into possible sources with strong time dependence (such as automobile traffic) and possible production and exchange mechanisms strongly dependent on the time of day (such as photochemistry). Table D1.30 presents the diurnal variation of wind speed at Sterling Park, South Ramp, and Dulles and stability class at Dulles. These results are plotted in Figure 6-1. On the average for the June to September 1976 time period (Dulles data are for January to December 1976) both wind speed and stability class exhibit strong diurnal variation, with night characterized by stable, low wind speed cases and day by unstable high wind speed cases. Thus, if wind speed and stability are, on the average, deemed variables for time of day, they need not be considered independent variables for the purpose of correlation analyses. For the present analysis, time of day was assumed to determine the wind speed category and stability class.

Tables D1.31 through D1.35 present the results for each pollutant and site. A comparative picture of the diurnal variation of four major species, CO, O_3, NO_2, and THC, at Sterling Park is extracted from these results and given in Figure 6-2. The following features characteristic of the urban environment may be noted: (a) a morning "traffic" peak during hours 7 and 8 in CO, NO_2 and THC, (b) an afternoon depression for these same species due to increased mixing during the unstable afternoon period, (c) an afternoon peak in the O_3 concentration due to its photochemical source, and (d) a late evening peak in CO, NO_2 and THC as the atmosphere becomes stable and mixing decreases. Similar features are found for all of the regional sites, particularly as regards the morning peaking of CO, NO_2 and, of course, the variation of O_3. As an example, the data for Lewinsville (next closest site to Dulles) are presented in Figure 6-3. On the basis of these data, one would expect to find positive correlations between CO and NO_x and negative correlations between either CO or NO_x and O_3. The calculations are carried out in Section 8.1. Since particular sources may be characterized by unique CO versus NO_x

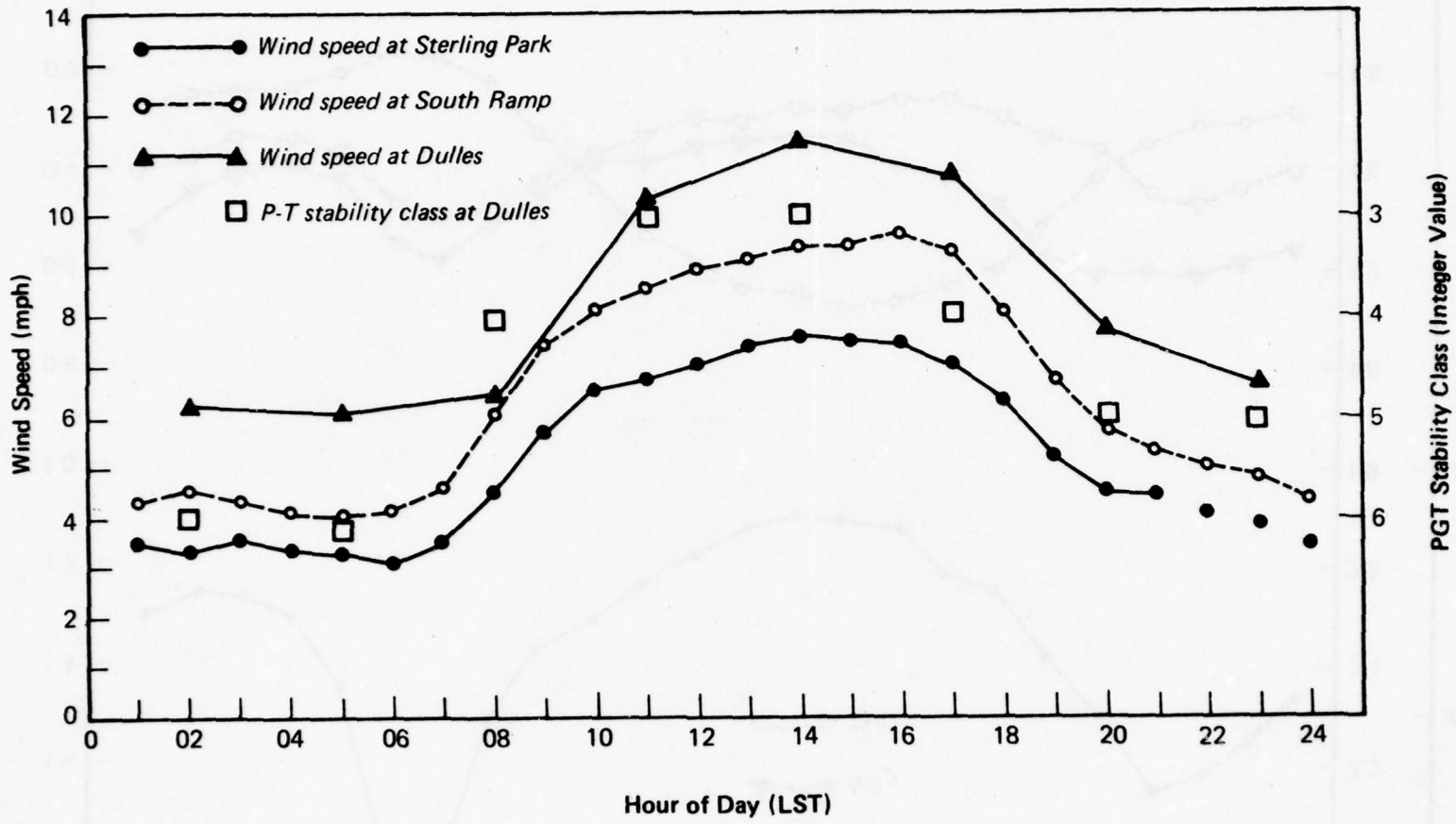

Figure 6-1 Diurnal Wind Analysis (June-September 1976)

710147
710145

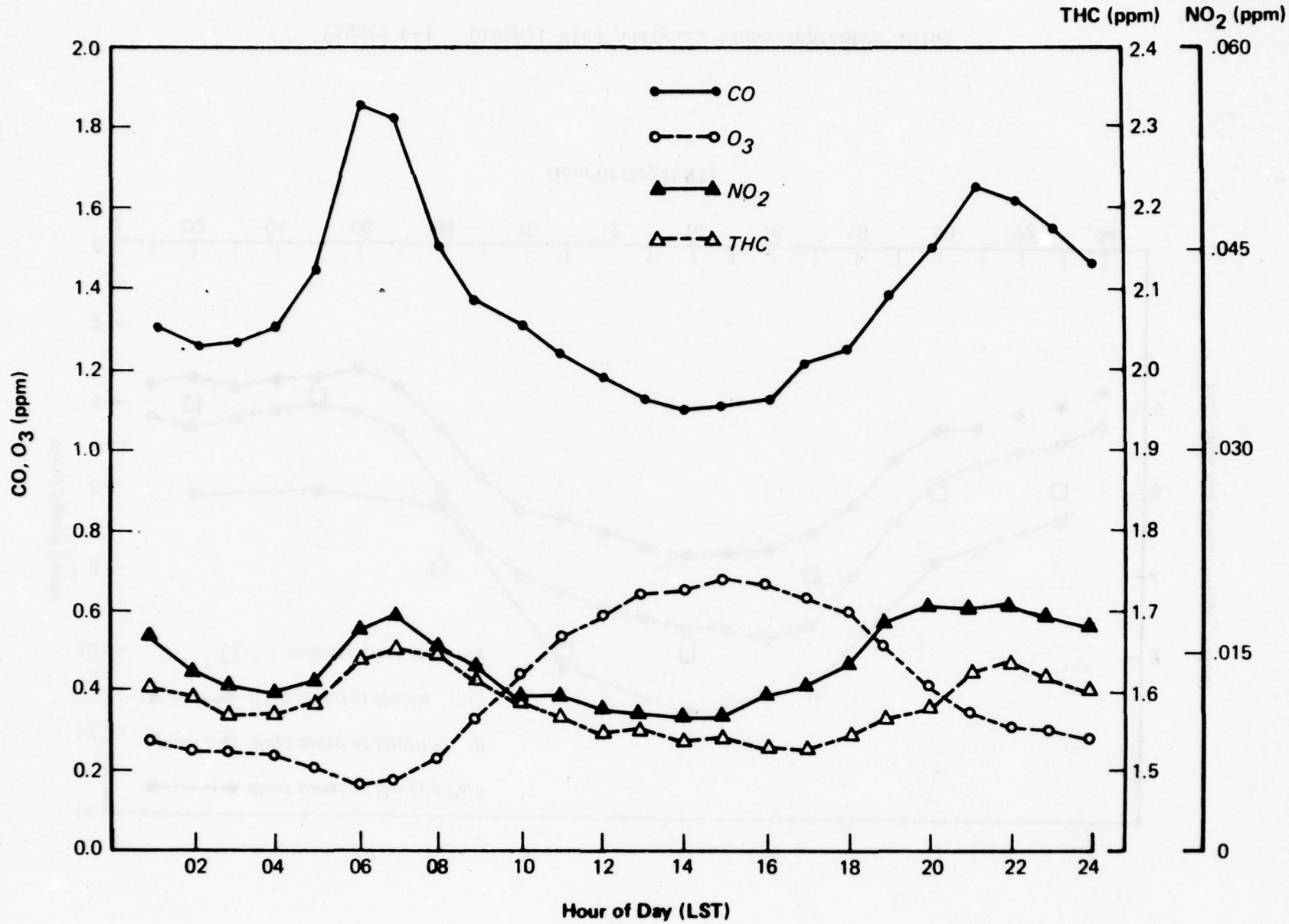

Figure 6-2 Diurnal Pollutant Analysis for Sterling Park (June-September 1976)

710146
710145

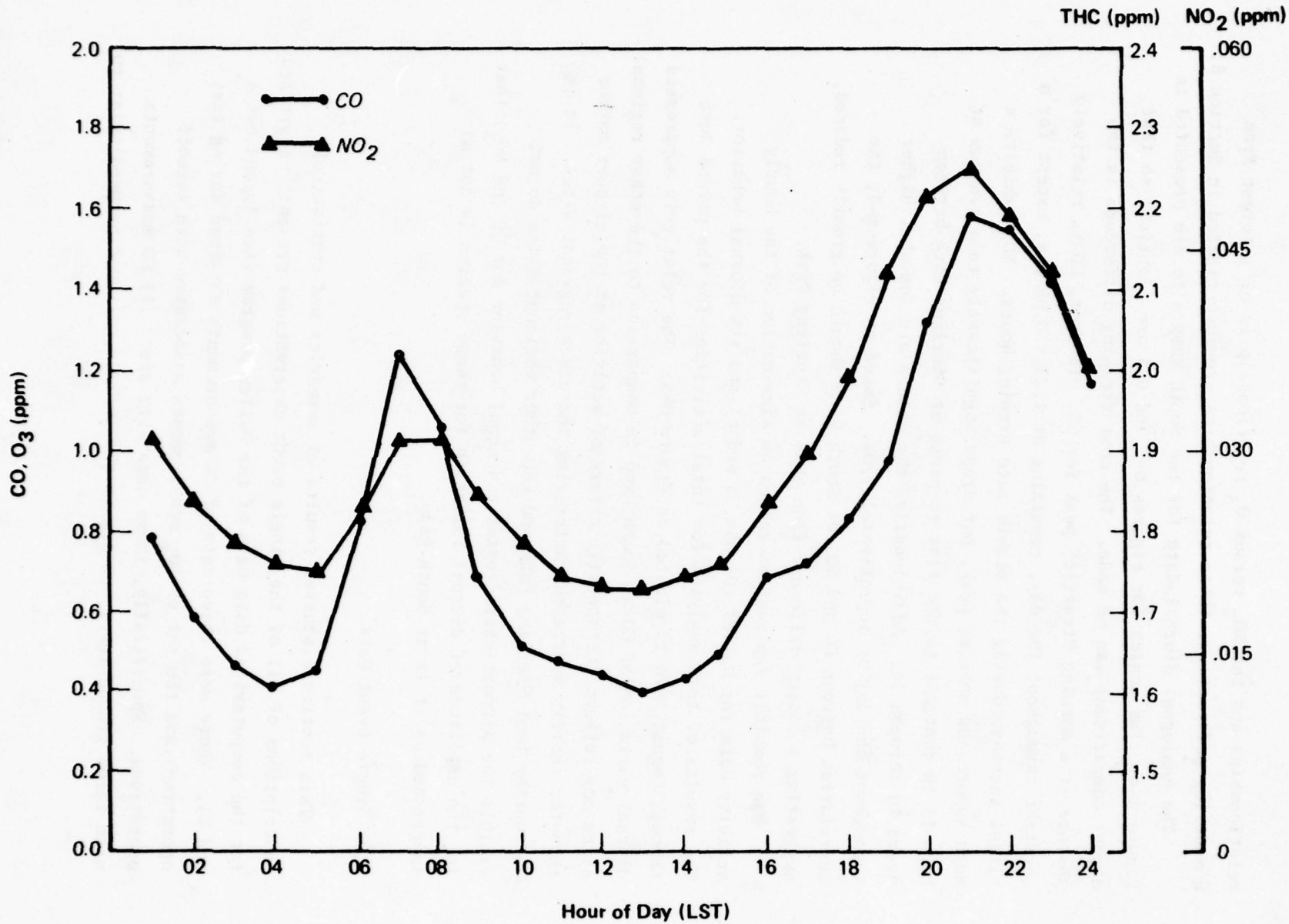

Figure 6-3 Diurnal Pollutant Analysis for Lewinsville (May-September 1976)

relationships and the NO_2 versus O_3 relationship is of interest from a modeling perspective, these relationships are investigated in Section 8.

The analogous diurnal data for the South Ramp site are presented in Figure 6-4. The scales for Figures 6-3 and 6-4 are identical so that direct comparisons can be made. The most striking difference is the absence of a morning "traffic" peak for CO. In fact, CO is relatively constant throughout the day, remaining at 1.25 ± 0.05 ppm, except for a slight increase during the stable late evening hours. NO_2 exhibits a much suppressed morning peak, but drops significantly to a minimum at hour 13 in contrast to the flat response at Sterling Park between hours 10 through 16. Additionally, the values are somewhat higher throughout the day by approximately 20%. Based on Figure 6-4, the correlation between CO and NO_2 at South Ramp should be greatly reduced, suggesting a source different from that at Sterling Park.

One possible explanation relies on examination of the hourly activity data for Dulles (D1.36a, b and c) and its diurnal behavior. The results of this analysis for total activities for the period June through August 1976 is plotted in Figure 6-5. The relatively suppressed diurnal variation of CO at South Ramp in comparison to the other regional sites may reflect the specific nature of activity at the airport rather than the traffic source characterizing the other regional sites. It is noteworthy that Sterling Park and the other regional sites do not exhibit the airport-characteristic diurnal behavior for CO and NO_x; that is, the amplitude of diurnal variation for these species is not as suppressed as it is at South Ramp.

6.2 Single Event Data

This section discusses results of summaries and statistical descriptions of all of the single event observations presently digitized for the computerized data base of the Dulles program (see Appendices A and C). There were three sets of CO measurements obtained during taxi operations and the set of NO_x measurements associated with takeoff operations. Specifically, these data sets are: (1) CO measurements with three ground-level sensors in the infield, aligned perpendicular to

710148
710145

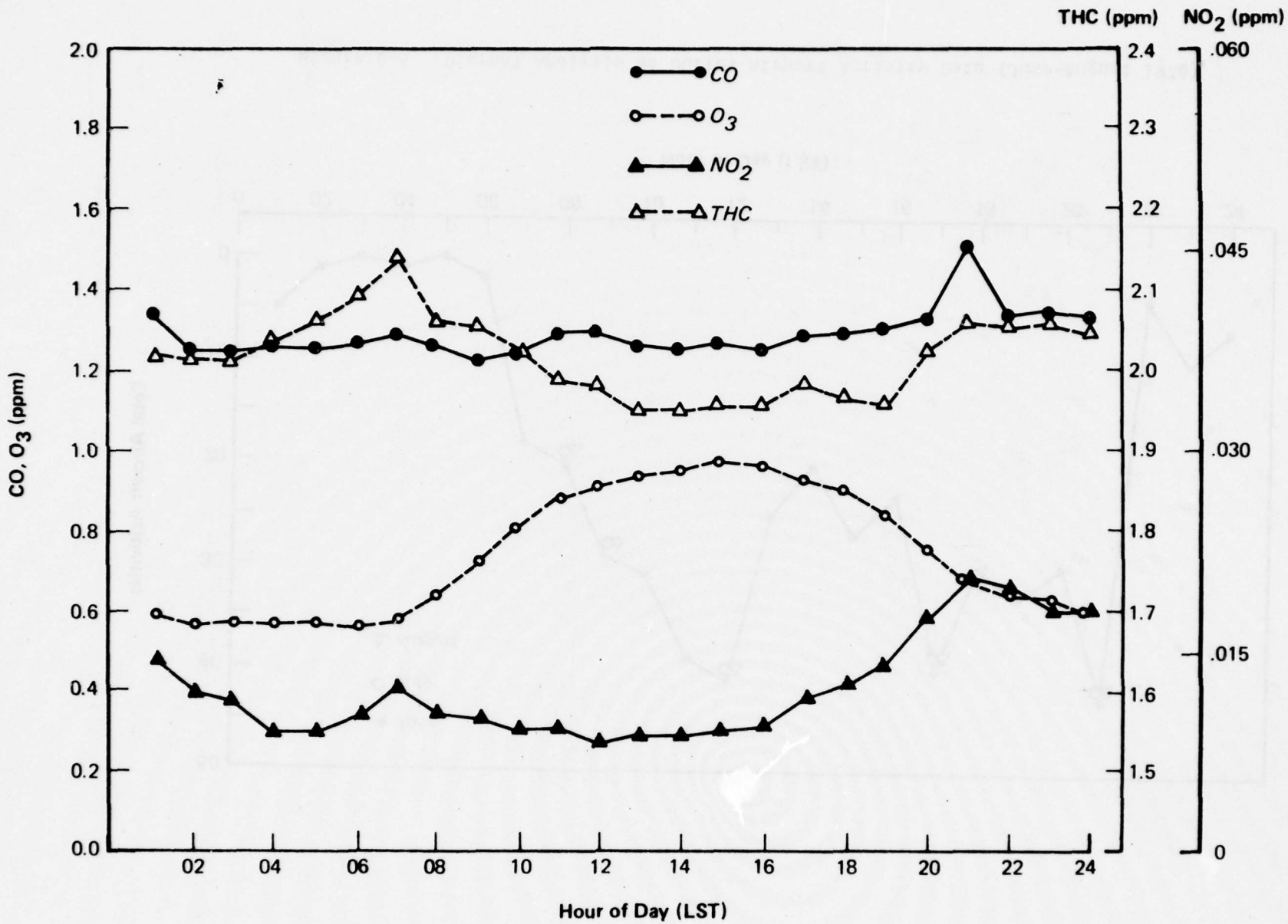

Figure 6-4 Diurnal Pollutant Analysis for South Ramp (June-September 1976)

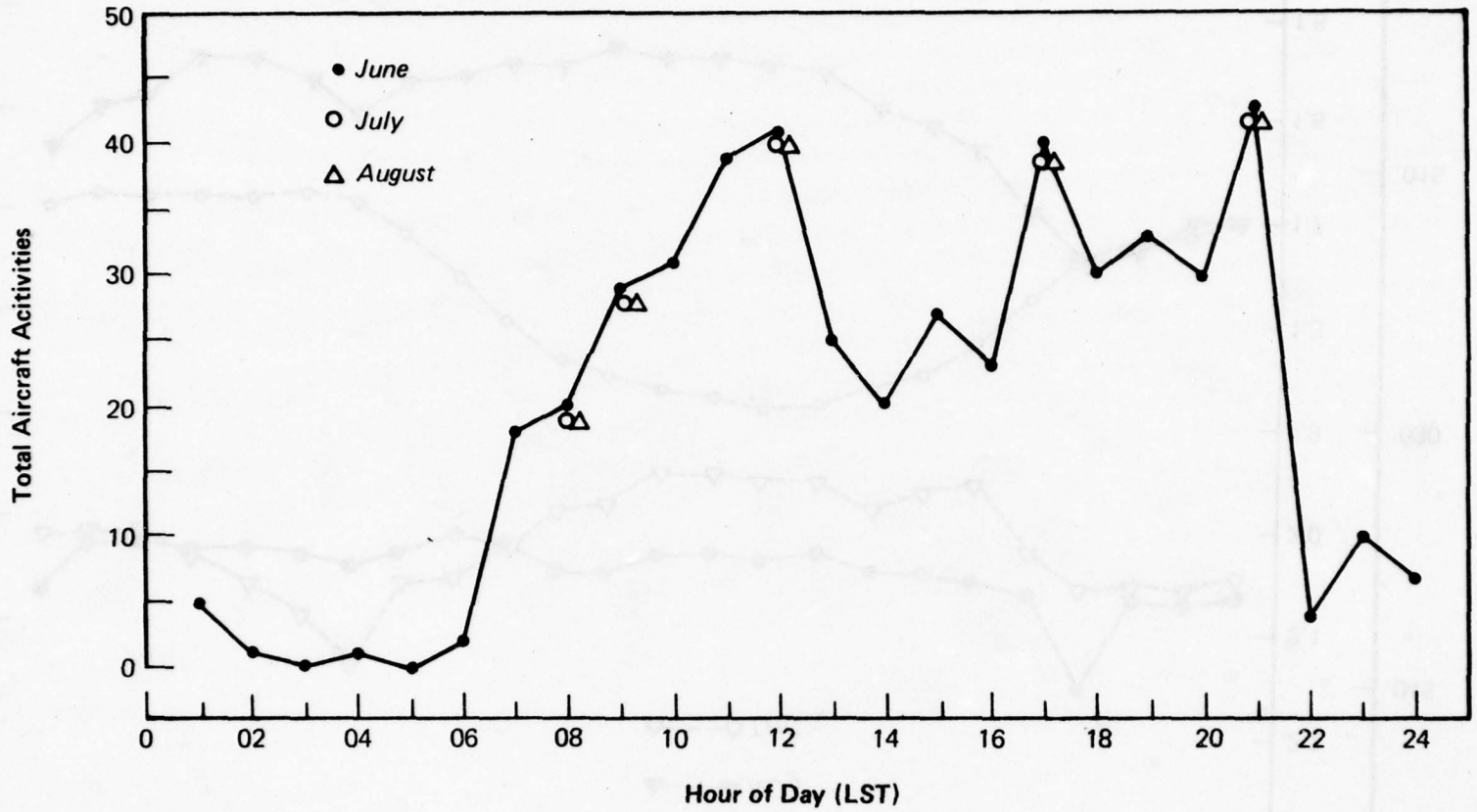

Figure 6-5 Diurnal Analysis of Dulles Airport Activity Data (June-August 1976)

the east-west taxiway at the northern edge of the jet ramp (called the "infield CO" set); (2) CO measurements at four levels on a single 58-ft tower and at two other 14-ft "surface" locations along a line perpendicular to the same east-west taxiway, but at the southern edge of the jet ramp (called the "one-tower CO" set); (3) CO measurements at five levels on two 82-ft towers and at a third distance at the "surface" level, with the same orientation as the single tower experiment (called the "two-tower CO" set) and (4) NO_x measurements at the surface level at three distances east of the north-south runways 19L and 1R (called the "NO_x takeoff" set). All sensor locations have been shown in Section 2.

Although Concorde observations are summarized below, the primary emphasis in defining interrelationships between pollutant concentrations and meteorological variables involved B707 or B727 events in the two-tower CO set because these were the greatest numbers of measurements in those two subsets. Thus, the particular correlation plots and tables and the multilinear regression results given in this section relate to these non-Concorde aircraft. But it was expected that the relations identified as most important for these two aircraft types would also be relevant for assessing transport and dispersion of exhaust emissions from the Concorde. After these preliminary analyses were completed, the results were applied to developing a parameterization model and a quasi-instantaneous transport model. These models were used to test predictions of Concorde influence on air quality against the measurement data obtained for Concorde operations.

6.2.1 Summaries

Tables 6-2 through 6-4 provide summaries of means and standard deviations for measured concentration, pulse duration, dose, wind speed and wind direction for all Concorde events. Summaries for all other aircraft types are presented in Appendix C. That appendix also contains a number of scatter plots showing the variation of peak CO concentrations versus wind direction, wind speed or turbulence level (σ_θ) for B707 and B727 aircraft. The large amount of scatter discourages attempts at

TABLE 6-2

STATISTICAL SUMMARY OF ONE TOWER CO TESTS FOR SST

		KEY		MEAN	S.D.	S.E. OF MEAN	SAMPLE	MAXIMUM	MINIMUM
		1	WS (mph)	13.33	6.32	2.10	9	21.00	2.00
		2	WD (deg)	315.99	16.58	5.52	9	346.00	302.00
Tower #1	56'	3	χ (ppm)	2.20	1.43	0.47	9	5.25	0.62
		4	Γ (sec)	36.00	6.00	2.00	9	48.00	30.00
	41'	5	χ	2.04	1.02	0.34	9	3.87	0.55
		6	Γ	38.66	7.41	2.47	9	54.00	30.00
	26'	7	χ	2.48	1.44	0.48	9	5.12	0.47
		8	Γ	38.00	5.19	1.73	9	48.00	30.00
	14'	9	χ	2.17	2.05	0.68	9	5.75	0.25
		10	Γ	44.66	13.45	4.48	9	72.00	30.00
Station	25	11	χ	0.26	0.36	0.16	5	0.75	0.00
		12	Γ	20.40	28.64	12.81	5	60.00	0.00
Station	26	13	χ	0.13	0.21	0.09	5	0.50	0.00
		14	Γ	31.20	42.93	19.20	5	84.00	0.00
Tower #1	56'	15	dose	75.48	40.44	13.48	9	157.50	22.50
	41'	16	dose	75.63	32.89	10.96	9	139.50	25.10
	26'	17	dose	91.55	49.91	16.63	9	184.50	19.95
	14'	18	dose	86.78	71.21	23.73	9	215.25	9.00
Station	25	19	dose	13.83	20.32	9.08	5	45.00	0.00
Station	26	20	dose	10.92	18.21	8.14	5	42.00	0.00

TABLE 6-3

STATISTICAL SUMMARY OF INFIELD CO TESTS FOR SST

	KEY	MEAN	S.D.	S.E. OF MEAN	SAMPLE	MAXIMUM	MINIMUM	RANGE
	u (mph)	25.00	36.32	14.83	6	99.00	7.00	92.00
	θ (deg)	202.00	23.61	10.55	5	230.00	165.00	65.00
Station #4	χ_1 (ppm)	5.41	2.04	0.83	6	7.60	1.90	5.70
	Γ_1 (sec)	21.00	4.69	1.91	6	30.00	16.00	14.00
Station #5	χ_2 (ppm)	1.96	1.14	0.46	6	3.50	0.90	2.60
	Γ_2 (sec)	35.83	20.83	8.50	6	65.00	10.00	55.00
Station #11	χ_3 (ppm)	1.43	1.15	0.66	3	2.50	0.20	2.30
	Γ_3 (sec)	22.50	10.60	7.50	2	30.00	15.00	15.00
Station #4	$Dose_1$ (ppm-sec)	106.83	31.67	12.93	6	152.00	57.00	95.00
Station #5	$Dose_2$ (ppm-sec)	52.50	16.30	6.65	6	80.00	32.00	48.00
Station #11	$Dose_3$ (ppm-sec)	25.50	31.81	22.50	2	48.00	3.00	45.00

TABLE 6-4

STATISTICAL SUMMARY OF TAKEOFF NO_x TESTS FOR SST

	KEY	MEAN	S.D.	S.E. OF MEAN	SAMPLE	MAXIMUM	MINIMUM	RANGE
	u (mph)	9.00	4.24	3.00	2	12.00	6.00	6.00
	θ (deg)	235.00	35.35	25.00	2	260.00	210.00	50.00
Station #4	χ_1 (ppm)	0.52	0.02	0.02	2	0.54	0.50	0.04
	Γ_1 (sec)	17.50	3.53	2.50	2	20.00	15.00	5.00
Station #5	χ_2 (ppm)	0.39	0.31	0.22	2	0.61	0.17	0.44
	Γ_2 (sec)	22.50	3.53	2.50	2	25.00	20.00	5.00
Station #11	χ_3 (ppm)	0.01	0.00	0.00	2	0.02	0.01	0.00
	Γ_3 (sec)	22.50	3.53	2.50	2	25.00	20.00	5.00
Station #4	$Dose_1$ (ppm-sec)	9.15	2.33	1.65	2	10.80	7.50	3.30
Station #5	$Dose_2$ (ppm-sec)	8.22	5.62	3.97	2	12.20	4.25	7.95
Station #11	$Dose_3$ (ppm-sec)	0.40	0.14	0.10	2	0.50	0.30	0.20

trend analysis for Concorde events until a larger number of tests becomes available. Appendix C comparisons indicate that maximum peak concentrations at the first tower are associated with wind directions that are within ± 45° of wind normal to the taxiway or runway.

For Concorde events, Tables 6-5 through 6-8 outline the average profile of measured concentrations and doses for various heights and distances for all four data sets. The surface level (i.e., 14 ft) concentrations and doses presented in these tables are plotted against the mean values for all other major aircraft types in Figures 6-6 through 6-9. Each pair of figures represents a separate set of tests.

6.2.2 Correlations

Table 6-9 provides correlation coefficients for a variety of variables from the two-tower experiment for B707 and B727 aircraft. By definition, these correlation coefficients can range from +1.00 or "perfectly correlated," to -1.00, a "perfect negative correlation," through zero which indicates no correlation or relationship between the two variables.

However, it is quite possible that entirely random variations between two variables can lead to seemingly important differences in coefficients. Thus, for a data set of 31 to 34 cases (the number of B707 and B727 two-tower events, respectively), there is a high probability that the correlation between two variables is "real" (and not induced by random errors) only if the correlation is greater than about 0.30. Of the two-tower data, only the B707 and B727 data sets are large enough to support correlation coefficient analysis. For small samples, threshold values for meaningful correlations are so large that it is very doubtful that real correlations can be found. Therefore, the purpose of this section is to analyze the important parameters for dispersion of pollutants from B707s and B727s and assume that the relationships identified here generalize to all aircraft types, including the Concorde.

An example of random errors leading to correlation coefficients near this threshold value is the correlation between the aircraft taxi speed, s, and the meteorological variables wind speed u, wind azimuth θ,

TABLE 6-5

AVERAGED THC PEAK CONCENTRATIONS AND DOSES

MEASURED AT 14 FT ON FIRST TOWER*

Aircraft Type	Sample Size	Average Peak Concentration (ppm)	Average Dose (ppm-sec)
Concorde	1	0.49	14.0
B-727	34	0.11	2.5
B-747	3	0.95	22.7
B-707	31	1.00	33.5
DC-8	5	1.82	32.0

*THC was only measured (at this 215 ft distance) after February 1, 1977.

TABLE 6-6a

CONCORDE PEAK INSTANTANEOUS CO CONCENTRATION (PPM)
VERSUS HEIGHT AND DISTANCE:
ONE- AND TWO-TOWER DATA (10 EVENTS)

	Distance from Source (ft)		
Height (ft)	215	379	543
80	2.50*	0.55*	-
56	2.21	0.79*	-
41	2.04	0.76*	-
26	2.48	0.80*	-
14	2.17	0.27	0.14

*From the single two-tower Concorde event measured.

TABLE 6-6b

CONCORDE CO DOSE (PPM-SEC) VERSUS HEIGHT AND DISTANCE:
ONE- AND TWO-TOWER DATA (10 EVENTS)

	Distance from Source (ft)		
Height (ft)	215	379	543
80	69.0*	24.7*	-
56	75.5	29.2*	-
41	75.6	27.4*	-
26	91.6	79.0*	-
14	86.8	13.8	10.9

*From the single two-tower Concorde event measured.

TABLE 6-7

CONCORDE PEAK INSTANTANEOUS CO CONCENTRATION (PPM), AND DOSE (PPM-SEC), VERSUS DISTANCE: INFIELD DATA

	Distance from Source (ft)		
	190	480	680
CO Peak Concentration (ppm)	5.9	2.0	1.4
CO Dose (ppm-sec)	105	48	28

TABLE 6-8

CONCORDE PEAK INSTANTANEOUS NO_x CONCENTRATION (PPM), AND DOSE (PPM-SEC), VERSUS DISTANCE: TAKEOFF DATA

	Distance from Source (ft)		
	450	635	920
NO_x Peak Concentration (ppm)	0.58	0.32	0.21
NO_x Dose (ppm-sec)	15.1	4.3	1.5

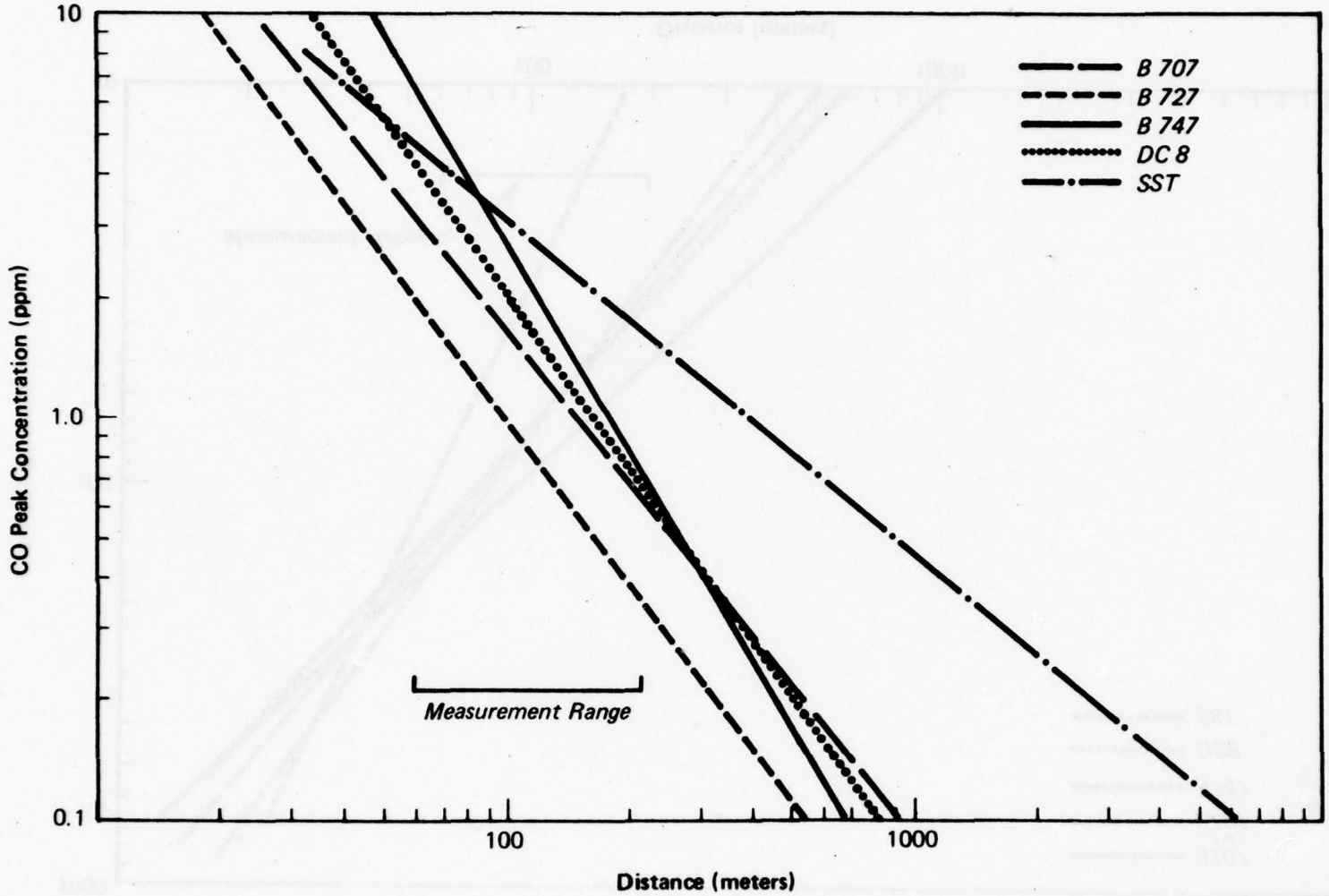

Figure 6-6a CO Concentration (14ft) Vs. Distance: Infield Data (May-September 1976)

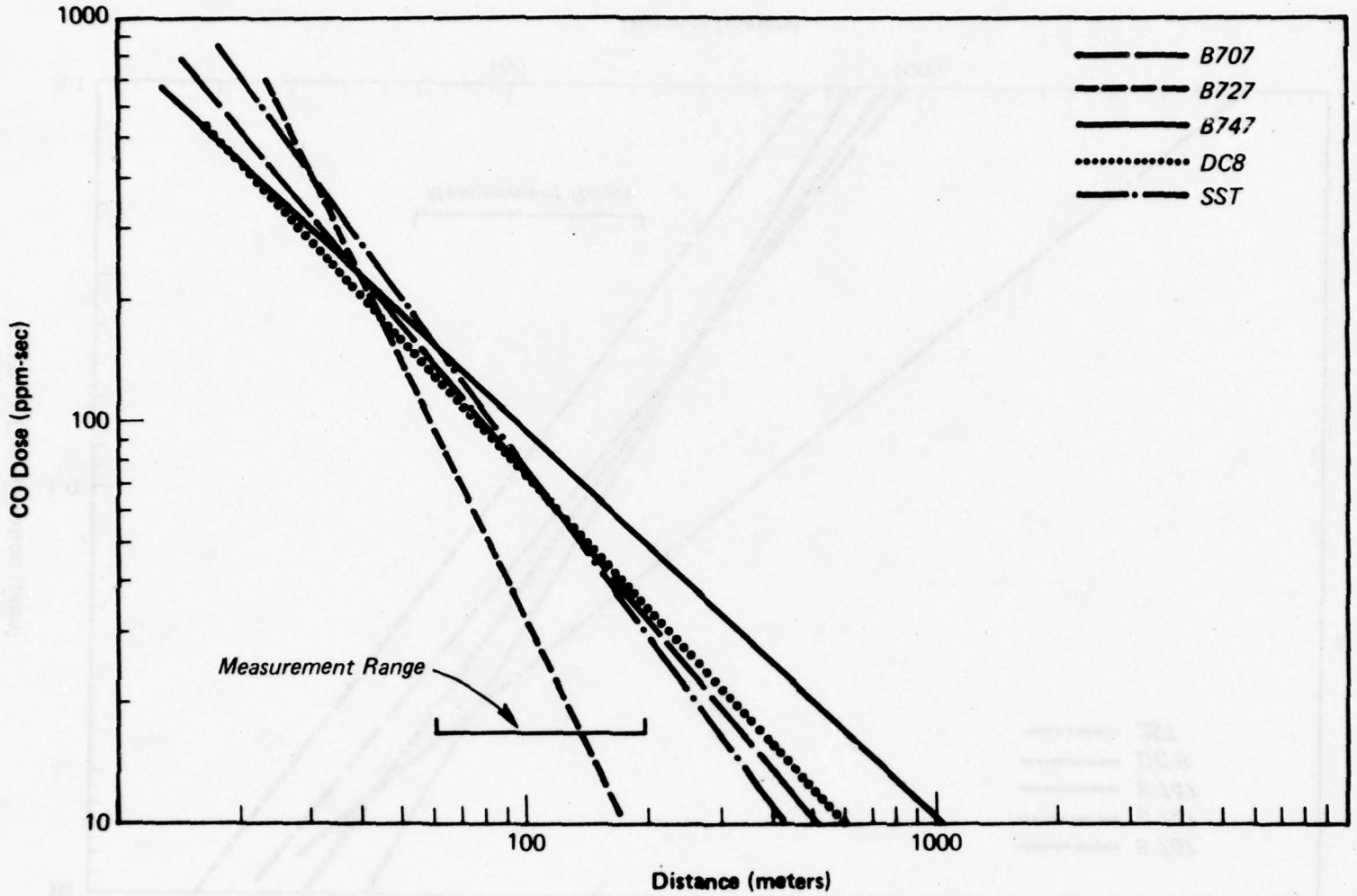

Figure 6-6b CO Dose (14ft) Vs. Distance: Infield Data (May-September 1976)

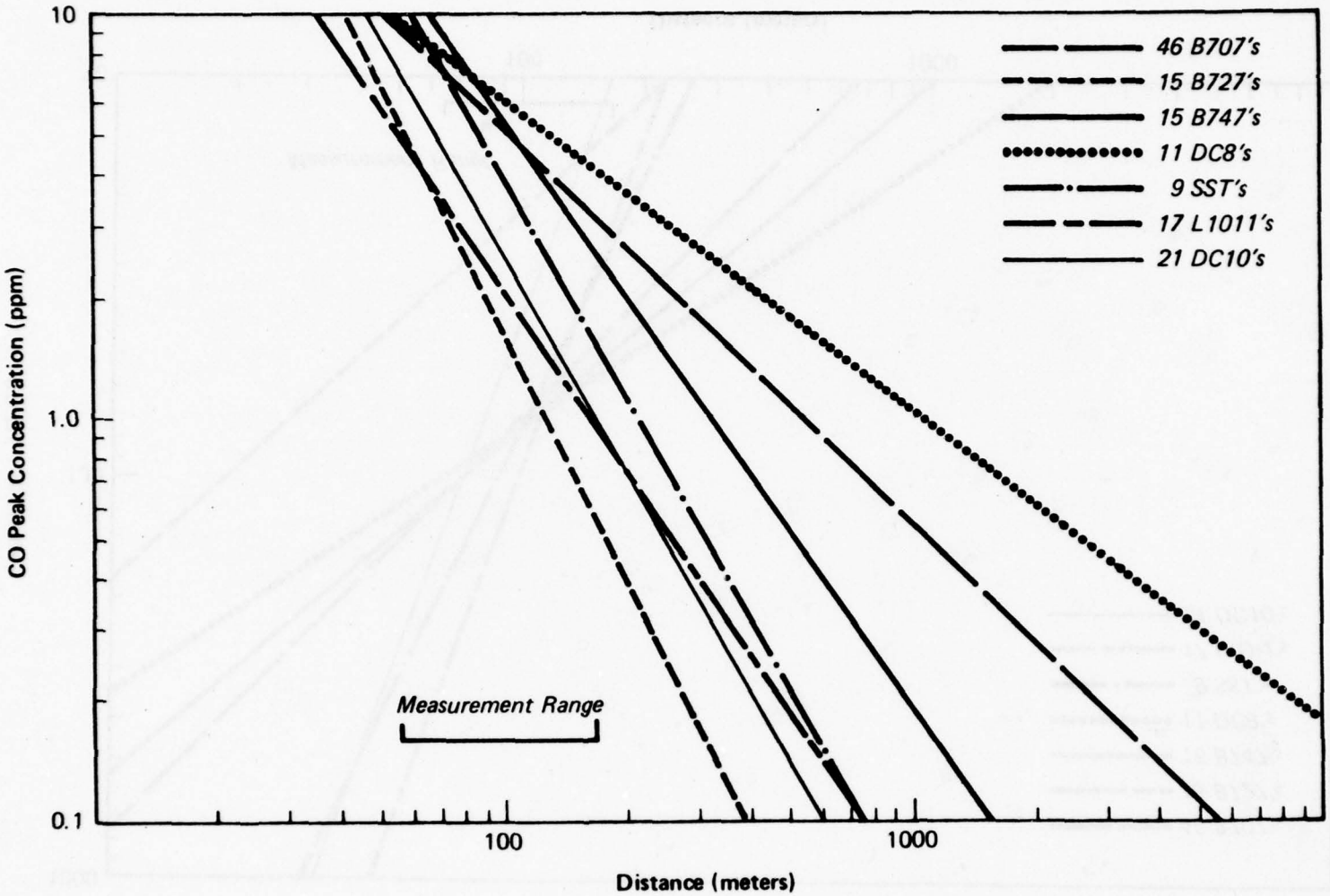

Figure 6-7a CO Concentration (14 ft) Vs. Distance: One Tower Data (November 1976)

710245

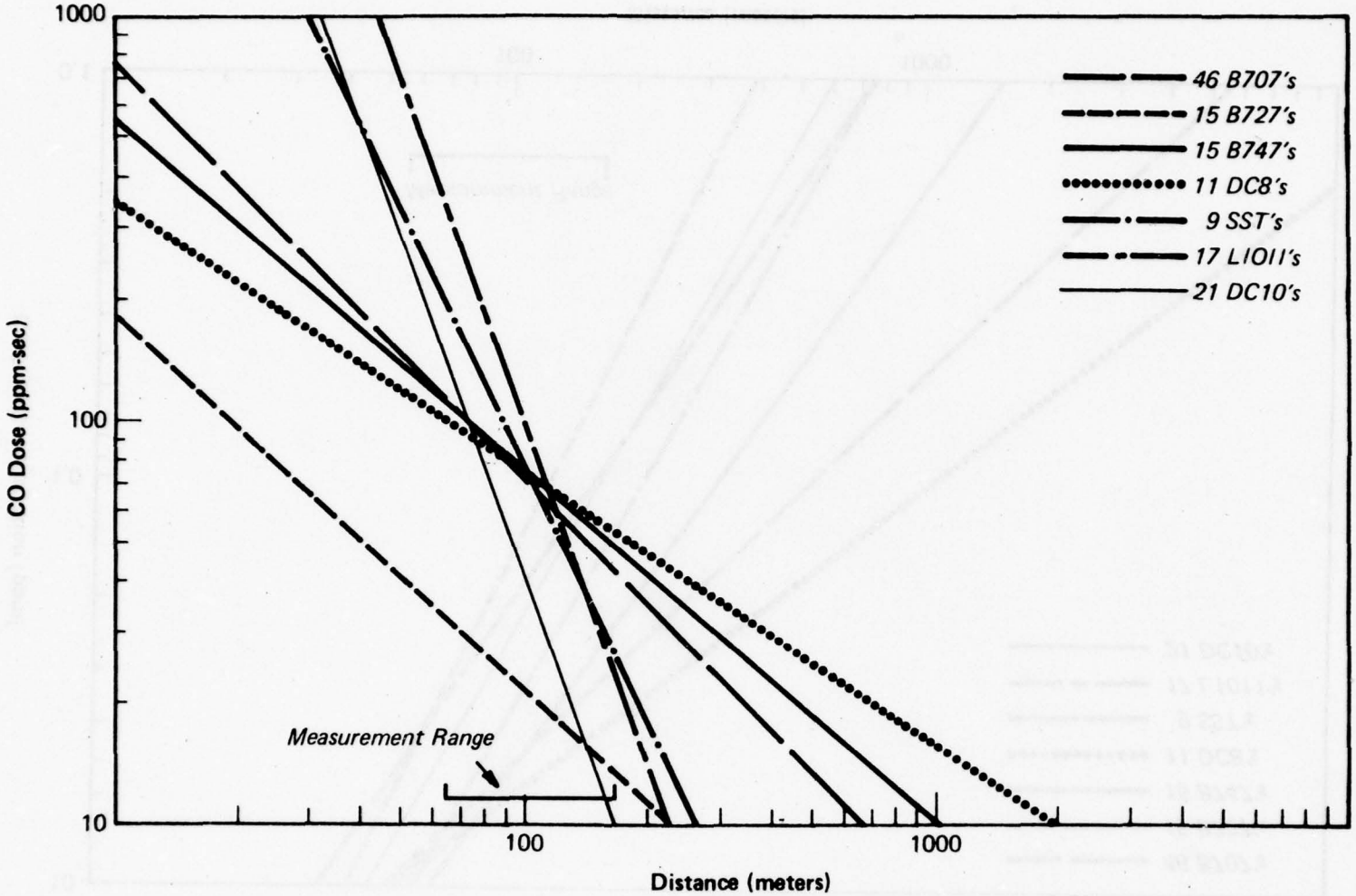

Figure 6-7b CO Dose (14 ft) Vs. Distance: One Tower Data (November 1976)

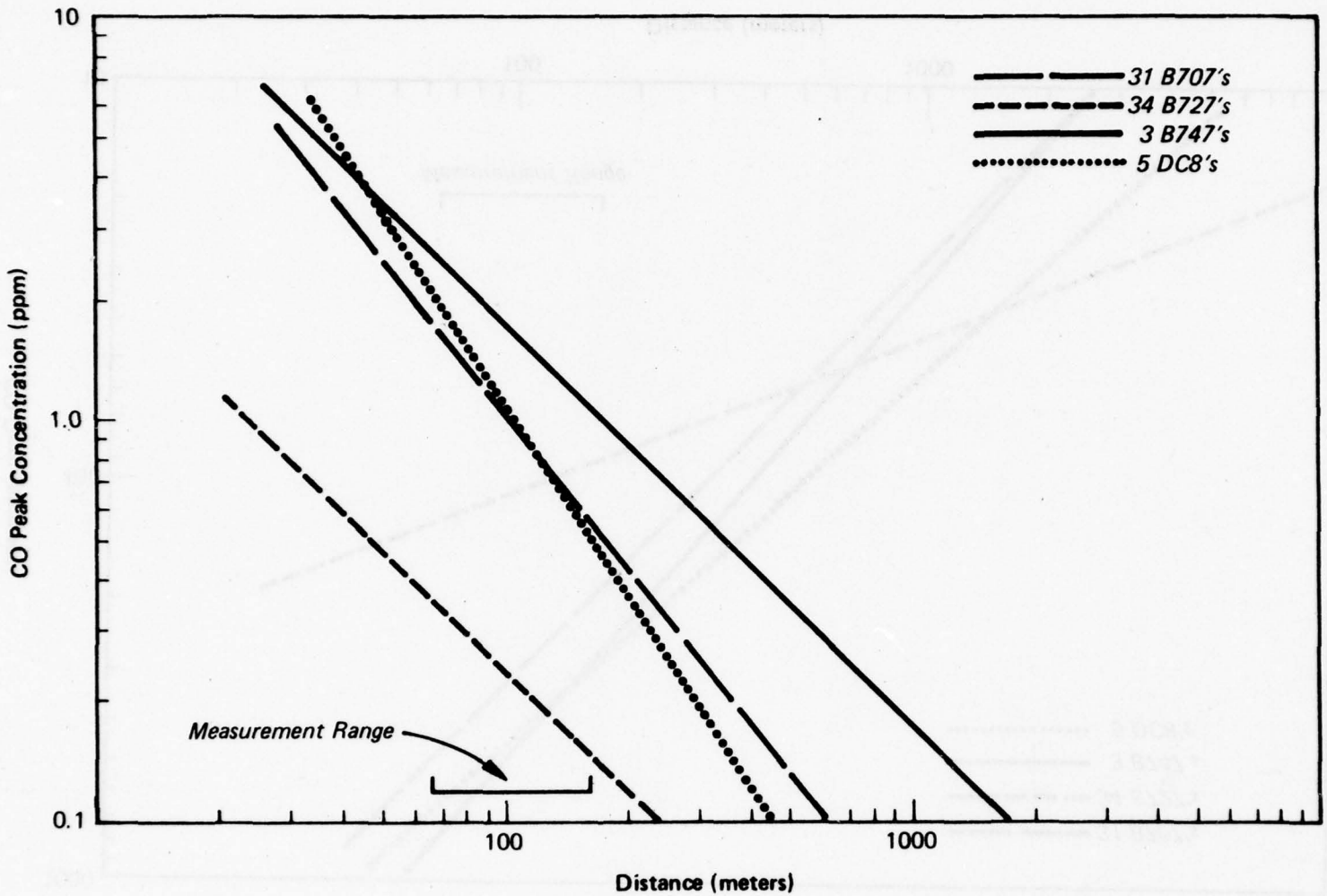

Figure 6-8a CO Concentration (14 ft) Vs. Distance: Two Tower Data (February-March 1977)

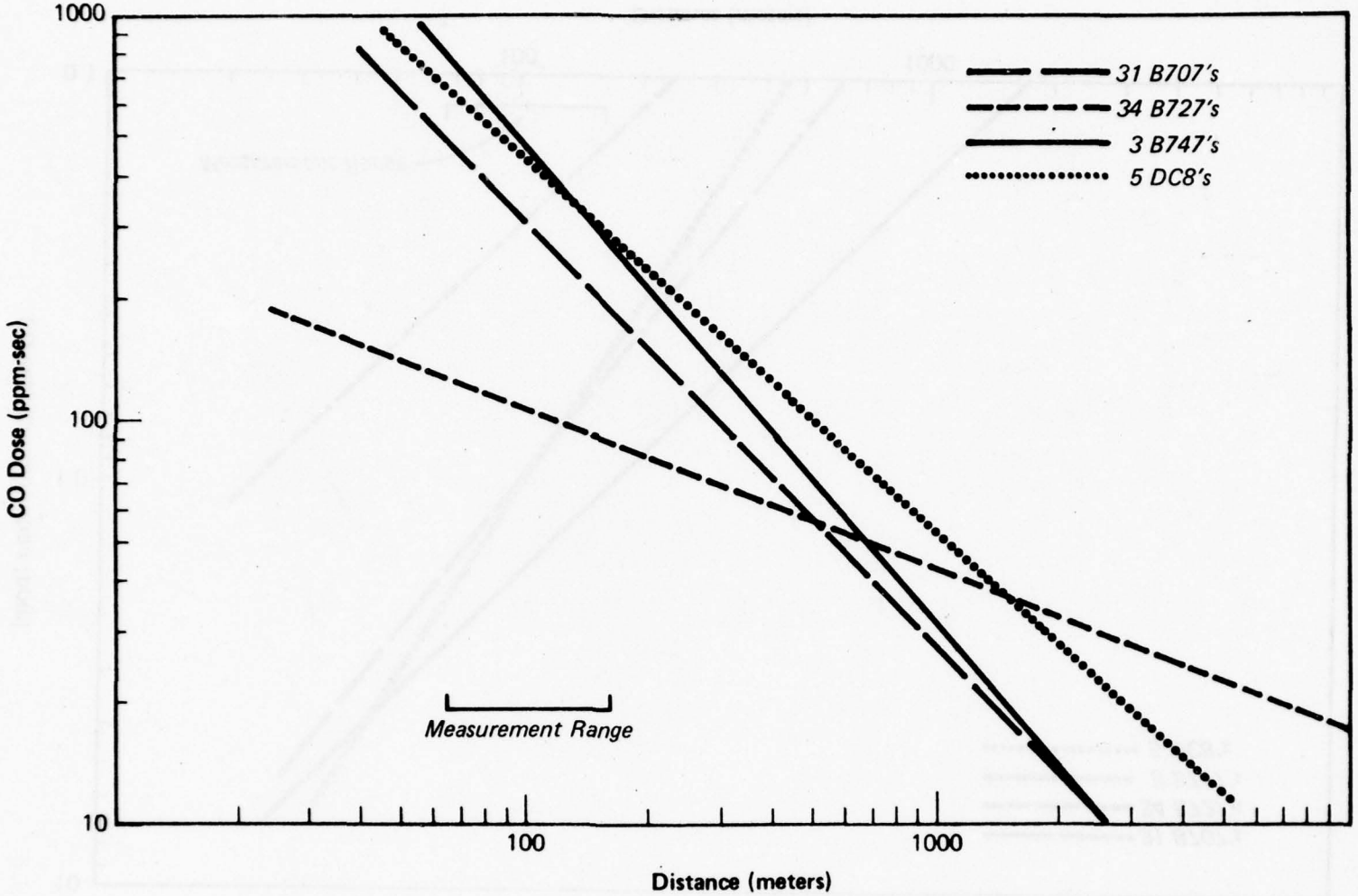

Figure 6-8b CO Dose (14 ft) Vs. Distance: Two Tower Data (February-March 1977)

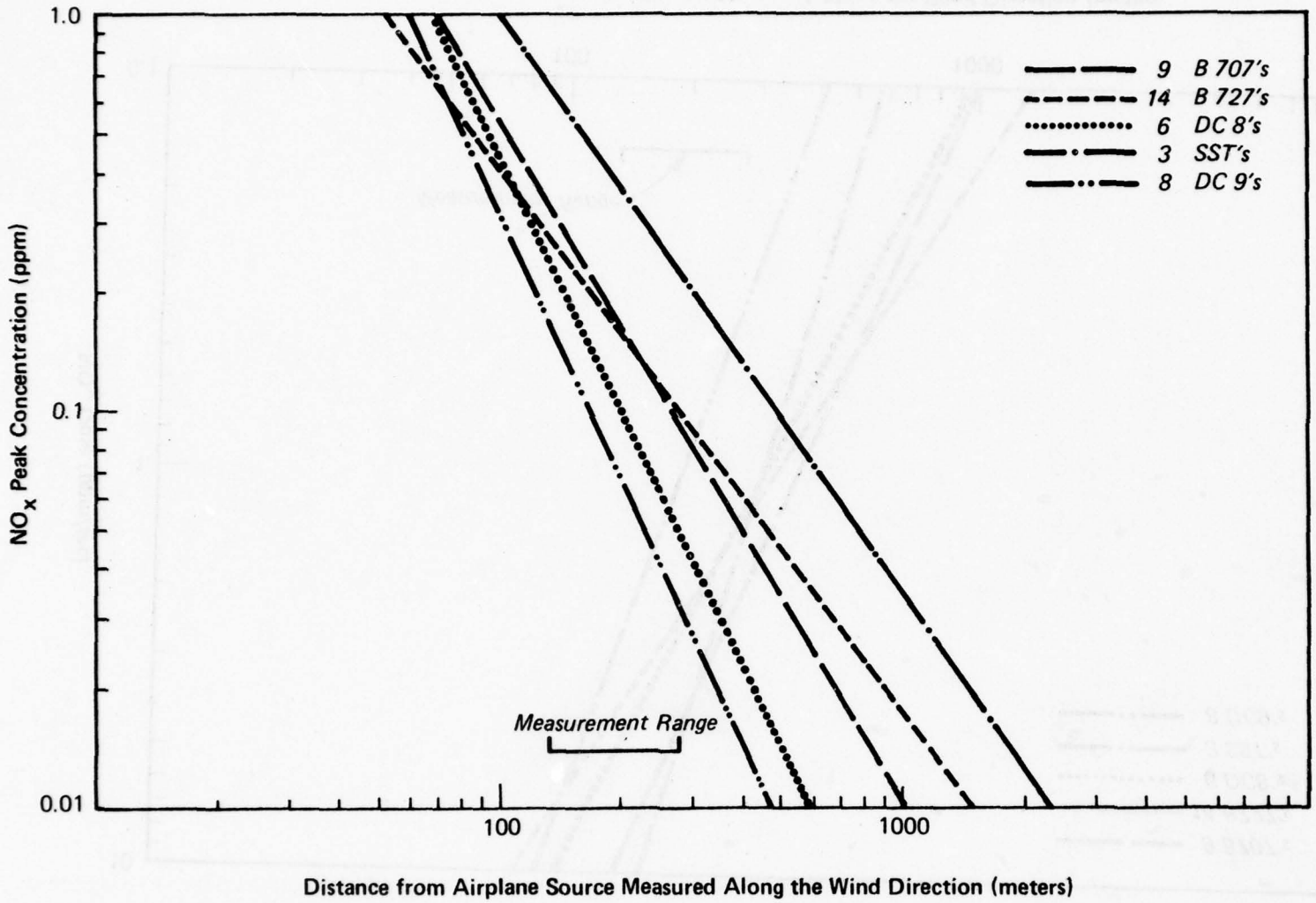

Figure 6-9a NO_x Measured Concentration (14 ft) Vs. Distance : End of Runway During Takeoff

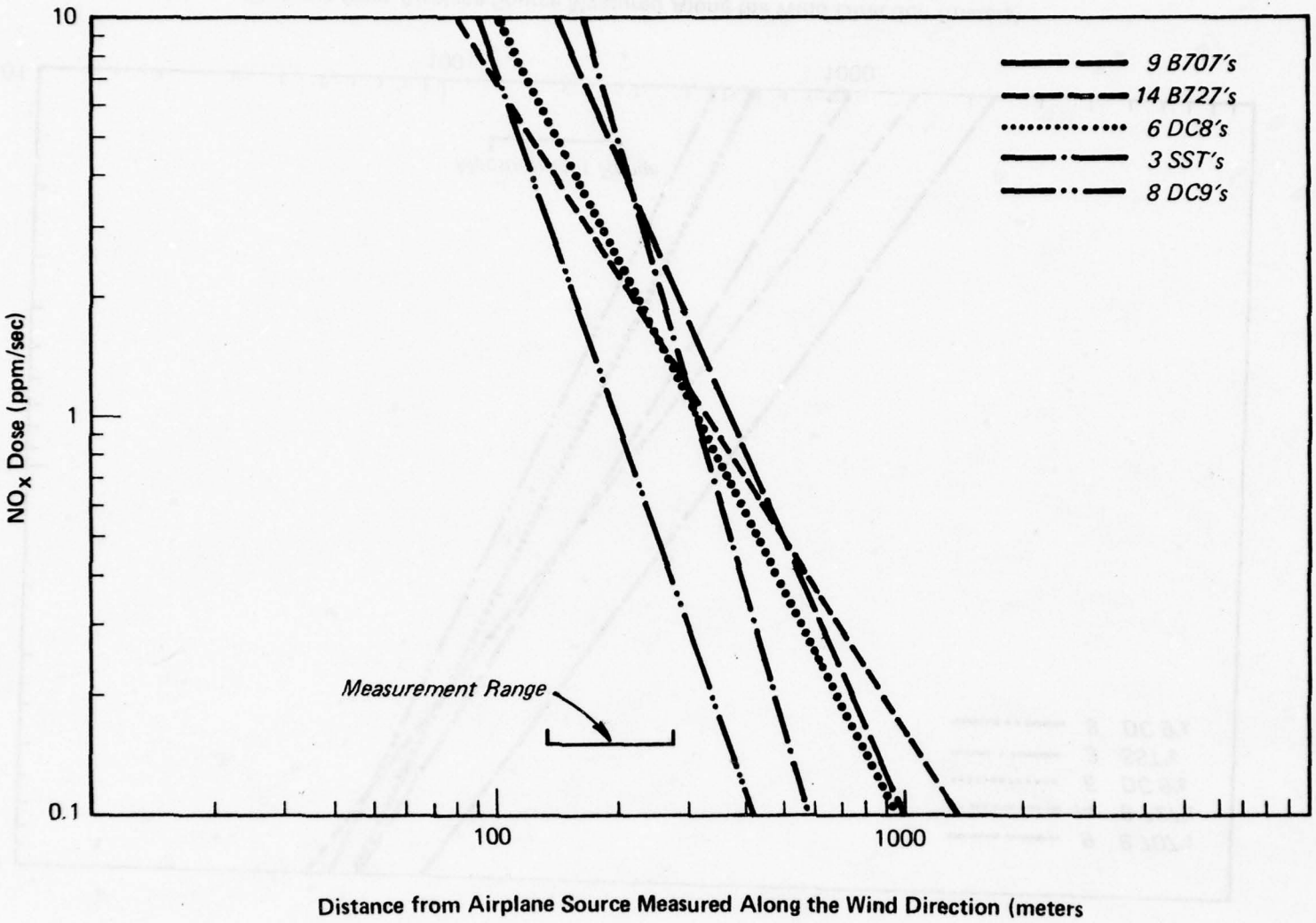

Figure 6-9b NO_x Measured Dose (14 ft) Vs. Distance: End of Runway

azimuthal turbulence parameter σ_θ, longitudinal turbulence parameter σ_u, lateral turbulence parameter σ_v, and longitudinal turbulence intensity σ_u/u. One would not normally expect that aircraft taxi speed would be strongly related to a wind or turbulence variable.

In the correlation table (Table 6-9), correlations are given at four different sensor locations for concentration (χ), pulse duration (Γ), and dose vs. several different variables. The most complete portion of the table is that for the sensor at 14 ft on the first tower, where correlation coefficients for "hybrid" variables (e.g., σ_u/u) are also given. Intercorrelations between wind and turbulence-related variables are also given for this 14 ft first tower sensor.

In general, due to the large variability within the measurement set, correlations are quite low. Only naturally related variables (such as χ vs. dose, and σ_u/u vs. u) show very high correlations. However, when the correlations were analyzed in greater detail, significant relationships were revealed. Table 6-10 provides an example. Here, χ, dose and Γ vs. wind vector and turbulence data variables are blocked together to illustrate the change in the correlation coefficient with sensor height. For χ and dose, a significant reversal is seen in the correlation coefficients with height. That is, the variables χ and u are positively correlated at low levels and negatively correlated at high levels. The change in the correlation coefficient with height (-0.74 for the B707) is statistically significant. Evidently, with high wind speeds, the CO impact is greater near the ground, and vice versa. This suggests, as theory would indicate, that plume rise increases with decreasing wind speed. The comparative change in the correlation coefficient with height for σ_θ indicates that increased turbulence and mixing decrease concentrations and doses near the ground, and increase them at higher levels as the pollutant plume material is mixed upwards.

6.2.3 Multilinear Regressions

Multilinear regression, another useful tool for extracting relationships between variables, can identify how one variable (χ, for example) is related to a combination of variables (such as wind speed and wind direction). For relatively reliable results, the number of cases examined should be several times the number of variables examined.

TABLE 6-9

RESULTS OF LINEAR CORRELATION ANALYSIS FOR SINGLE EVENT MEASUREMENTS
Correlation Coefficients for B-707 Aircraft

	χ (ppm)		Pulse Duration (sec)		Dose (ppm-sec)		s (m/s)		u (m/s)		θ (deg)		σ_θ		σ_u		σ_v		σ_u/u		s+ usin θ		ucos θ		Pasquill Stability	
14' 1st Tower	707	727	707	727	707	727	707	727	707	727	707	727	707	727	707	727	707	727	707	727	707	727	707	727	707	727
χ			-.33	-.05	.81	.63	.04	-.02	.30	.23	.31	.32	-.24	-.03	.14	.26	.13	.23	-.44	-.07	-.14	-.01	.09	-.07	0.40	.08
pulse duration					.14	.60	-.34	.50	.36	-.17	-.02	.03	.14	-.08	-.41	-.24	-.34	-.22	-.01	-.11	-.22	.27	-.01	.11	-.17	.01
dose							-.06	.37	.09	.02	.31	.18	-.18	-.09	-.07	.03	-.13	.04	-.40	-.07	-.06	.30	0	.15	.21	.04
s									-.24	-.10	.29	.05	.21	-.29	-.10	-.27	-.14	-.31	.53	-.20	.31	.48	.09	.13	.08	.04
u											-.37	.13	-.50	-.22	-.78	.49	.53	.40	-.47	-.37	.22	.16	.06	.09	.63	.62
θ													.35	-.73	-.52	-.38	-.11	-.44	.07	-.57	-.08	-.06	.06	.13	.04	.29
σ_θ															-.37	.44	.27	.72	.32	.66	-.02	-.15	-.03	-.17	.65	-.18
σ_u																	.58	.69	.06	.58	.30	-.12	.10	-.12	.38	.24
σ_v																			-.11	.33	.03	-.12	.09	-.11	.07	.25
σ_u/u																					.17	-.23	.07	-.15	-.45	-.32
s+ usin θ																							.06	.35	0	.03
ucos θ																									.04	.13
Pasquill Stability																										
41' 1st Tower																										
χ			-.09	.14	.77	.78	-.10	.07	-.14	.03	.22	.21	.07	.01	-.21	.35	.04	.15							0	0
pulse duration					.40	.65	-.12	.06	-.28	-.15	.19	-.02	.13	.07	-.31	-.15	-.27	-.01							-.26	-.52
dose							-.19	.08	-.38	-.04	.20	.14	.21	.04	-.42	.12	-.17	.11							-.22	-.29
41' 2nd Tower																										
χ			-.35	.31	.87	.60	-.10	.36	-.04	-.01	.28	.22	-.19	-.10	-.11	-.15	0	-.03							.21	.03
pulse duration					-.11	.87	.31	.23	-.23	.12	.13	.22	.03	.12	-.26	-.13	-.33	-.03							-.24	.01
dose							-.04	.45	-.19	.62	.16	-.20	-.19	-.12	-.37	-.21	-.31	-.07							.15	.01
80' 1st Tower																										
χ			.65	.48	.93	.92	.04	-.14	-.44	-.38	-.15	-.17	.43	-.06	-.41	-.23	-.19	-.27							-.45	-.38
pulse duration							-.34	.24	-.53	-.44	.09	-.10	.29	-.09	-.47	-.53	-.34	-.34							-.62	-.52
dose							-.06	.18	-.47	-.40	-.06	-.14	.40	-.04	.43	-.34	-.21	-.26							-.48	-.49

TABLE 6-10

CORRELATIONS BETWEEN CO CONCENTRATION AND WIND SPEED AND TURBULENCE

X	u				σ_θ			
	14 ft	41 ft	80 ft	$\Delta\gamma$*	14 ft	41 ft	80 ft	$\Delta\gamma$*
Peak Concentration:								
B707	0.30	-0.14	-0.44	-0.74	-0.24	0.07	0.43	+0.67
B727	0.23	0.03	-0.38	-0.61	-0.03**	+0.01**	-0.06**	-
Pulse Duration:								
B707	-0.36	0.28	0.53	-	0.14	0.13	0.29	-
B727	-0.17	-0.15	-0.44	-	-0.08**	0.07**	-0.09*	-
Dose:								
B707	0.09	-0.38	-0.47	-0.56	-0.18	0.21	0.40	-0.58
B727	0.02	-0.04	-0.40	-0.42	-0.09	0.04	-0.04	-

*Change in correlation coefficient between 14 ft and 80 ft level $\Delta\gamma$, not given if value is less than 0.30.

**Could be highly influenced by one anomalous value.

For the two-tower B707 and B727 data sets, multilinear regression was carried out for the concentration, χ, at 14 ft on the first tower. Table 6-11 illustrates the results of this regression for both aircraft types. Here, the variable that explains the greatest part of the variance in χ is entered first in the regression, followed by the variable that explains the greatest part of the remaining variance, and so on.

For a particular set of variables, the fit of the regression is optimized when the standard error reaches a minimum value. The correlation coefficient, R, may improve slightly for the addition of extra variables in the regression, but the fit ceases to improve. It is seen that the turbulent mixing parameter, σ_u/u, is influential in determining the value of χ at 14 ft on the first tower for both aircraft types.

Several different methods can be employed in order to arrive at a better multilinear regression than that in Table 6-11. For example, a "hybrid" variable, such as

$$1 + \left(\frac{s + u \sin\theta}{u \cos \theta}\right)^2$$

may be important in a regression fit since it theoretically describes the speed with which an emitted puff would reach a sensor (see Section 7, Figure 7-2). For the current set of experiments, the aircraft direction was essentially constant and thus the effect of reversing the sign of s was not explored. Since the dependent variable is assumed to be normally distributed and χ cannot be less than zero, the distribution of χ, constrained by this boundary is likely not to be normal, but a logarithmic transformation of this variable may be nearly normal. This type of transformation of the dependent variable is also often effective in reducing the overall variance or improving a regression.

Table 6-12 illustrates the results of a multilinear regression of the natural log of χ, considering the variables:

$$\sqrt{1 + \left(\frac{s + u \sin\theta}{u \cos\theta}\right)^2}$$

pulse duration, $s + u \sin\theta/u \cos\theta$, σ, u, σ_θ, σ_u, σ_v, σ_u/u, Pasquill-Turner stability, $u \cos\theta$, $u \sin\theta$, $s + u \sin\theta$ and s. Again, variables

TABLE 6-11

STEPWISE MULTILINEAR REGRESSION SCREENING

RESULTS FOR PEAK CO CONCENTRATIONS*

B707				B727			
Order	Dependent Variable	$R_{cum.}$**	S.E.***	Order	Dependent Variable	$R_{cum.}$**	S.E.***
1	σ_u/u	0.44	1.098	1	θ_2	0.31	0.307
2	T_p	0.55	1.037	2	σ_u	0.37	0.305
3	P-T	0.58	1.034	3	σ_u/u	0.41	0.304
				4	u	0.53	0.288
No. of Cases = 31				No. of Cases = 34			

*For 14 ft level on first tower

**$R_{cum.}$ = Cumulative correlation coefficient with variable added to stepwise multilinear regression.

***S.E. = Standard error in predicted CO conccentration at first tower distance.

TABLE 6-12

STEPWISE MULTILINEAR REGRESSION RESULTS FOR THE LOGARITHM OF PEAK CO CONCENTRATIONS (LN_χ)

	B707			B727		
Order	Dependent Variable	$R_{cum.}$	S.E.	Dependent Variable	$R_{cum.}$	S.E.
1	$\sqrt{1+\left(\frac{s+u\ \sin\theta}{u\ \cos\theta}\right)^2}$	0.53	1.028	$u\ \cos\theta$	0.20	2.418
2	Pulse Duration	0.68	0.900	σ_v	0.261	2.424
3	$\frac{s+u\ \sin\theta}{u\ \cos\theta}$	0.71	0.879	σ_u	0.371	2.367
4	θ_2	0.76	0.831	s	0.42	2.356
5	σ_θ	0.79	0.804			
6	σ_u/u	0.81	0.788			
7	$u\ \cos\theta$	0.82	0.775			
No. of cases = 31				No. of cases = 34		

added to the regression after the minimum standard error is attained are not included in the table. There is a marked improvement in the regression fit for the B707 data set, although a slight decrease in the fit for the B727s. Evidently, the latter measured values are so close to background pollutant levels, or so near the threshold of sensor response (see Section 4.3) that much of the variation in the B727 data set is due to random errors. (It should also be noted from Table 6-9, that the correlation coefficients generated for the B727 data set are in general lower than those for the B707 data set.)

The relative success of the regression fit for B707s encouraged the development of a new quasi-instantaneous concentration model to be used in predicting aircraft emissions impact. The importance of the travel-time related parameters and turbulence mixing parameters suggested that a quasi-instantaneous Gaussian plume model would be most sensitive to physical details of release geometry and ambient meteorology. Therefore, this type of model was developed to evaluate the assumptions about initial plume geometry used in more complex transport models. Comparison of measured concentrations with those predicted by both simple and complex models is presented in Section 8.2.

6.2.4 Dose Versus Emission Index

It was important in assessment of the potential impact and/or area of influence of the Concorde to substantiate the Concorde pollutant emission factor, as tabulated in the Concorde Environmental Impact Statement final report. The measured pollutant data from the one- and two-tower experiments have been plotted as estimated dose vs. emission rate for each aircraft type monitored in the experiment. The dose (measured peak height times the pulse duration between half-peak heights) is a measure of the total mass distributed in the aircraft emission plume. If other factors are equal (e.g. vertical dispersion, plume rise, aircraft speed, initial wake dispersion), the measured dose is expected to be linearly proportional to the aircraft emission rate.

Figures 6-10 through 6-12 depict CO dose vs. emission rates for sensor locations at 14-ft and three different downwind distances. It is evident that, although the dose does increase with increasing emission rate up to the B707 and DC8 rates of 54.9 g/sec, the dose from Concorde is far below the increase one would expect for a nearly three-fold increase in emission rate above the B707 emission factor (as given by the FEIS values). This comparison for the surface sensors was also supported by a similar comparison shown in Figure 6-13 for an average of doses at all sensor levels (representing an average plume concentration). In fact, the measured Concorde dose for the composite set of ten one- and two-tower events is about the same as that for the B707, DC8 and B747 events. One possible explanation of this discrepancy is that the published Concorde emission factor is overestimated by a factor of three. However, there are at least two other explanations. The Concorde plume rise may be greater than that for other aircraft so that only a portion of the plume would be detected by a low level sensor. The wake induced by the Concorde as it taxies may also be larger than that for other aircraft, producing significantly more mixing in the vertical. This could result in somewhat lower measured surface level doses than those otherwise expected.

6.2.5 Turbulence Measurements

To determine the appropriate dispersion rates for use in single event transport models, effective jet plume geometries and local turbulence fields were examined. The major factor determining the effective height of jet exhaust plumes is the plume rise, which is related to the magnitude of the exhaust temperature and the exit velocity. The initial distribution of the exhaust is determined by the engine geometry. It is possible that the aerodynamic wake of the aircraft also influences this distribution. However, the turbulence directly measurable at Dulles was primarily that of the ambient atmosphere.

During the dual-tower test series, the reduction of the wind data included the determination of the cross-wind and the along-wind components of turbulence intensity according to a method suggested by

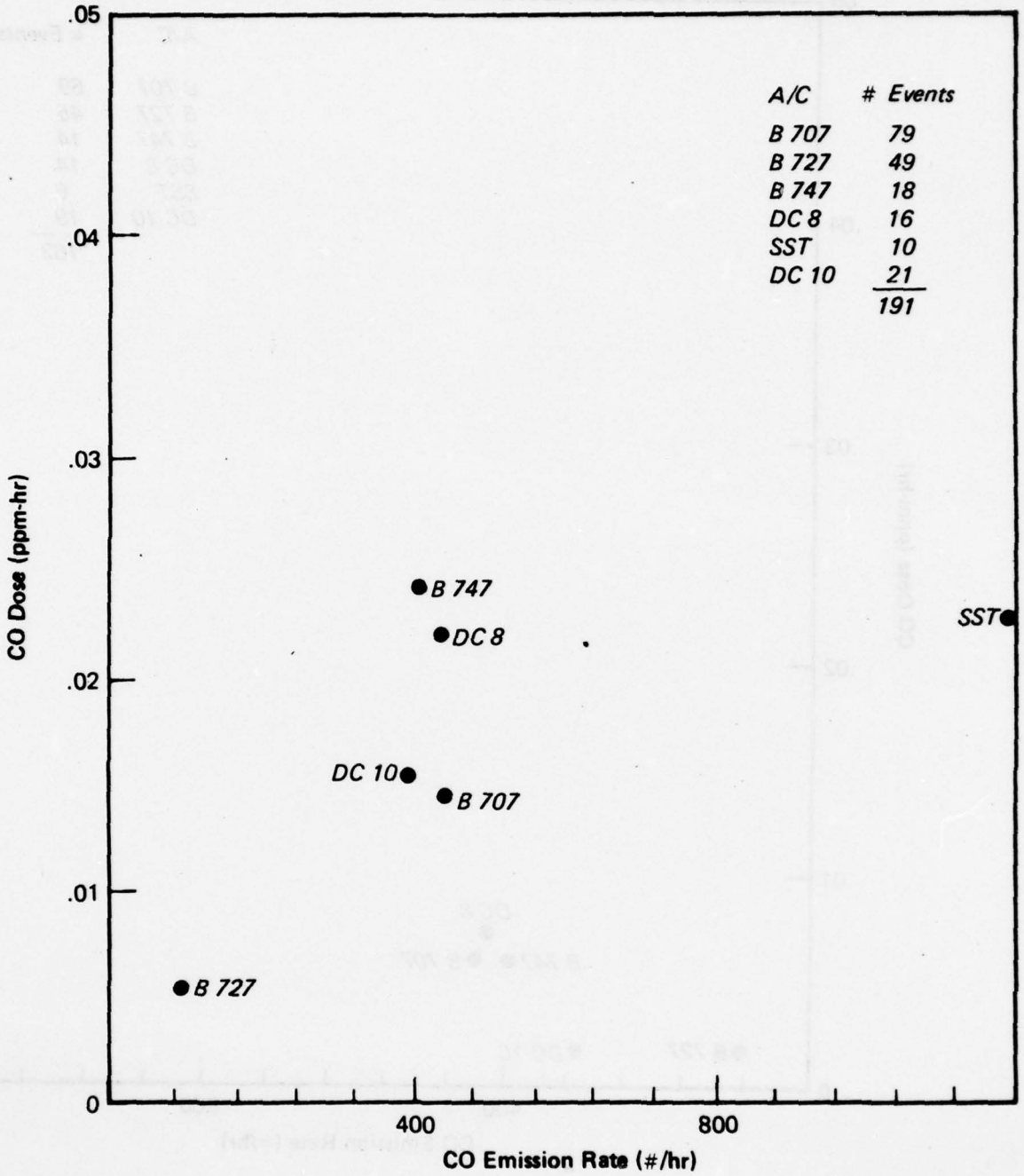

Figure 6-10 CO Dose Vs. Emission Rate, 1st Tower at 14 ft

710168

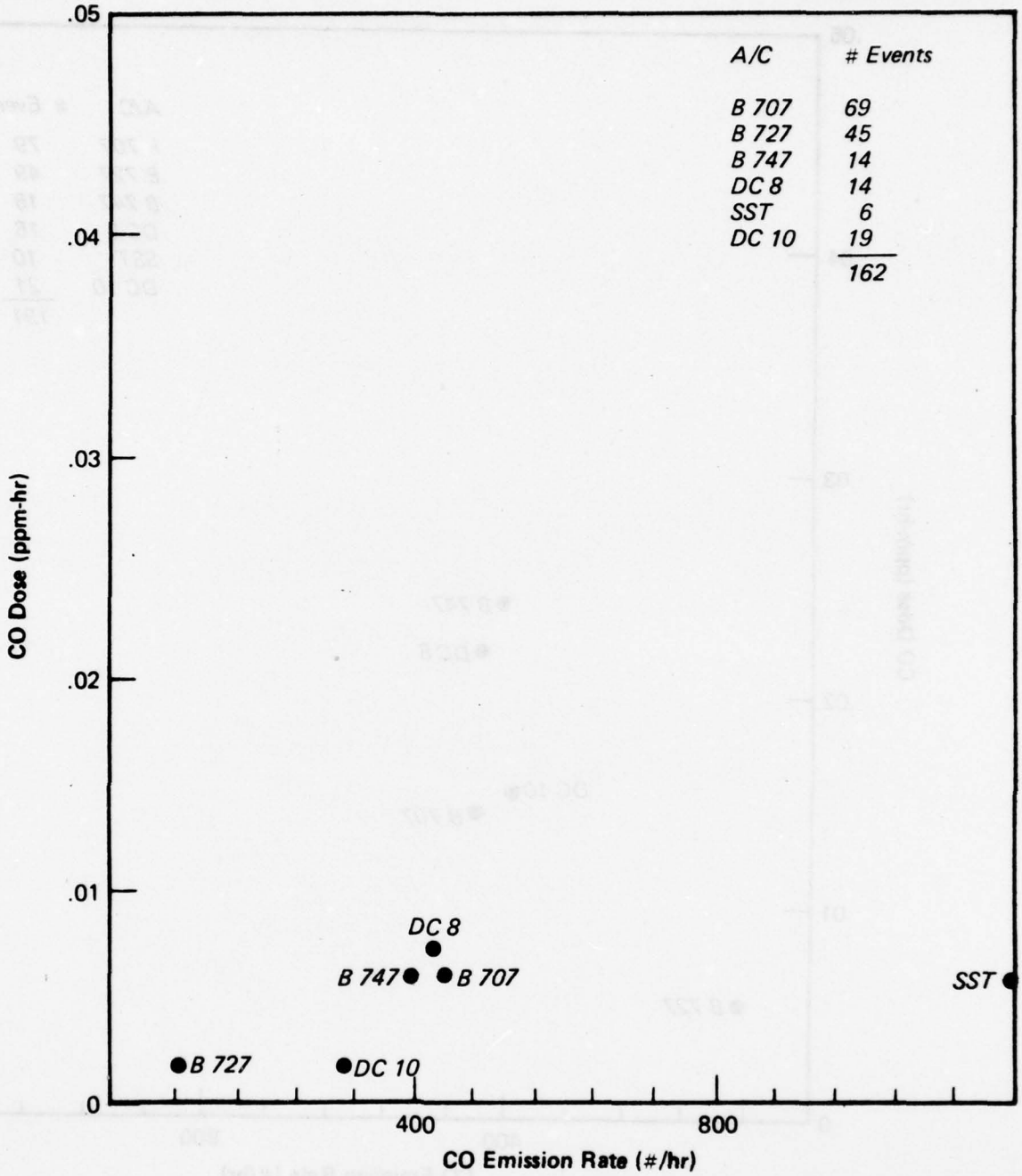

Figure 6-11 CO Dose Vs. Emission Rate, 2nd Tower at 14 ft

710143

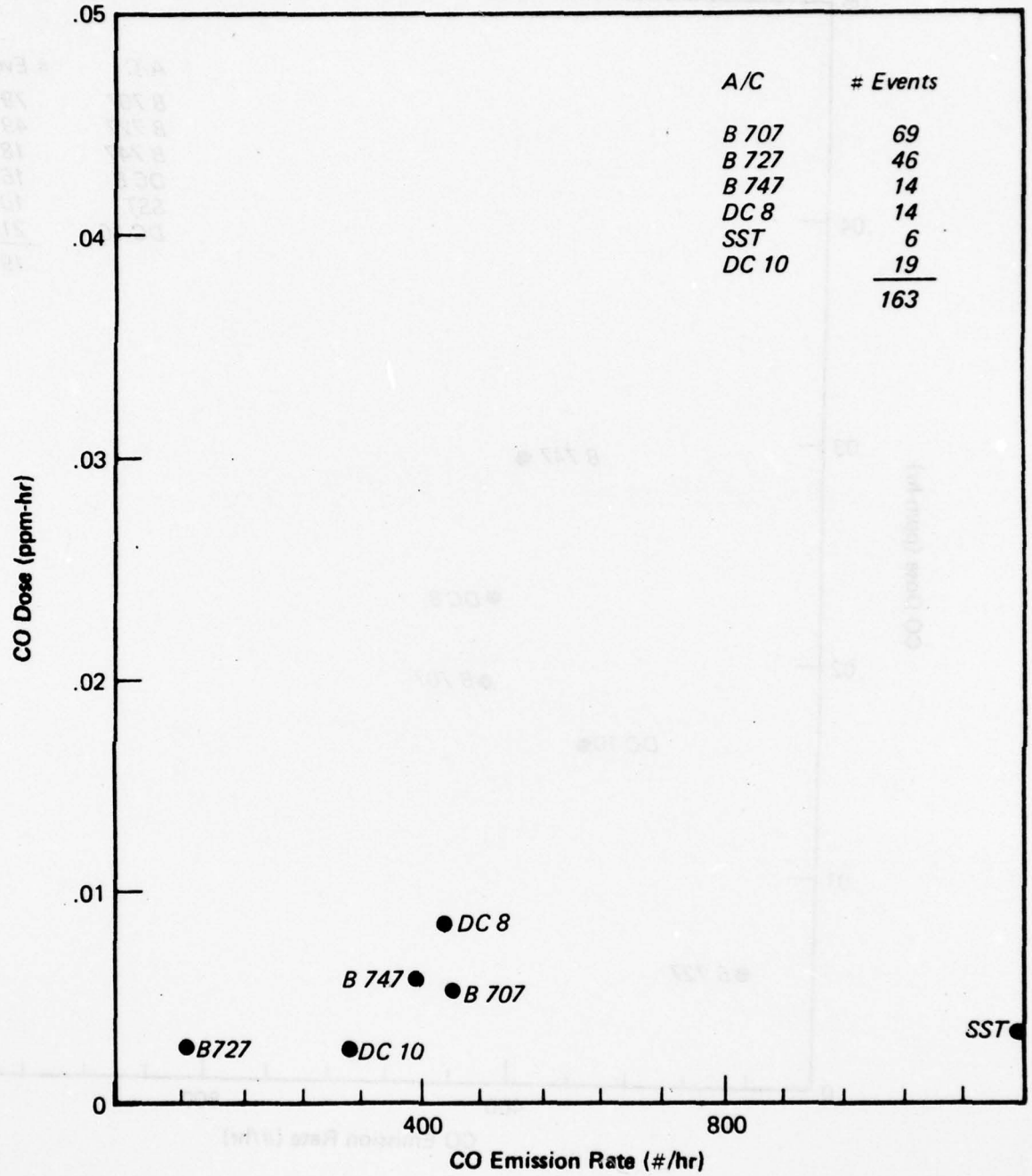

Figure 6-12 CO Dose Vs. Emission Rate, Last Sensor at 14 ft

710141

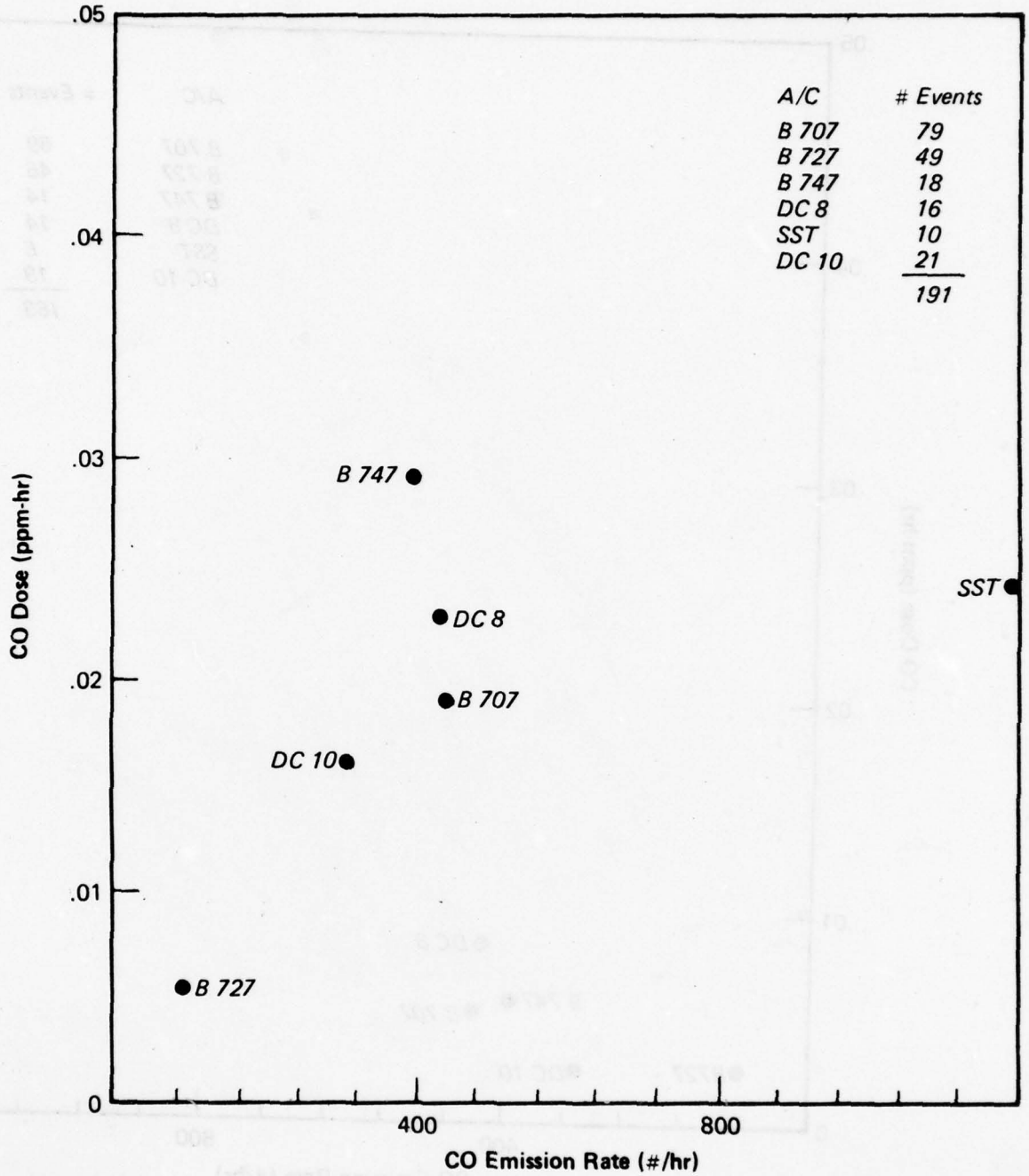

Figure 6-13 CO Dose Vs. Emission Rate, 1st Tower, Composite of all Heights

710142

Pasquill (1974). These turbulence measurements were then compared with values from the literature. Figure 6-14 compares the averages of the lateral dispersion parameter, σ_θ, derived from the dual-tower test series data with the values generally accepted (Slade 1968) as representative of the Turner (1964) stability categories. After some adjustment for the cases during which precipitation had fallen, the distribution of ambient turbulence measurements made during the dual tower tests (Figure 6-15) compared quite well with the estimates derived by use of the Turner scheme, which relies only on the surface meteorological observations conventionally available at or near each airport from the local weather bureau. Note, however, that the estimates of σ_θ from the measurement data are based on 3-minute periods, not the 1-hour periods that the Slade values assumed. On the basis of Turner's (1970) 1/5 power law adjustment for averaging time, a ratio of 1.7 between the hourly and the 3-minute dispersion parameters would ordinarily be expected.

This comparison indicates that normal use of the Turner stability method may underestimate the ambient turbulence at Dulles and yield concentrations almost double those predicted from measured turbulence levels. However, these measured levels may be affected by extraordinary sources of local turbulence at Dulles.

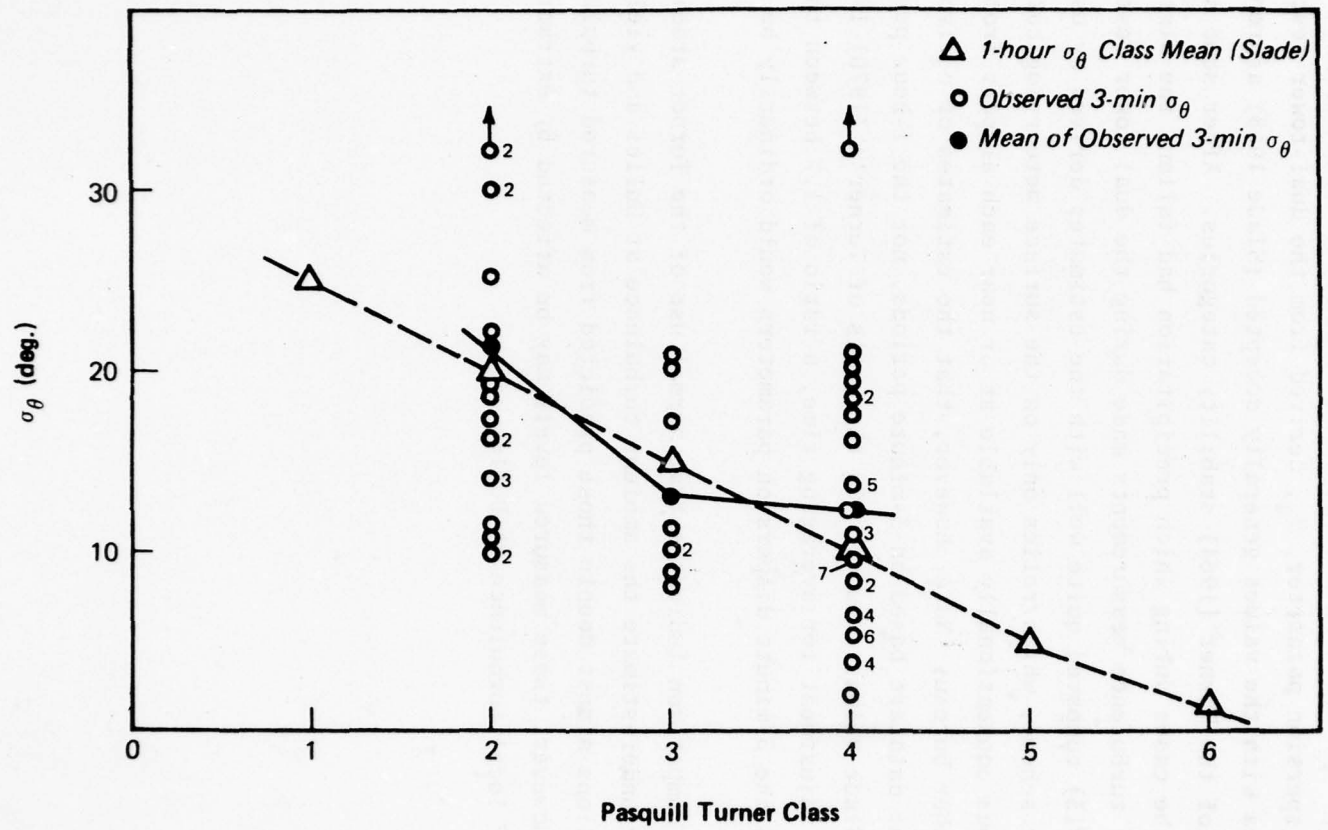

Figure 6-14 Comparison of Observed 3-Minute σ_Θ with 1-Hour Average Value (Slade 1968) Stratified by Pasquill-Turner Stability Class

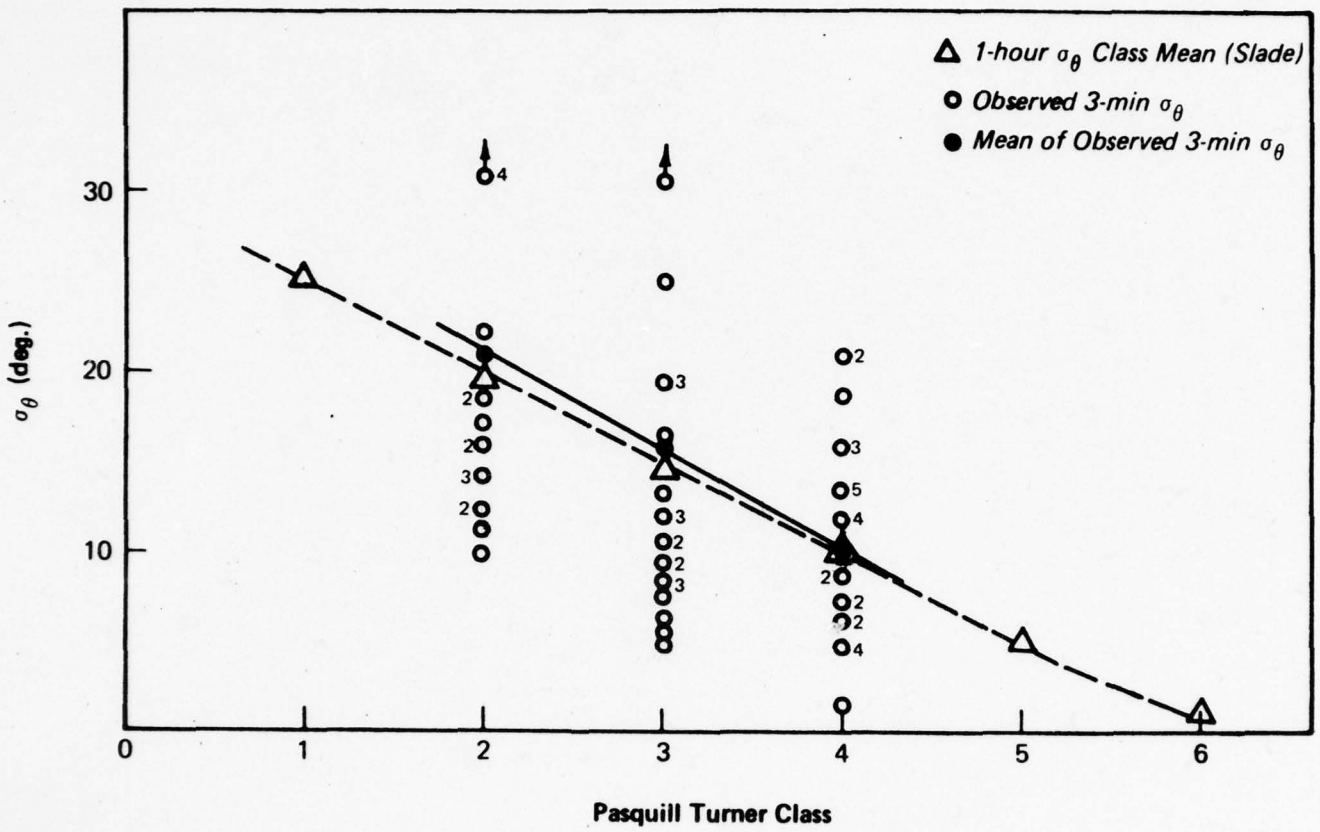

Figure 6-15 Comparison of Observed 3-minute σ_Θ with 1-Hour Average Value (Slade 1968) Stratified by Modified Pasquill-Turner Stability Class

7. AIR QUALITY MODELING APPROACH

A number of modeling methods were used in the present analysis. Statistical modeling techniques were employed for the regional impact analysis. For the final analysis of the area of air quality influence of the Concorde and other aircraft within the airport, a modified version of the Argonne line source model (ALSM) was used. The ALSM model is a submodel of the Airport Vicinity Air Pollution (AVAP) model developed at Argonne National Laboratory; AVAP was utilized in the original FEIS (1975) for the Concorde.

In the original FEIS (1975), the AVAP model was applied without specific data regarding the exhaust plume geometry for individual aircraft. The tower measurements made as part of the experimental program permitted a detailed examination of (a) the character of the plume rise, (b) the initial plume size, and (c) the rate of plume growth as it is transported downwind. The character of plume rise was determined by applying a multiple parameter fit (a parameterization model) to the tower data. The best calculation technique to incorporate the effects of plume rise and engine geometry was evaluated by comparing predictions of three variants of a quasi-instantaneous Gaussian model with the measured data. The difference between the variants involved the assumption that the rate of plume spread was best described by (a) a circular jet; (b) Pasquill-Turner dispersion parameters or (c) the local turbulence data measured at Dulles. The final analyses using ALSM and AVAP incorporated the best estimates of plume geometry and plume rise derived from the above comparisons with empirical measurements.

At present, a number of air quality models have been specifically designed or modified for calculating pollutant concentration patterns generated by aircraft operations in and around airports or military airbases. Eight of these models are listed in Table 7-1, along with the contracting agency and/or developing corporation (Haber, 1975). Most of the modeling efforts subsequent to the NREC model rely on its basic framework, including the use of a Gaussian plume transport model. Many differ in their degree of detail in treating initial source geometry, or in accounting for the variety of aircraft operations that constitute the time period modeled. The NREC model covers all basic operations taking

AD-A056 644 ENVIRONMENTAL RESEARCH AND TECHNOLOGY INC CONCORD MASS F/G 1/3
CONCORDE AIR QUALITY MONITORING AND ANALYSIS PROGRAM AT DULLES --ETC(U)
DEC 77 D G SMITH, R J YAMARTINO, C BENKLEY DOT-FA76WA-3816
UNCLASSIFIED ERT-P-2495-VOL-1 FAA-AEQ-77-14-VOL-1 NL

2 OF 2
AD
A056644

END
DATE
FILMED
9-78
DDC

OF

6644

TABLE 7-1

AIRPORT AIR POLLUTION DIFFUSION MODELS

Model Name	Developer	Contracting Agency
AIREC or NREC	Northern Research Engineering Corporation	EPA
GEOMET	Geomet Incorporated	EPA
ERTAQ/MARTIK	Environmental Research & Technology Northern Research Engineering Corporation	FAA
AVAP	Argonne National Laboratory	FAA
AQAM	Argonne National Laboratory	Air Force
BOEING	Boeing Computer Services	Proposal to FAA
LMSC	Lockheed Missile and Space Company	Proposal to FAA
PAL	Environmental Protection Agency	EPA

place at an airport with primary emphasis on developing a typical LTO cycle for passenger aircraft.

Since the NREC model was first published, considerable developmental effort has gone into improving the calculation of the distribution of the pollutants among the sources defining the LTO cycle and the dispersion of the pollutants from the point and line sources to receptors. This effort has resulted in the detailed airport/military air base models represented by AVAP/AQAM (Airport Vicinity Analysis Program and Air Quality Airport Model, respectively), developed by the Argonne National Laboratory (Rote, et al., 1973 and Rote and Wangen, 1975). For example, in the climbout portion of the LTO cycle, the NREC model has all aircraft (12 classes) follow the same departure path. This path is approximated in the dispersion algorithm as a series of point sources of varying strength; whereas in AQAM, 50 aircraft types are represented with each following a different departure path, which is treated as an inclined line source using the Argonne-developed line source model (ALSM). ALSM represents an improvement over the line source algorithm used in the NREC and ERTAQ/MARTIK codes, particularly for predicting concentration associated with inclined source paths and for wind directions nearly paralleling the aircraft pathways. ALSM is also much simpler than AVAP/AQAM in that it models single aircraft operations.

The family of transport model types available for airport analysis is dominated by the Gaussian plume models, as indicated above; but in the development and validation program a distinction has been drawn between Gaussian models based on instantaneous line source equations, called quasi-instantaneous in this report, and those based upon a segmentation of a continuous line source, called quasi-continuous here. The form of Gaussian model used in the Concorde FEIS for the assessment of regional influence of the Concorde was the quasi-continuous source model (AVAP).

Most of the models cited do not treat the details of emission geometry for single aircraft accurately, particularly initial plume rise and wake dispersion. Some modes of operation, such as engine start and idle or taxiing on a path perpendicular to the mean wind, are treated realistically enough to draw conclusions about off-airport impact; but when the wind blows almost along the aircraft path, the assumptions made

by the method of analytic approximation in earlier models may not be adequate for estimating local concentrations. However, since making measurements at the ends of taxiways and runways is often not permitted, model validation must usually be carried out with measurements made at the sides of these pathways, as in the present studies. It is apparent that analysis of pollution impacts upon occupants of the airport, as well as the surrounding area, should improve in accuracy when concentration predictions are based upon models successfully validated with monitoring data.

For evaluation of input parameter assumptions, such as initial source volume and plume rise estimates (derived from multi-parameter data fitting method), the quasi-instantaneous models described below proved to be more efficient and sensitive. Thus, they were used primarily to validate final parameters used by ALSM.

Even with all of the refinements made to the airport air pollution simulation models, it has not yet been possible to obtain conclusive tests of their predictive capabilities. It appears that a major reason for the difficulty with previous validation efforts has been the failure to identify the specific operations of all individual aircraft contributing to the monitored concentrations. The current test program provides a remedy to this situation by placing primary emphasis upon developing models that correlate well with measurements made in the immediate vicinity of individual aircraft operations.

In the following paragraphs, brief descriptions of regional modeling methods and each of the single event modeling techniques applied to the Dulles monitoring data are provided. The ALSM and AVAP models are also briefly discussed. These two models, incorporating the results of the single event model analyses, were used for estimating Concorde areas of influence (Section 9.3) and for comparison with the original EIS assessments (Section 10). Rote and Wangen (1975) and Wang, Conley and Rote (1976) provide complete descriptions of ALSM and AVAP, respectively.

7.1 Regional Modeling Methods

This part of the program involved examination of relations between airport concentration data and the concurrent concentration data collected at Sterling Park (Virginia), Bethesda (Maryland) and three other air pollution monitoring stations in Virginia. The period between June and September 1976 that was examined was the period coincident with the initial Concorde operations at Dulles airport. This phase was designed to develop and evaluate models that predict the impact of the airport on its community, specifically from aircraft-related pollutant concentrations. More generally, examination of the regional data base provides better understanding of the sources and processes that affect regional air quality. The model development and application effort was limited to statistical models for photochemical reactants, such as NO_x, THC and O_3; whereas, transport models receive principal emphasis for nonreactive or slowly reacting species, such as CO.

Modeling of regional air quality may be approached in one of three ways. First, the region may be considered as a closed box, with each local source and sink specified, with transport mechanisms (such as diffusion and advection) analytically modeled and with chemical interchange mechanisms defined and boundary conditions introduced. This full analytical treatment requires considerable understanding of all the processes involved and the exact nature of the relevant sources.

Alternatively, impacts on an intermediate scale of regional distances can sometimes be evaluated by extension of a local scale transport model. The original Concorde EIS attempted to assess the incremental impact of changes in the number of supersonic aircraft operating at Dulles by using the comprehensive AVAP plume transport and diffusion model. In the current program, estimates of plume rise and initial dispersion parameters derived from a statistical parameterization model (discussed in Section 7.2) have been used to revise the AVAP model and perform comparative analyses of projected Concorde impacts on both local and regional scales of distance. However, pilot analyses indicated that all significant concentrations were restricted to the immediate vicinity of the airport. Thus AVAP-predicted concentrations are limited to the local scale and are discussed separately in Section 9.

A third approach is the statistical/empirical model described here. In this case the data base itself is the source of clues to the identity of the important mechanisms that determine regional air quality. For example, consider a steady-state situation with one source whose pollutant output is characterized by a particular CO/NO_x ratio and a loss rate by transport to the boundary of the region. Measurements made within the region should, upon close examination, reveal that the ratio of measured CO to measured NO_x was constant and very close to the ratio at the source. Therefore, the motivation for this form of first order model is the prior knowledge that certain of the parameters are related functionally, either as a direct consequence of a predominant source (such as the CO/NO_x ratio from auto exhaust) or through related production and loss mechanisms (such as the photochemical processes determining the ratio of O_3/NO_2).

As introduced in Section 6.1, the process of data stratification often leads to apparent relationships that require further quantification. The simplest forms of analysis are simple linear correlations and regressions. Thus, for example, regression of CO with NO_x for a given site in the form:

$$(CO) = a\,(NO_x) + b$$

should help identify such parameters as the predominant CO/NO_x ratio which characterizes the local source, a, and the ambient value of CO, b. In particular, this method should help to isolate whether regional air quality parameters correlate with specific airport-related data, such as activity, particularly when measurement data are stratified by wind direction. Conversely, correlations with airport activity due to mutual dependence on time of day (such as for photochemically dependent mechanisms and local events) may be identified.

In cases where the cross correlation of variables described above prevents identification of significant relationships between measurements and potential sources, multilinear regression techniques generally provide the additional selectivity needed to isolate such a relationship.

As the second step in the statistical analysis, therefore, a multilinear regression model:

$$Y = ax_1 + bx_2 + \ldots + c$$

has been used. This type of model allows the influence of secondary continuous scale variables to be evaluated quantitatively and eliminates the need to stratify the data into the many subsets often needed with simple linear regression models. Results of the application of this multilinear regression model to the regional data base are presented in Section 8.1.

7.2 Multi-Parameter Models

Measurements of peak CO concentrations, CO doses and wind variability, obtained during the two-tower phase of the experiment, have also been used to determine the parameters of a Gaussian-puff type of dispersion model. The seven model parameters include the initial plume concentration (χ_o), initial alongwind and vertical plume dimensions, $\sigma_x(o)$ and $\sigma_z(o)$, alongwind and vertical growth rates of the plume, b_x and b_z, plume height at the first tower, H_1, and the incremental plume rise between towers, ΔH. The theoretical model used assumes Gaussian vertical profile equations:

$$\chi_T = \frac{\chi_o \, \sigma_x(o) \, \sigma_z(o)}{f_1 \, \sigma_x(t) \, \sigma_z(t)} \left[e^{-1/2\left(\frac{z-H}{\sigma_z(t)}\right)^2} + e^{-1/2\left(\frac{z+H}{\sigma_z(t)}\right)^2} \right] \operatorname{erf}\left(\frac{L}{2\sqrt{2}\,\sigma_y(t)}\right)$$

$$t = \frac{d}{u \cos \theta}$$

and

$$\Gamma_T = \sqrt{8 \ln 2}\,\frac{\sigma_x}{\bar{u}} = \Gamma_T' - \frac{\tau \ln 2}{f_2}$$

where

χ_T = theoretical peak concentration

H = H_1 = plume height at first tower

$H_1 + \Delta H$ = total plume height at second tower and beyond

L = length of taxiway (3,000 ft)

t = travel time to sensor from runway centerline

d = sensor distance from runway centerline

$\bar{u}$ = mean wind speed

θ = mean wind direction

f_1 = sensor response correction factor for peak concentrations

$= 1.00 + 0.79\ (t/\Gamma_T)^{1.2}$

f_2 = sensor response correction factor for pulse duration

$= 1.00 + 0.09\ (\Gamma_T/t)^{1.4}$

Γ_T = theoretical pulse duration

Γ_T' = theoretical pulse duration, corrected for sensor response

The form and values of parameters for the f_1 and f_2 correction factors were based on a best fit to an analytic simulation of the response of a first order measurement system (with time constant, τ) to a Gaussian input pulse having Γ_T = full width at half maximum. For the CO sensors (Ecolyzer systems) $\tau \simeq 12$ sec; for the THC sensor (flame ionization system) $\tau \simeq 4$ sec; for NO/NO_2 sensors (chemiluminescent system) $\tau \simeq 0.5$ sec. The error function term in the equation above (approximately 1.00 for downwind distances << L) is simply the factor describing the effect of the finite length of the source line segment. This model, together with the additional meteorological assumptions listed below, is then used to estimate peak CO concentrations and doses as a function of downwind (i.e., alongwind) distance from the taxiway centerline for single taxi operations of various aircraft types.

Additional Meteorological Constraints

$$\sigma_x = \sigma_x(o) + b_x \bar{u}\, t \tan \sigma_\theta$$

$$\sigma_y = b_x \bar{u}\, t \tan \sigma_\theta$$

$$\sigma_z = \sigma_z(o) + b_z \bar{u}\, t \tan \sigma_\theta$$

where $b_x = 0.4$ and $b_z = 0.24$ or 0.40, whichever provides the better fit, and where t is plume travel time and $\bar{u}$ is mean wind speed. For t > 100 seconds a puff growth rate proportional to $t^{.85}$ was assumed.

Doses (concentrations accumulated over the period that a pollutant puff passes a sensor) were computed with the expression:

$$D = \chi_T \frac{\sqrt{2\pi}\, \sigma_x(\tau)}{\bar{u}}$$

where the quantities are defined as above.

A chi-square value, based upon summing relative errors in the following equation, is minimized by the program MINUIT (described in Appendix B):

$$\chi^2 = \frac{\Sigma(\chi_T' - \chi_M)^2}{(\Delta\chi)^2} + \frac{\Sigma(\Gamma_T' - \Gamma_M)^2}{(\Delta\Gamma)^2}$$

where

χ_T' is theoretically predicted concentration, corrected for sensor response (as in Section 4.1)

χ_M is measured concentration

Γ_T' is theoretical pulse duration, corrected for sensor response (as in Section 4.1)

Γ_M is measured pulse duration

Δ is uncertainty in observed value (for CO $\Delta\chi$ assumed at 0.25 ppm and $\Delta\Gamma$ assumed at 10 seconds).

7.3 Quasi-Instantaneous Models

The instantaneous line source equation given by Turner (1970) has been used as the basis of a model that predicts peak concentrations along taxiways and runways. A brief introduction to its major variants is given in this section. Details of its derivation are given in Appendix B.

The quasi-instantaneous models all use the following instantaneous line source as their basis:

$$\chi(x,y,z,h) = \frac{Q}{2\pi(s + u_p)\sigma_x\sigma_z} \exp -1/2\left(\frac{x-u_n t}{\sigma_x}\right)^2$$

$$\cdot \left\{\exp -1/2\left(\frac{z-H}{\sigma_z}\right)^2 + \exp -1/2 \left(\frac{z+H}{\sigma_z}\right)^2\right\}$$

where

(x,y,z) are the (alongwind, cross-wind and vertical) components of a Cartesian coordinate system, assuming mean wind is predominantly normal to aircraft pathway.

χ is the pollutant concentration (mass/volume)

H is the effective height (engine height plus plume rise) of emission, and therefore the centerline height of the plume (length)

Q is the source strength (mass/time)

σ_x, σ_z are dispersion coefficients that are measures of alongwind and vertical plume spread. These two parameters are functions of downwind distance and atmospheric stability (length)

s is aircraft speed (length/time)

u_p is average wind speed parallel to aircraft pathway (length/time)

u_n is average wind speed normal to aircraft pathway (length/time)

The source base is at $z = 0$ in the coordinate system, and the plume centerline reaches the equilibrium height H at some distance downwind from the source. In the present analyses, plume rise was assumed to be complete by the time the plume reaches the first tower. Thus, H was assumed to be identical at all sensor distances downwind of the taxiway or runway.

At the first tower, the plume centerline height is calculated by (Yamartino, 1977):

$$H = A_{1,2} + B_{1,2}/\sqrt{u}$$

where u(mph) is the wind speed for each single event. The subscripts 1 and 2 refer to two sets of aircraft analyzed. Values for the parameters are given in Table 7-2.

The line source strength Q (gm/m) is replaced in the previous equation by $Q/(s + u_p)$. Actually there is a third velocity vector which may significantly alter the effective source strength. That factor is $u_j(y)$ the jet exhaust velocity as a function of position along the taxiway or runway. This function is not yet well known. Therefore it was assumed to be a uniform factor affecting all results similarly and was not considered further in the modeling analysis. The range of the observational data also did not allow further analysis of the effects of negative values of s nor of wind angles nearly parallel to the taxiway via the quasi-instantaneous models.

It must be emphasized that the source geometry and near field plume behavior of exhaust pollutants from an aircraft are not precisely described by either a purely "instantaneous" line source Gaussian model or a continuous line source version (see Figure 7-1). However, with appropriate adaptations, it was anticipated that either form could be transformed into a model that adequately described the behavior of pollutant concentrations or dosages at the given receptors. (Dosages are concentrations accumulated over the period of time that the pollutant passes a sensor or receptor.)

Jet engine exhausts expel hot air and gases at high velocity. Since the exhaust plume is warm and buoyant relative to its surroundings, it rises as it is transported downwind. Knowledge of the rise of

TABLE 7-2

PLUME RISE ESTIMATES DERIVED FROM TWO TOWER TESTS AT DULLES*

Assumption**	No Plume Rise	Mean Measured Height	Gaussian Centerline Height
A_1 (ft)	Mean exhaust height	24.7	-2.6
A_2 (ft)	Mean exhaust height	29.7	9.1
B_1 (ft $mph^{1/2}$)	0	20.5	65
B_2 (ft $mph^{1/2}$)	0	9.9	43

*Source: Yamartino, 1977.
**Set 1 - includes B707, B727, B747 aircraft
Set 2 - includes DC8, DC9, DC10, L1011, Concorde aircraft

EXHAUST PLUME DISPERSION AND MEASUREMENT GEOMETRY

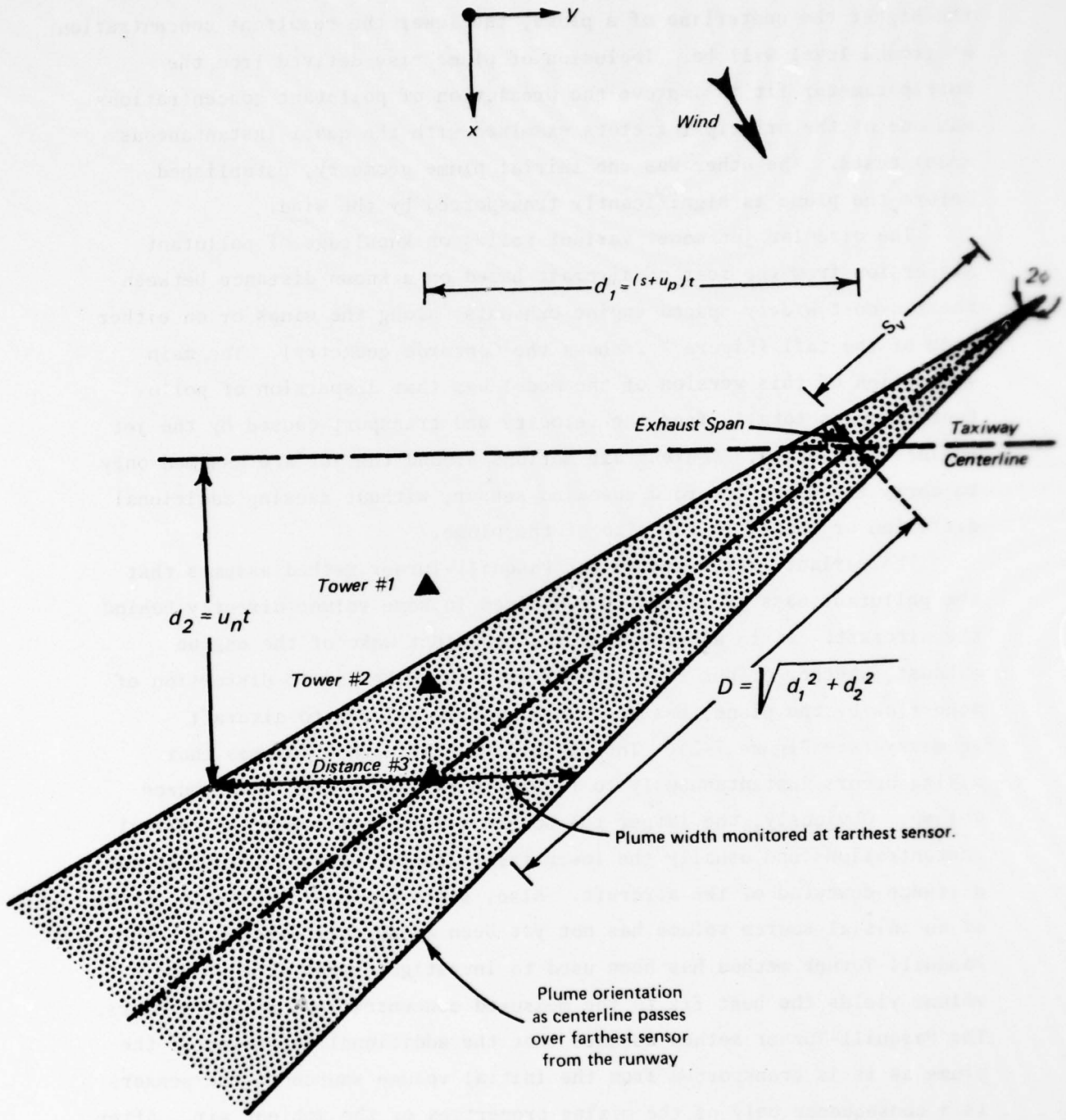

Figure 7-1 Aircraft Exhaust Plume Dispersion Geometry

707130

the plume is important to the modeling of pollutant concentrations, for the higher the centerline of a plume, the lower the resultant concentration at ground level will be. Inclusion of plume rise derived from the multiparameter fit to improve the prediction of pollutant concentrations was one of the principal factors examined with the quasi-instantaneous model tests. The other was the initial plume geometry, established before the plume is significantly transported by the wind.

The circular jet model variant relies on knowledge of pollutant dispersion from the rear of aircraft based on a known distance between the two most widely spaced engine exhausts, along the wings or on either side of the tail (Figure 7-2 shows the Concorde geometry). The main assumption of this version of the model was that dispersion of pollutants results totally from the velocity and transport caused by the jet engines themselves. Ambient air motions around the jet are assumed only to carry the plume toward a downwind sensor, without causing additional diffusion or change in the size of the plume.

The variant identified as the Pasquill-Turner method assumes that the pollutant mass is initially contained in some volume directly behind the aircraft. It is assumed that the turbulent wake of the engine exhaust, whether or not it interacts with the wake due to distortion of wind flow by the plane, has an initial volume related to aircraft geometry (see Figure 7-2). The Pasquill-Turner method assumes that mixing occurs instantaneously to result in the above-mentioned source volume. Obviously, the larger the source volume, the lower the initial concentrations and usually the lower the pollutant concentrations at any distance downwind of the aircraft. Also, since the most realistic choice of an initial source volume has not yet been adequately determined, the Pasquill-Turner method has been used to investigate what size source volume yields the best fit to the measured concentrations at all sensors. The Pasquill-Turner method assumes that the additional diffusion of the plume as it is transported from the initial volume source to the sensors is a consequence only of the mixing properties of the ambient air. After the initial volume is defined, further effects of the velocity or mixing properties of the engine exhaust itself are not considered. Thus, this approach represents a quite different assumption from that of the circular jet model with respect to the relative importance of ambient and jet

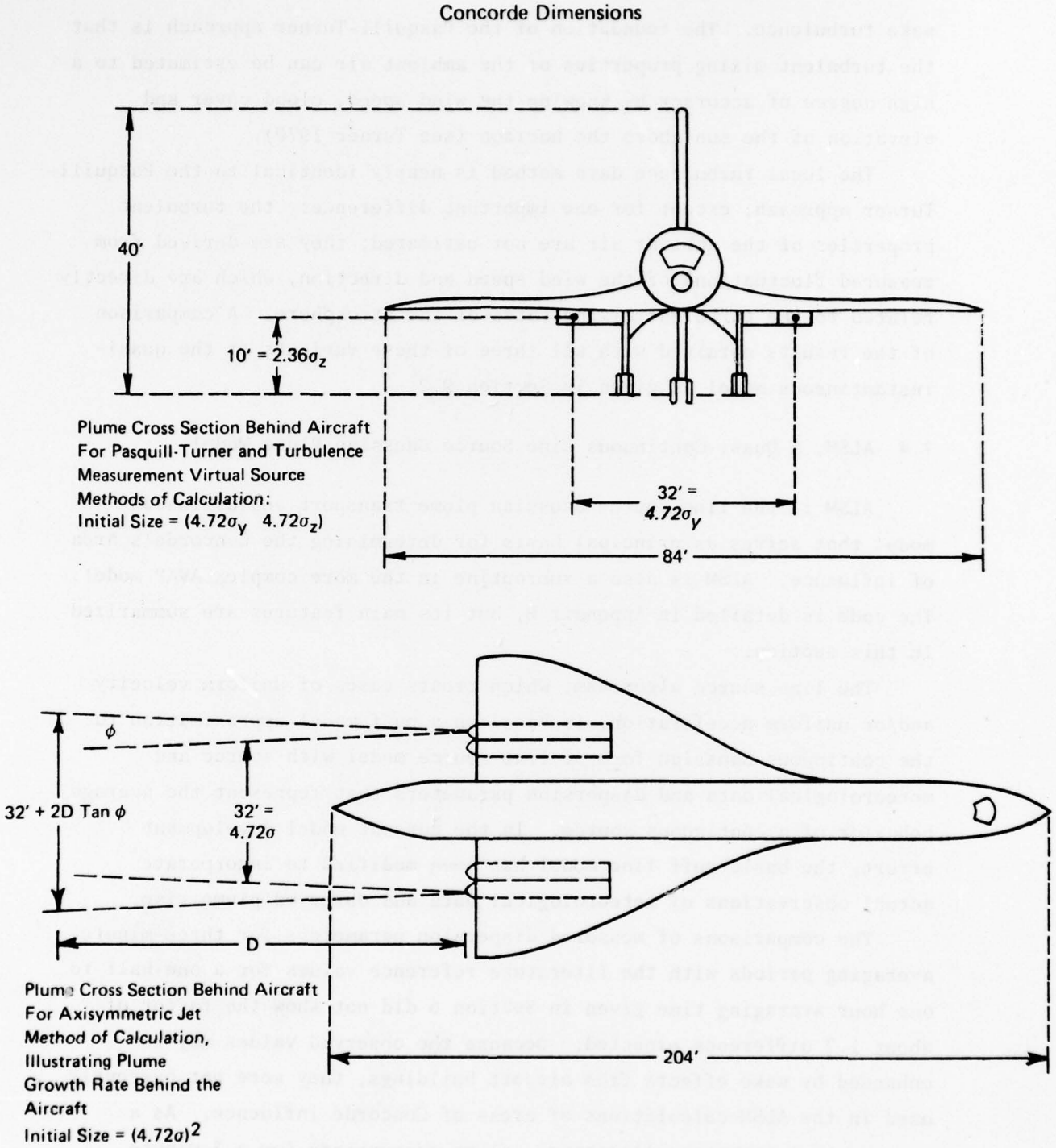

Figure 7-2 Geometry of Concorde and Its Exhaust Plume

707131

wake turbulence. The foundation of the Pasquill-Turner approach is that the turbulent mixing properties of the ambient air can be estimated to a high degree of accuracy by knowing the wind speed, cloud cover and elevation of the sun above the horizon (see Turner 1970).

The local turbulence data method is nearly identical to the Pasquill-Turner approach, except for one important difference: the turbulent properties of the ambient air are not estimated; they are derived from measured fluctuations of the wind speed and direction, which are directly related to the turbulent mixing rates of the atmosphere. A comparison of the results obtained with all three of these variants of the quasi-instantaneous model is given in Section 9.2.

7.4 ALSM, A Quasi-Continuous Line Source Gaussian Plume Model

ALSM is the line source Gaussian plume transport and diffusion model that serves as principal basis for determining the Concorde's area of influence. ALSM is also a subroutine in the more complex AVAP model. The code is detailed in Appendix B, but its main features are summarized in this section.

The line source algorithm, which treats cases of uniform velocity and/or uniform acceleration, is based on a puff model approximation to the continuous Gaussian form of line source model with source and meteorological data and dispersion parameters that represent the average behavior of a continuous source. In the current model development effort, the basic puff line model has been modified to incorporate actual observations of meteorological data and observed plume rise.

The comparisons of measured dispersion parameters for three-minute averaging periods with the literature reference values for a one-half to one hour averaging time given in Section 6 did not show the factor of about 1.7 difference expected. Because the observed values may be enhanced by wake effects from airport buildings, they were not currently used in the ALSM calculations of areas of Concorde influence. As a conservative approach, literature values appropriate for a 3-minute averaging time were employed since this represented a maximum release period for a single taxiing and takeoff operation (assuming no idling on the runway). The use of measured turbulence parameters would result in lower concentration and smaller influence area predictions.

It is assumed that the effluent emitted over a time duration τ, from a finite straight line segment, can be treated as a sequence of long thin "puffs" or "linear puffs" extending over the length of the line segment. The duration τ is taken to be the averaging time (= three minutes) over which the meteorological parameters are considered constant. It is further assumed that the time of formation τ_1 of each puff is short compared to the averaging time τ and that each puff rapidly comes to rest relative to the ambient air mass. With these assumptions, the transport of a linear puff of pollutant is treated by the Green's function technique to obtain the concentration at any receptor point (Rote and Wangen, 1975; Wang and Rote, 1975).

The initial width Δy and height Δz of a physical line source are treated in analogy with the physical point and area sources by first assigning initial values of horizontal and vertical dispersion σ_{yo} and σ_{zo} and then computing the corresponding position of pseudo upwind line sources. Choices of these input parameter values were based on the results of quasi-instantaneous model investigations (Section 9.2).

The boundary conditions, the ground and the mixing lid, are treated as recommended by Bierly and Hewson (1962) for point sources; however, multiple images are not considered. The critical downwind distance x_c for uniform vertical mixing beneath the "lid" of an elevated inversion is also calculated according to their method and is measured downwind from the center of the line segment. If an inclined line segment penetrates the lid, that portion above the lid is excluded from the calculation. Only the source and ground reflection are considered for $x \leq x_c$. Beyond $2x_c$, uniform mixing is assumed, and for $x_c < x < 2x_c$, a linear interpolation is performed.

7.5 AVAP, A Continuous Line Source Gaussian Plume Model

The Airport Vicinity Air Pollution (AVAP) Model was designed to predict the impact of pollutant sources at commercial airports upon local air quality for averaging time intervals ranging from one hour to one year and the emissions are simulated by a combination of point, area or line sources, according to the approximate geometrical shape of the source. Point sources include smoke stacks, vents or small sources of

evaporated materials. Area sources include complex mixtures of motor vehicles (cars, trucks, aircraft) operating in parking lots, aircraft ramp areas, etc. Line sources are divided into uniform and nonuniform, according to whether the vehicles moving along the line are moving with approximately constant speed or are accelerating (or decelerating). Uniform lines include access roadways and taxiways. Nonuniform lines include takeoff and landing operations on runways and approach and departure paths (treated as inclined lines).

The AVAP code operates by applying a Gaussian puff-plume dispersal mechanism to the wide variety of source types and configurations found in modern airports. Because of its flexibility and detailed treatment of aircraft LTO cycles, AVAP was used in predicting the air quality impact of Concorde operations for the original Concorde FEIS (1975). The strategy in the FEIS was to first consider the normal operations at Dulles between 9 A.M. and 3 P.M. and then consider the change in air quality resulting from the substitution of one B 747 operation (landing during the hour 9 to 10 A.M. and departing the following hour) with two Concorde operations.

The meteorological and aerometric measurements program at Dulles led to the following modifications in the model.

1) Jet exhaust plume rise was added in the taxi mode.

2) Taxi/idle mode emissions were lowered by a factor of three to reflect the reduced impacts monitored, within 600 feet of the taxiways.

8. RESULTS OF REGIONAL MODELING ANALYSIS

The results of the regional modeling analysis are based on an air quality data set consisting of hourly averaged concentrations of CO, O_3, THC and NO_x at four regional air quality monitoring sites in Virginia and Maryland, as well as at Sterling Park in the immediate vicinity of Dulles International Airport. To characterize the vicinity of the airport itself, the South Ramp site was included. Predominant sources around South Ramp include automobiles on access roads and in parking lots in addition to taxiing aircraft. Additional data available for this analysis included meteorological parameters such as wind speed and direction, stability class and airport activities data. Extensive statistical analyses such as those described in Section 6.1 and 7.1 were performed on the regional data set.

The purpose of the regional study was twofold:

1) To characterize the regional air quality characteristics for the vicinity of the airport and

2) To identify any significant correlations between airport activity and regional air quality.

The methodology employed progressed from the simplest to the more sophisticated statistical techniques as required. In particular, parametric relationships between pollutants at the same location (such as CO versus NO_x at Sterling Park) and between locations for the same pollutant (such as CO at South Ramp versus CO at Sterling Park) were investigated to examine predominant sources at one location and the influence of one location on another in a statistical sense. The inherent assumption is that particular sources (and combinations of sources) will exhibit unique CO versus NO_x relationships and that receptors influenced by similar sources will produce similar relationships. Additionally, the NO_2 versus O_3 relationship was computed at each site for comparison. Complete analysis results referred to in this section are included in Appendix D.

8.1 Regression and Correlation Analyses

To assess regional air quality effects, standard statistical tools including simple linear regression, correlation analysis and multilinear regressions were applied to the regional data base. Both intersite and intrasite comparisons of statistical parameters were examined to determine whether specific influences on regional data due to airport activities could be isolated. For this purpose, South Ramp data were assumed to characterize the airport. In this section calculations are performed for all wind directions.

Table 8-1 presents the results of a simple linear regression between South Ramp and Sterling Park for O_3, NO_2, THC and CO. In each case, the equation $y = ax + b$ was fitted to the data where y is the dependent variable, x the independent variable, a the regression slope and b the regression constant. Additionally, the correlation coefficient, r, was computed. In each case, the value at Sterling Park was assumed to be the dependent variable. Mean values of x and y are given.

These calculations are elucidated by an examination of the diurnal data for Sterling Park and South Ramp (Figures 6-2, 6-4). A high correlation coefficient implies similar duirnal trends. As long as transport lag is small, a low correlation coefficient implies independent sources. Both CO and THC appear to have a statistically small correlation between the two sites. Ozone has a high correlation coefficient due to the common photochemical source, while NO_2 has an intermediate value. NO_2 has both natural and source contributions.

Correlation analysis was performed between NO_2 and O_3 for the South Ramp and Sterling Park regional sites. Results are given in Tables 8-2a and 8-2b where each entry is the correlation coefficient between the respective parameters at sites found in the vertical and horizontal legends (for example, Massey NO_2 and Lewisville NO_2, correlation coefficient: 0.547). Wind speed data were taken at South Ramp. These tables show that for all cases NO_2 correlates negatively with O_3. It was earlier suggested, based on evaluation of diurnal analysis at South Ramp, that the diurnal behavior of NO_2 there differed markedly from that at Sterling Park. It was suggested that a different source, namely aircraft activity, was responsible. Quantitively, it is expected that

TABLE 8-1

REGRESSION RESULTS FOR STERLING PARK ($\bar{y}$) VS. SOUTH RAMP ($\bar{x}$)

Parameter	a	b	r	$\bar{x}$	$\bar{y}$
O_3	0.9542	0.0089	0.8428	0.0338	0.0412
THC	0.1400	1.3967	0.1559	2.0615	1.6854
NO_2	0.6084	0.0066	0.6337	0.0132	0.0146
CO	0.1320	1.2204	0.0882	1.1089	1.3669

TABLE 8-2a

CORRELATION COEFFICIENTS NO_2, O_3, WS

	Massey NO_2	Lewinsville NO_2	Seven Corners NO_2	Massey O_3	Lewinsville O_3	Seven Corners O_3	Wind Speed
Massey NO_2	1.000	0.547	0.514	-0.309	-0.310	-0.183	-0.279
Lewinsville NO_2		1.000	0.772	-0.194	-0.392	-0.294	-0.407
Seven Corners NO_2			1.000	-0.121	-0.262	-0.254	-0.364
Massey O_3				1.000	0.875	0.868	0.289
Lewinsville O_3					1.000	0.891	0.373
Seven Corners O_3						1.000	0.298
Wind Speed							1.000

TABLE 8-2b

CORRELATION COEFFICIENTS NO_2, O_3, WS

	Sterling Park NO_2	South Ramp NO_2	NIH NO_2	Sterling Park O_3	South Ramp O_3	Wind Speed
Sterling Park NO_2	1.000	0.626	0.573	-0.336	-0.270	-0.351
South Ramp NO_2		1.000	0.568	-0.082	-0.206	-0.285
NIH NO_2			1.000	-0.229	-0.226	-0.295
Sterling Park O_3				1.000	0.865	0.319
South Ramp O_3					1.000	0.270
Wind Speed						1.000

the correlation between O_3 and NO_2 at each of the regional sites, affected primarily by automobile sources, should be of similar magnitude (NO_2 peaks during the O_3 minimum in the early morning and late afternoon "traffic" hours) while this correlation is expected to be lower at South Ramp due to the broader distribution of the aircraft activity data (Figure 6-5) throughout the day. Table 8-3 lists the relevant correlation coefficients for NO_2 vs. O_3 at each site. Note that the South Ramp correlation coefficient is somewhat lower than the other regional sites.

The relationship between the two primary aircraft effluent pollutants CO and NO_x was investigated at both South Ramp and Sterling Park. Once again, Sterling Park is characteristic of the other regional monitoring sites. As discussed earlier, the diurnal behavior of CO and NO_x appears to differ considerably between the two sites. Stepwise linear regression was performed for each case. The first relationship sought was CO vs. NO_x of the form:

$$y = ax + b$$

where y is CO, x is NO_x, a is the regression slope and b is the regression constant. Results are given in Table 8-4.

Different relationships are found at each site. In particular, the correlation coefficient at Sterling Park is significantly higher than at South Ramp. CO and NO_x should correlate well for automobile sources, while it is expected that for random airport activities, which are sources of weakly correlated quantities of CO and NO_x (i.e., CO almost exclusively during taxi/idle and NO_x during takeoff), the relationship should be less well defined.

The resultant regression relationships indicate that the CO concentration at South Ramp is essentially constant (compare mean value and regression constant) with only about 1% of the remaining variance explained by NO_x variation. This was noted qualitatively in the previous diurnal analysis. Sterling Park, on the contrary, while not exhibiting a direct proportionality, indicates about 40% variance due to NO_x dependence. To isolate dependence on parameters not investigated by this simple linear regression, a step-wise multilinear regression was

TABLE 8-3

CORRELATION COEFFICIENT NO_2 VS. O_3

Site	South Ramp	Sterling Park	Massey	Lewisville	Seven Corners
Correlation Coefficient	-0.206	-0.336	-0.309	-0.392	-0.254

TABLE 8-4

CO VS. NO_x REGRESSION RESULTS FOR SOUTH RAMP VS. STERLING PARK

	a	b	r	$\bar{x}$	$\bar{y}$
South Ramp	0.130	1.049	0.005	0.018	1.051
Sterling Park	26.69	0.789	0.566	0.021	1.360

performed for both sites using a sample set consisting of both South Ramp and Sterling Park NO, NO_2, THC and CO. (Sterling Park NO_x was not included for the South Ramp calculation.) Results do not differ significantly from the simple regression with NO_x. Again, the Sterling Park results are characteristic of the regional data rather than the South Ramp measurements.

8.2 Wind Direction-Specific Analysis

Results presented in the previous section were based on calculations using the complete regional data base with no constraint on particular wind directions. Of particular interest, however, is the relationship between airport and regional parameters when the prevalent wind direction is from the airport toward each of the regional monitoring locations. To facilitate these calculations, specific ranges of wind direction were selected for each site using the Dulles wind data. These 60° wind direction segments are summarized in Table 8-5.

Correlation analyses were performed for each regional site and its corresponding wind direction selection range for the parameters NO_2, CO, O_3 and total aircraft activity at the airport.

Results of calculations to determine the correlation coefficients between pollutants at South Ramp and each of the regional sites when the wind was blowing from the airport are presented in Table 8-6. For comparison, the "all" wind direction values presented in the previous section for Sterling Park are given in parentheses.

The correlation coefficients are negligible for CO, of possible significance for NO_2, and indicate positive correlation for O_3. It may be inferred that South Ramp and the other regional sites (including Sterling Park) do not share a common CO source. The case for NO_2 is somewhat more ambiguous. However, it should be noted, for example, that the correlation coefficient for the wind direction-specific case with respect to the airport for Sterling Park (0.5524) decreases somewhat from the case for all wind directions (0.6337). For O_3, the high positive correlative is undoubtedly due to its common photochemical source.

TABLE 8-5

REGIONAL DATA WIND DIRECTION SELECTION CRITERIA
FOR AIRPORT UPWIND OF MONITORING SITE

Regional Site	Wind Direction Range (°)
South Ramp	300-360
Sterling Park	180-240
Massey	300-360
Lewinsville	280-340
Seven Corners	275-335

TABLE 8-6

WIND-SPECIFIC CORRELATION COEFFICIENTS BETWEEN SOUTH RAMP AND OTHER SITES FOR NO_2, CO AND O_3

	Sterling Park		Massey	Lewinsville	Seven Corners
NO_2	0.5224	(0.6337)	0.4780	0.5044	0.5438
CO	-0.1221	(-0.882)	0.1045	-0.0209	0.0316
O_3	0.8984	(0.8428)	0.8472	0.7835	0.7694

Relationships between pollutants at each site were previously discussed with respect to isolating differing sources for the "all" wind directions case where it was noted that conditions at South Ramp are distinctive from those at the off-airport regional monitoring sites. These findings were not substantially modified by subsequent examination of the wind specific cases. In particular, the local correlation between CO and NO_2 at each of the sites was evaluated. Results are presented in Table 8-7. In each case presented in this table, the wind was blowing from the 60° upwind angle, which includes the Dulles airport taxiways and runways.

Again, the correlation coefficient at South Ramp indicates negligible correlation between CO and NO_2, while those at the remaining sites imply marginal statistical significance for a CO vs. NO_2 correlation. Major roadways can be identified as nearby pollutant sources for the Massey and Lewinsville sources, and for these sites this correlation coefficient is most significant. Similarly, the correlation analysis data for NO_2 vs. O_3 (also given in Table 8-7) reinforce the previously observed differences evident between South Ramp and the regional monitoring sites. Due to the intermittent source of NO_x at the airport from daily activities, NO_2 is expected to be less correlated with O_3 (which has a well defined diurnal cycle) than NO_2 away from the airport's influence. The magnitude of the negative correlation at Sterling Park is in the same range as the other regional sites, even when the wind is from the airport's direction.

Assuming that the primary source of pollutants at the airport is aircraft activity, an investigation was made of the correlation between total activity data (see Figure 6-5) and downwind pollutants for both South Ramp and the regional monitoring sites. Results are presented in Table 8-8 for NO_2, CO and O_3. There appears to be no significant correlation between activity data and pollutant concentration at any of the regional sites or at South Ramp. The positive indication of correlation with O_3 at each site may be explained by examining Figures 6-2 and 6-5 and noting that both parameters are essentially zero at night and reach maximum values in the afternoon.

TABLE 8-7

WIND-SPECIFIC CORRELATION COEFFICIENTS CO VS. NO_2 AND NO_2 VS. O_3

	South Ramp	Sterling Park	Massey	Lewinsville	Seven Corners
CO vs NO_2	-0.0923	0.3880	0.5398	0.6966	0.3407
NO_2 vs O_3	-0.1715	-0.3920	-0.4475	-0.5032	-0.2446

TABLE 8-8

CORRELATION COEFFICIENTS FOR AIRCRAFT ACTIVITY DATA VS. POLLUTANT CONCENTRATIONS

	South Ramp	Sterling Park	Massey	Lewinsville	Seven Corners
NO_2	0.0665	0.0478	-0.1136	-0.0858	0.0355
CO	0.0772	-0.0492	-0.0477	-0.1438	0.1349
O_3	0.4611	0.4796	0.4515	0.4529	0.4174

8.3 Summary

The regional modeling analysis was accomplished by applying a number of statistical techniques to the regional data base. Significant results of these computations are presented in Appendix D. The methods employed progressed from the simplest to the more sophisticated techniques as required. The purpose of the regional study was: (1) to specify the regional air quality characteristics for the vicinity of the airport and (2) to identify any significant correlations between airport activity and regional air quality.

The most basic analysis tool used was simple stratification. Using available wind data for Dulles and corresponding hourly pollutant concentration values for each regional site, pollution rose plots were generated for O_3, CO, NO_2 and THC as a function of wind speed and stability class and for "all" wind cases. It was noted that in no location does the most significant direction in the pollution rose plot for a given pollutant correspond to the relative direction of the airport.

Stratifying the pollutant concentration data for each regional location by time of day (LST) isolated the diurnal variation of each species. The diurnal behavior of the regional sites with the exception of South Ramp follows a characteristic pattern with THC, NO_2 and CO maxima during peak automobile traffic hours and an O_3 miximum during the early afternoon. The diurnal variation of CO and NO_2 is greatly suppressed at the South Ramp site, however, suggesting that it may reflect the specific nature of activity at the airport rather than the traffic source characterizing the other regional sites.

To quantify these observations, simple linear regression, correlation analyses and multilinear regressions were applied to the data base both for all wind directions and for cases when the prevalent wind direction is from the airport toward each of the regional monitoring locations. Relationships between sites for particular pollutants and between pollutants at given locations were investigated.

In general the results indicate high correlation between sites for O_3, moderate correlation for NO_2 and little correlation for THC and

CO. The O_3 result is probably due to common photochemical production rather than source transport. For NO_2 the result is ambiguous suggesting both independent local sources and photochemical mechanisms. For CO and THC, however, the low correlation suggests independent local sources. These results are not modified when the prevalent wind direction is from the airport.

As suggested in the diurnal stratification, the relationships between CO and NO_x and NO_2 and O_3 appear to be somewhat different at South Ramp as compared to the other regional sites. This is quantitatively supported by the correlation and multilinear regression analyses. The nature of these relationships may be evaluated in terms of predominant sources at a given location and, therefore, it is inferred that the nature of the sources contributing at South Ramp are distinctive in comparison to those at the other regional sites.

Finally, no significant correlation was found between airport activity data and downwind pollutants at South Ramp and the regional monitoring sites.

9. RESULTS OF SINGLE EVENT MODELING ANALYSIS

Presented in this section are the analysis results of several different Gaussian transport and dispersion models that have been developed, modified and validated against measurement data to more accurately simulate the special dispersion conditions associated with the passage of a single aircraft on a taxiway or runway at Dulles. The results of parameterization model comparisons with data are presented below in Section 9.1. The comparisons of quasi-instantaneous models used to validate modifications for ALSM are presented in Section 9.2. ALSM was the model ultimately used in this study to define the Concorde "areas of air quality influence" for each pollutant (Section 9.3). The results of applications of the more complex AVAP model, and comparisons of the original results with those presented in the Concorde EIS, are presented in Section 10.

9.1 Plume Rise and Multi-Parameter Fit

Although near-ground-level measurements of pollution emanating from a nearby jet aircraft would appear adequate to address air quality impact questions, the potential for seriously underestimating this impact exists as the hot exhaust plume may simply rise up and over the low level receptors, only to diffuse back down to ground level further downwind. This uncertainty in the "vertical profile" of aircraft emitted pollutants served as motivation for a series of Dulles plume rise experiments, consisting initially of four receptors on a single 58 ft tower. Later the network was expanded to include a coplanar array of 11 CO detectors: five each on two 82 ft towers, and a single 14 ft high sampler 543 ft from the taxiway centerline.

A preliminary analysis of the 140 events recorded during the single-tower CO study in November 1976 indicated significant plume rise and determined that wind speed and aircraft type are important variables affecting plume rise (Yamartino, 1977). Estimating the plume centerline height by fitting the observed height dependent CO peak concentrations

with a Gaussian shape function, plume elevation was found to be inversely dependent upon wind speed. Results of ten Concorde observations suggested a mean plume centerline height of about 34 ft at the 215 ft downwind distance. The estimates of plume rise assumed for the Concorde for subsequent transport model analysis were the mean values derived from the second set of single tower experiments (see Table 7-2).

Although a crude model of plume rise had been derived for the one-tower experiment, it was unclear whether the final plume height had been observed. The addition of the second tower permitted further measurements on the plume's upward trajectory, while providing data on the plume's horizontal and vertical rates of expansion. Preliminary analysis of eighty observations obtained during February and March 1977 suggest an additional increment of plume rise of approximately 60% between the towers. For the set of all aircraft types, the distributions of plume heights at the first of the two towers and the incremental plume rise between towers are given in Figures 9-1 and 9-2, respectively. Respective estimates of vertical and horizontal (along wind) plume spread are plotted in Figures 9-3 and 9-4.

To estimate both the average and the worst-case rates of CO decrease with distance based upon observational data, the two-tower data on CO peak concentration and pulse duration, along with wind variability data (σ_θ) were input to the seven parameter Gaussian-puff dispersion model described in Section 7.2. The resulting peak CO concentrations (Figure 9-5) and doses (Figure 9-6) are presented as functions of downwind (i.e., alongwind) distance from the taxiway centerline for single taxi operations for various aircraft types. The curves suggest that for CO emissions during taxi, Concorde impact is only about one to one and one-half times that of a B707, in contrast to reported CO emission factors, which suggest a Concorde CO emission rate three times that of the B707.

Noting that the entire dose impact from a single taxi operation would occur in a time span of less than one hour for downwind distances $\leq$10,000 ft, Figure 9-6 also represents the contribution of a single taxi operation to the hourly average CO level. It is indicated by this figure that beyond 100 ft from the taxiway centerline no single taxi operation contributes more than 0.1 ppm CO to the hourly average CO

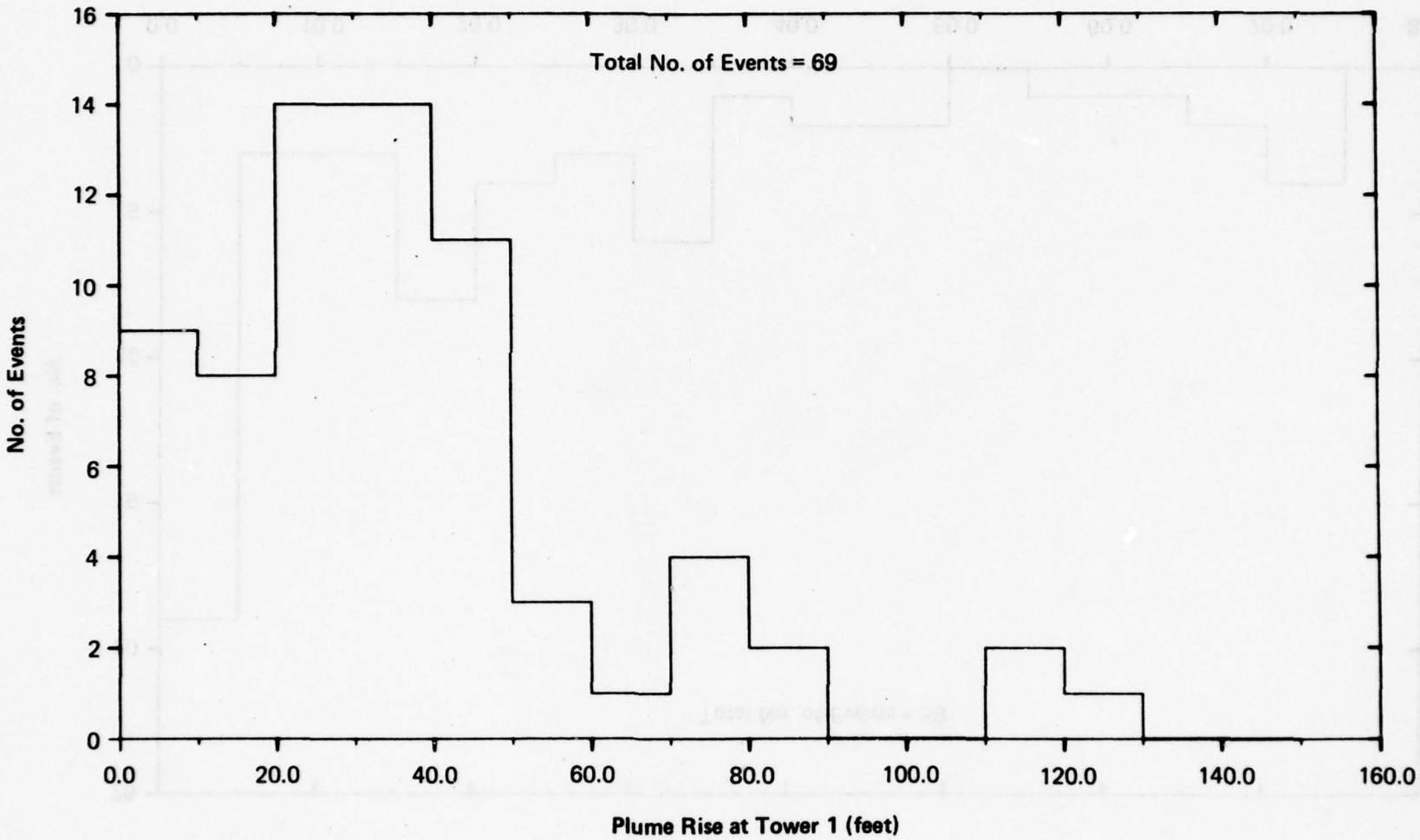

Figure 9-1. Distribution of Plume Rise at Tower 1, All Aircraft Types.

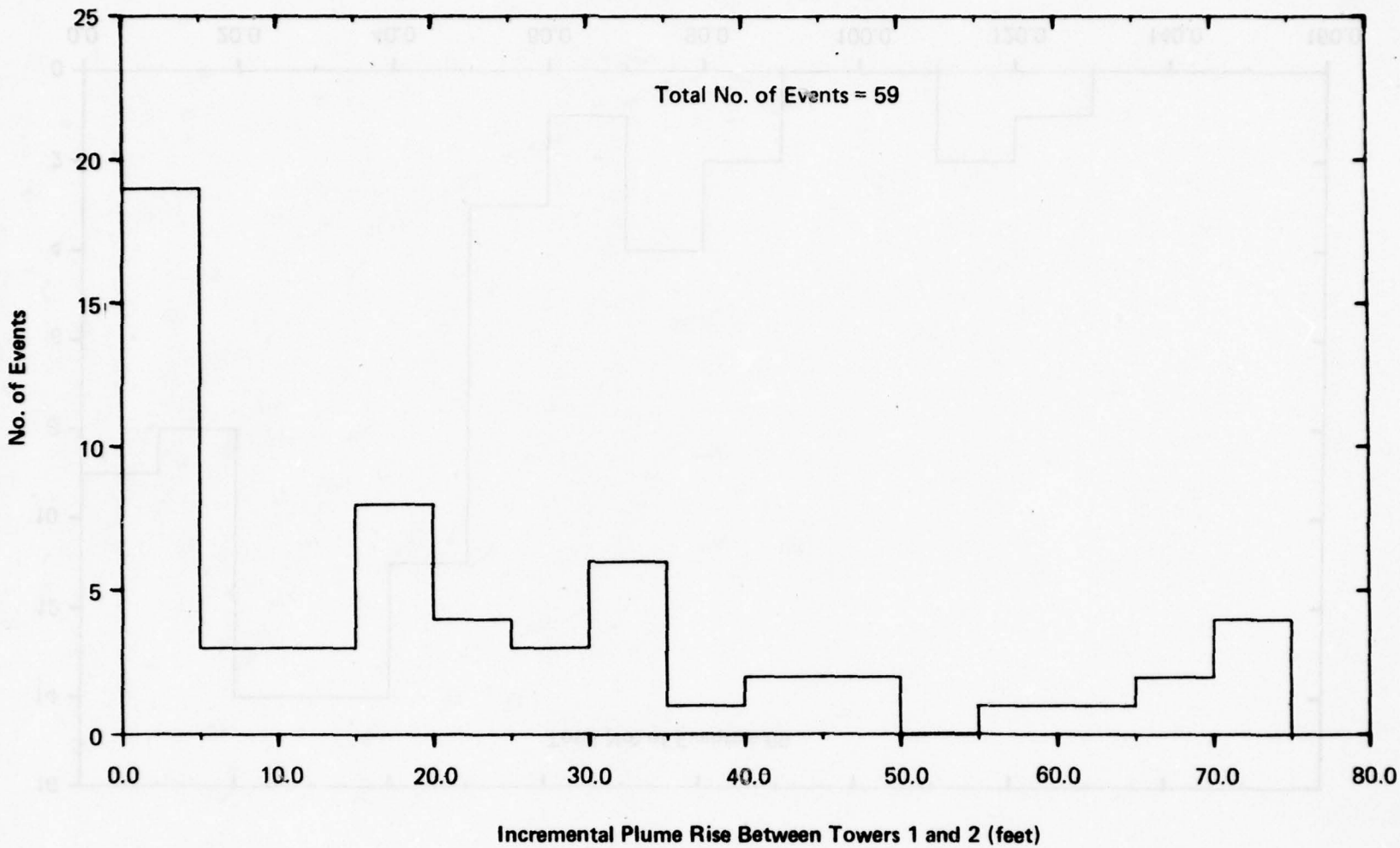

Figure 9-2. Incremental Plume Rise Between Tower 1 and Tower 2, All Aircraft Types.

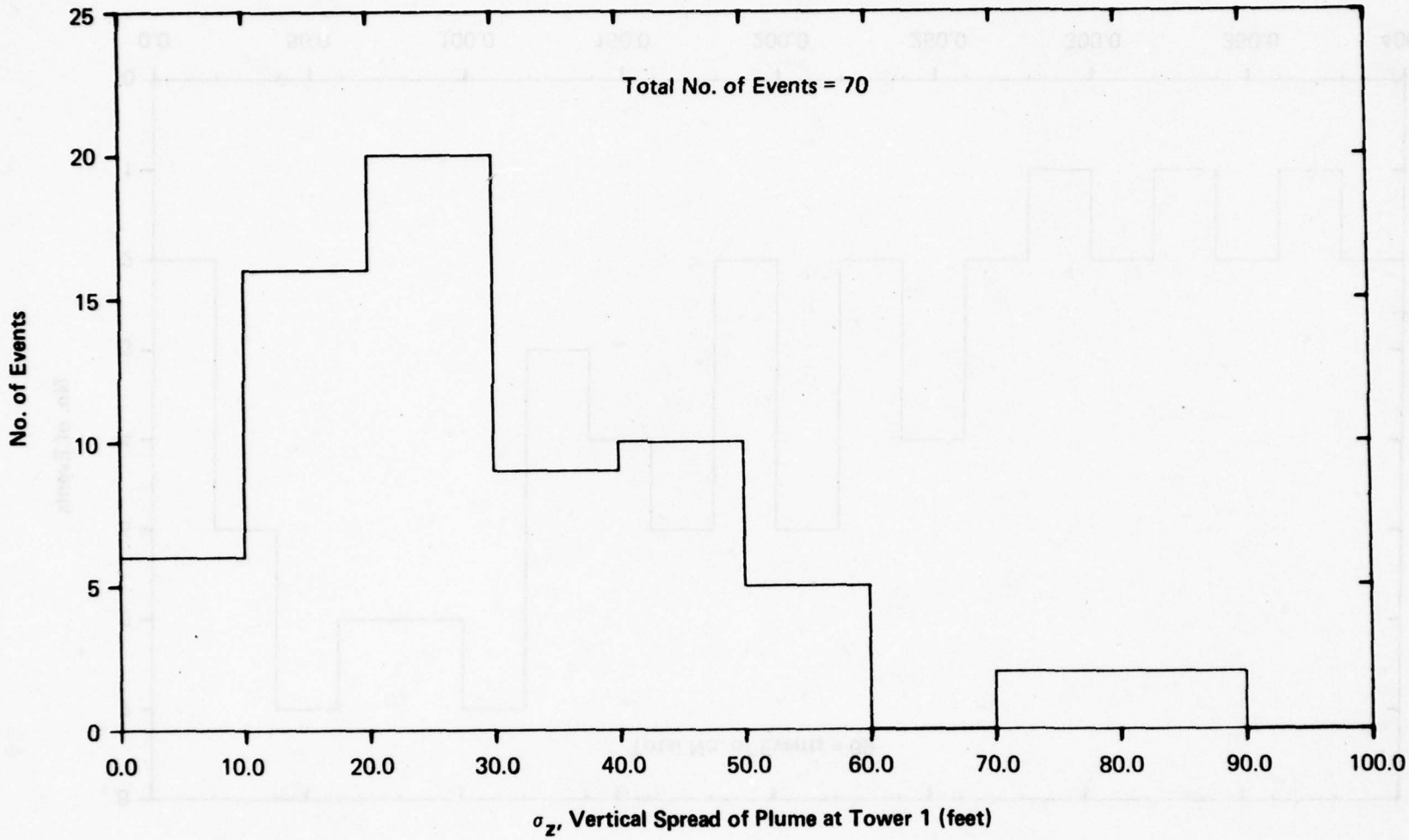

Figure 9-3. Vertical Spread of Plume at Tower 1, All Aircraft Types.

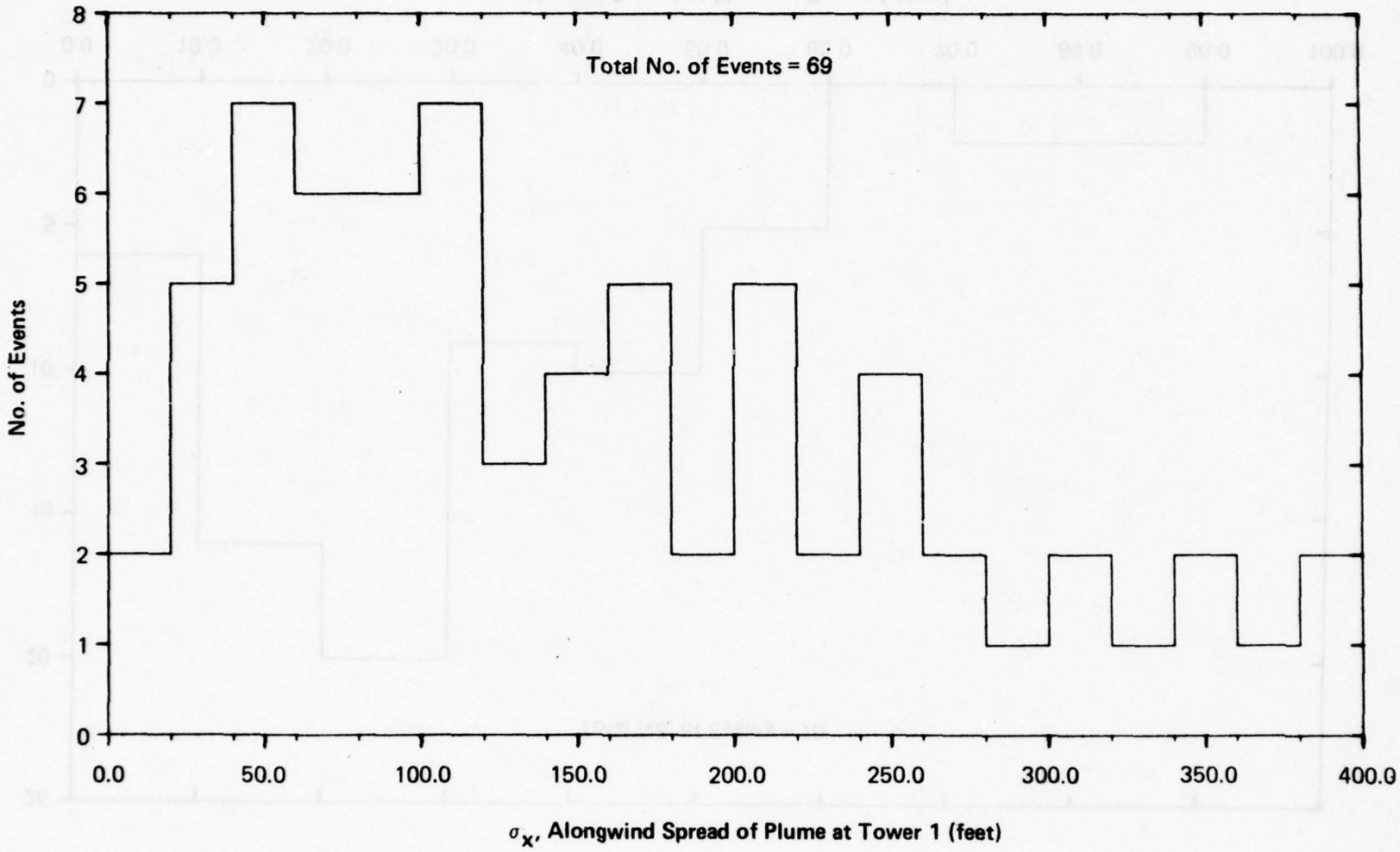

Figure 9-4. Alongwind Spread of Plume at Tower 1, All Aircraft Types.

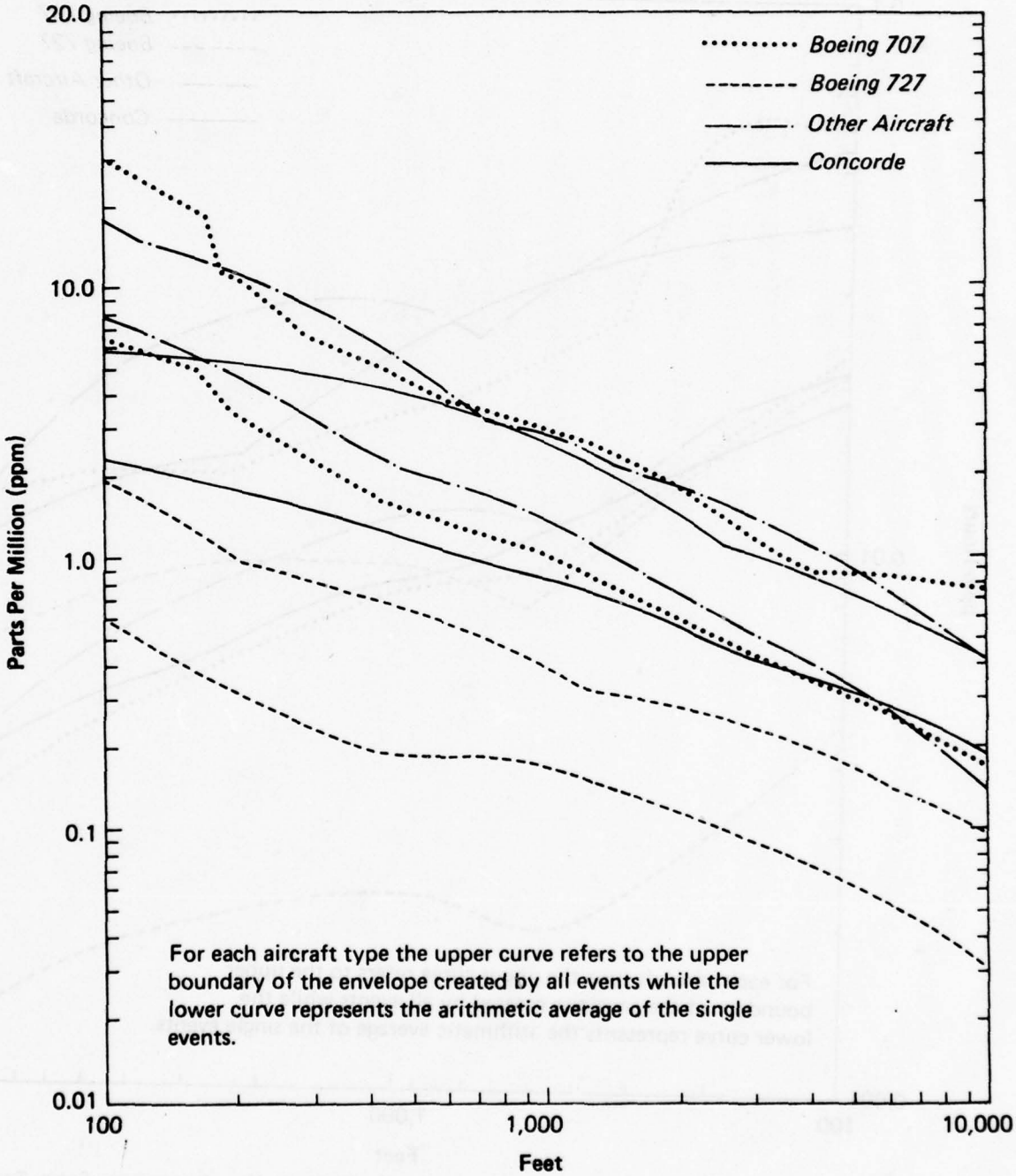

Figure 9-5 Multiparameter Estimate of Peak CO Vs. Distance from Taxiway

712066

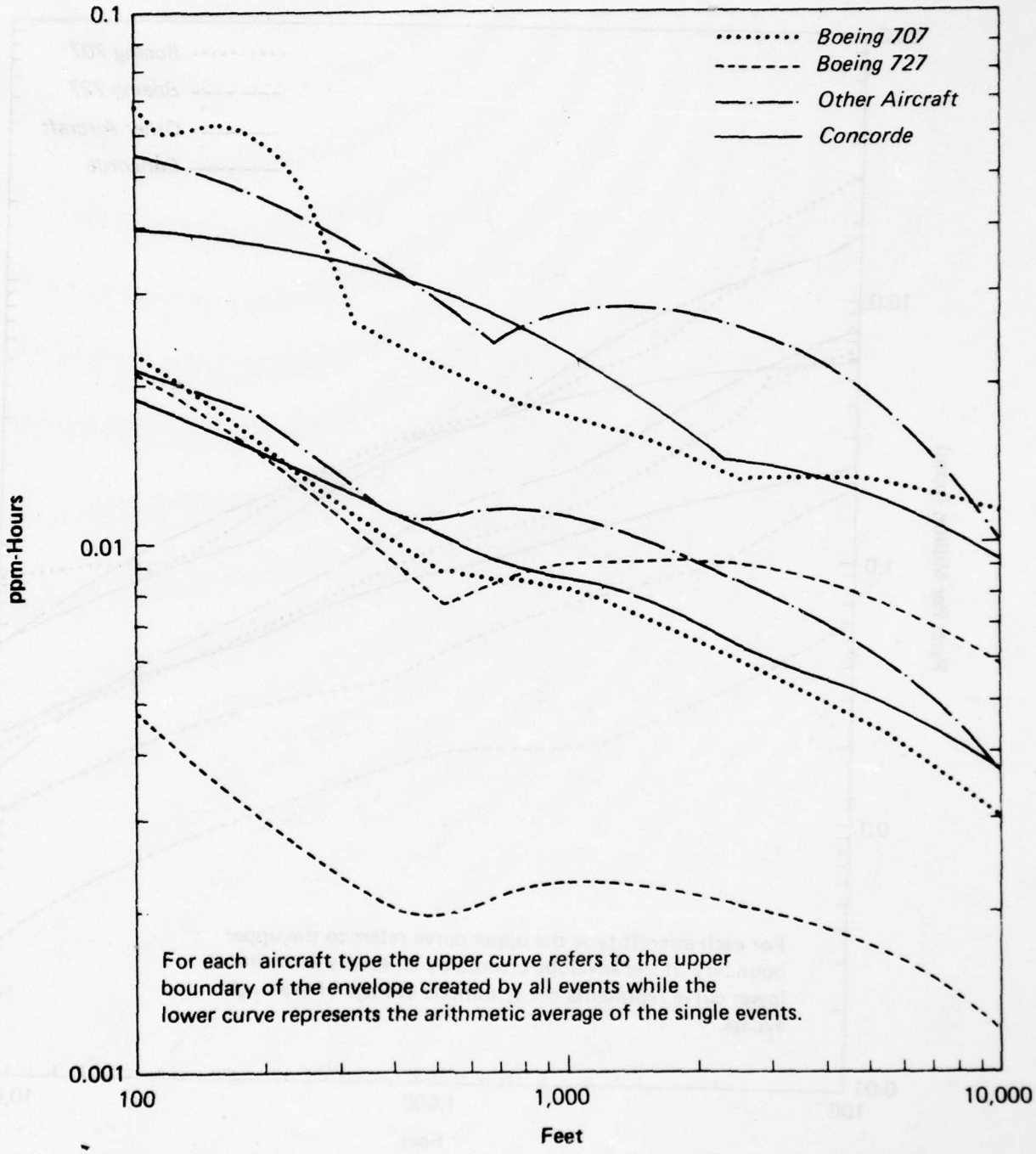

Figure 9-6 Multiparameter Estimate of CO Dose Vs. Distance from Taxiway

712067

level and that beyond 10,000 ft this contribution has dropped to <0.01 ppm. These concentrations may be compared to typical background levels of ~0.5 ppm CO and a NAAQS primary 1-hour standard of 35 ppm.

9.2 Results Obtained with Quasi-instantaneous Models

The three variants of a quasi-instantaneous Gaussian dispersion model introduced in Section 7.3 were compared with measured CO concentrations taken during the two-tower experiment (February and March 1977) for B707 and B727 events, and the one-tower experiment (November 1976) for the Concorde events. CO concentration data were chosen for principal comparisons since they represents the largest set of measurement data available. Only the above three aircraft types were used in the present analysis.

Figure 9-7 illustrates the importance of plume rise. In this figure, the average predicted concentration vs. height by the circular jet model is compared against the average measured concentration vs. height for 31 taxiing B707s during the two-tower experiment. This comparison was drawn for sensors located on the first tower at 215 ft from the centerline of the taxiway. In addition to the comparison shown in Figure 9-7, two sets of predictions for each variant of the model have been examined: (1) assuming a mean plume rise from the statistical analysis of Yamartino (1977, unpublished) from the November 1976 experiment, (2) assuming no plume rise. It is evident from Figure 9-7, that including plume rise improved the fit.

Figure 9-8 is a comparison of the jet, Pasquill-Turner, and turbulence methods with the observed data. Here, peak concentration is plotted vs. distance. All three models incorporate plume rise and the response correction factor. The Pasquill-Turner method provided a slightly better fit to the surface level concentrations observed for the 31 B707 events, but all three variants performed well. On the average, the predicted concentrations best matched those observed at the closest sensor to the runway. This is probably due to the fact that Yamartino's plume rise formula was developed from data obtained at this distance and assumed that its rise ceased there.

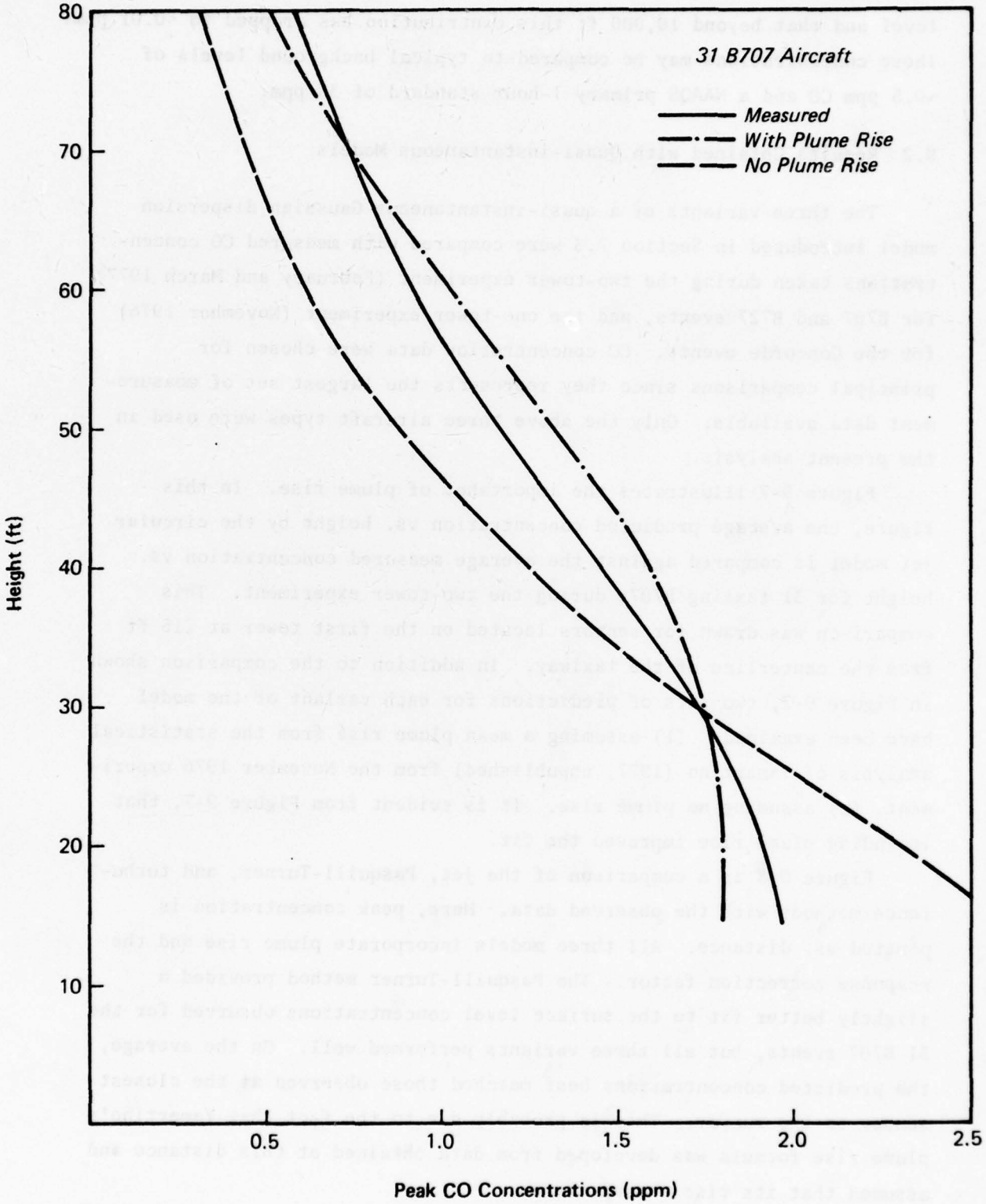

Figure 9-7 Effect of Plume Rise on Model Comparison with Observations

707036

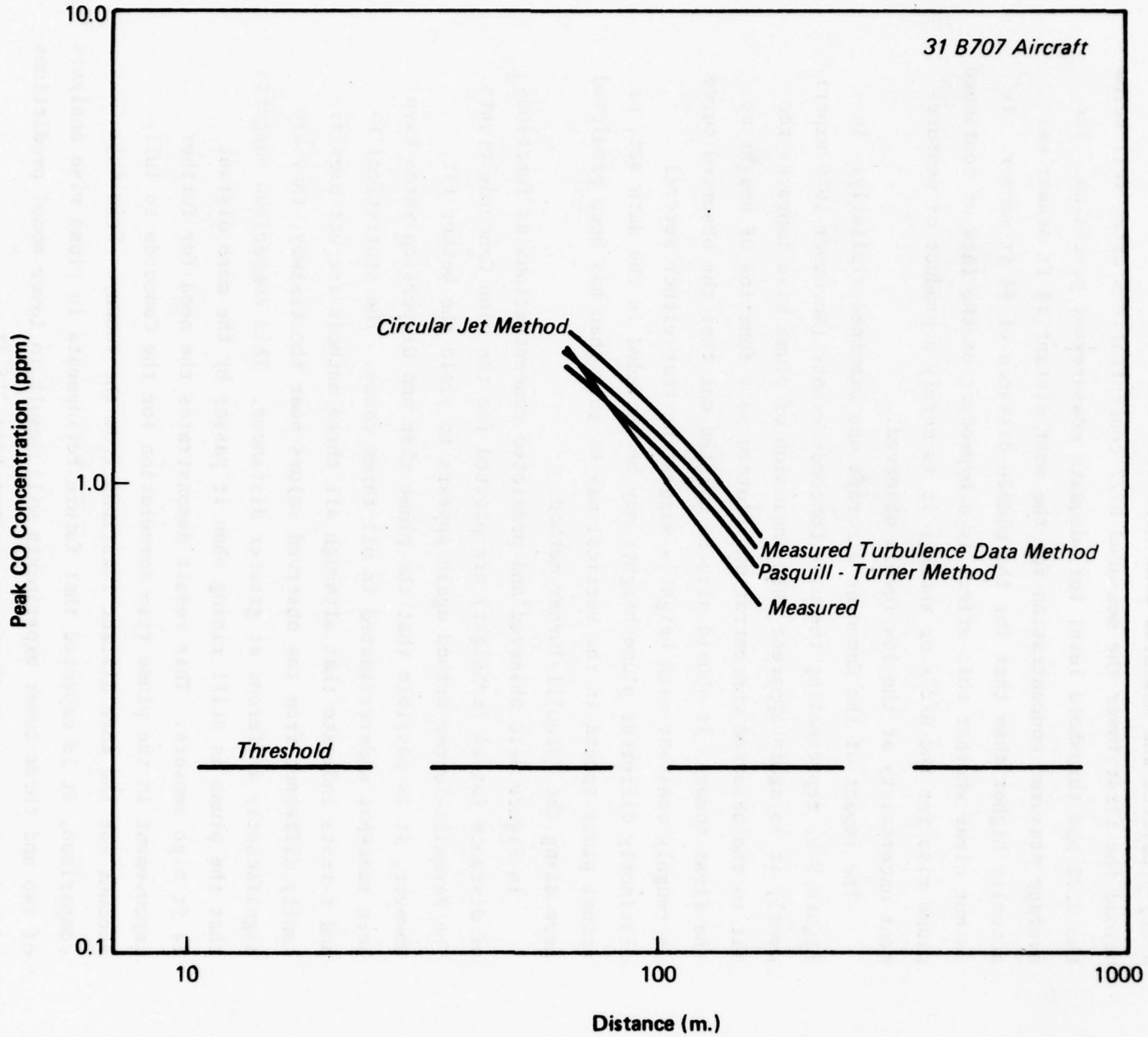

Figure 9-8 Effect of Initial Plume Size and Rate of Dispersion on Comparison of Model with Observations

The analysis of 34 B727 events has demonstrated similar results. Because the emission rates from a B727 are much lower than from the B707, predicted and measured concentrations are both lower. In fact, beyond the first tower the measured B727 concentrations often fell below the 0.25 ppm threshold level for adequate measurement precision. The average measured concentration for the most distant 14 ft sensor was actually higher than that for the middle distance of 14 ft sensor. It is not clear whether this effect is a byproduct of the lack of continued plume rise for the B727s or whether it is merely a product of measurement uncertainty at the low levels observed.

The impact of the Concorde aircraft was examined similarly. In Figure 9-9, representing the nine Concorde events (November 1976 experiment), it is again apparent that inclusion of plume rise improves the fit to the observed concentrations plotted as a function of height at the first tower. It should also be pointed out that the observed curve is roughly constant with height - suggesting that either several distinctly different plume heights may be included in the data set, or actual plume spread in the vertical may be more than has been predicted here using the Pasquill-Turner method.

In Figure 9-10 observed and predicted concentrations as functions of distance (at 14 ft height) are plotted for the nine Concorde events. The Pasquill-Turner method again appears to yield the better fit. However, it is possible that the plume rise and dispersion rates have been somewhat underestimated in all three cases. The statistical F- and t-tests indicate that although all three methods are not significantly different from the observed values near the taxiway, they are significantly different at greater distances. This comparison suggests that the plume is still rising when it passes by the more distant 14 ft high sensors. This result demonstrates the need for further improvement in the plume rise formulation for the Concorde to fully account for the more distant locations from the runway. From this comparison, it is expected that future refinements in plume rise analysis of two and three tower experiments will result in lower model predictions of concentrations at distances greater than 215 ft.

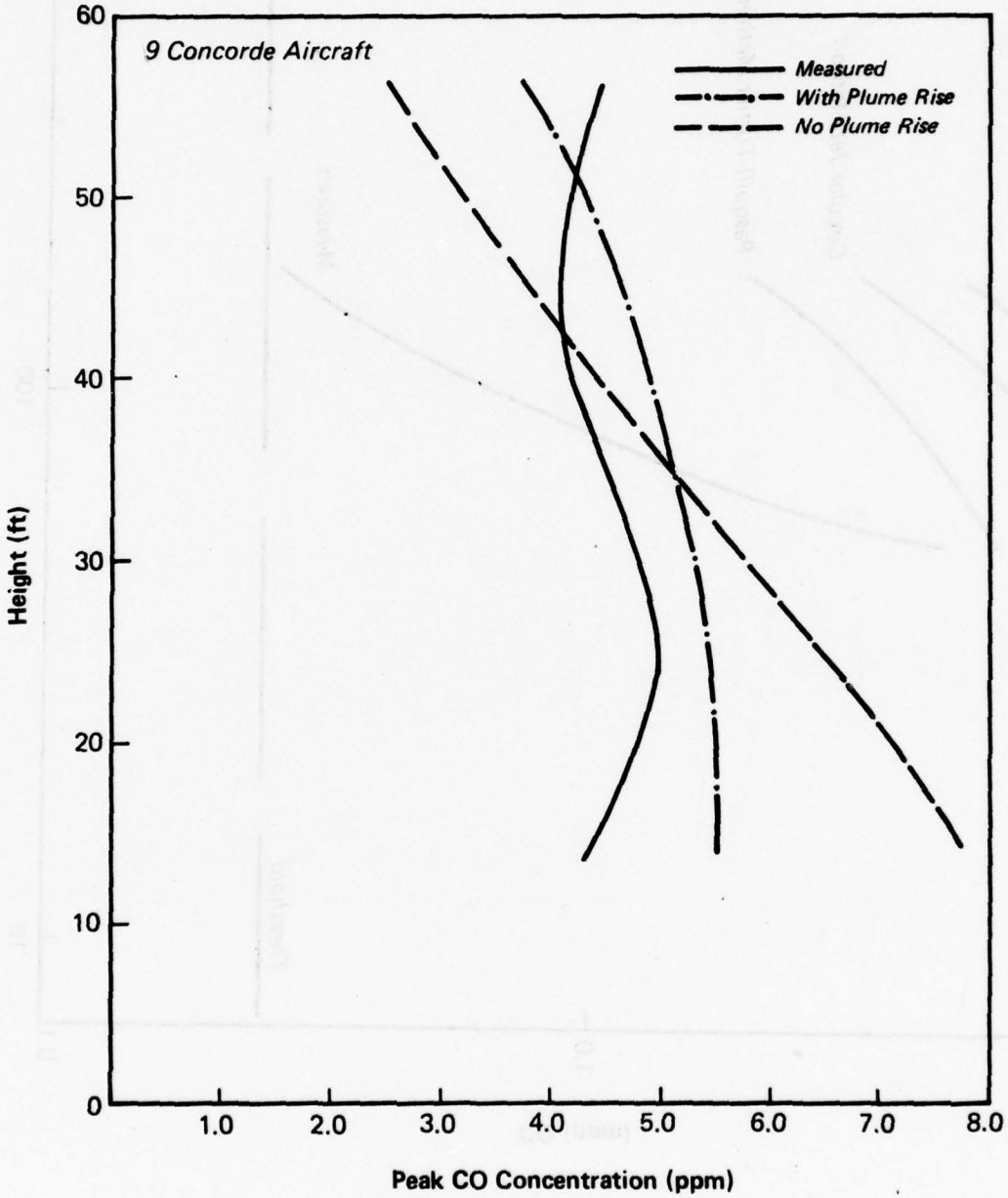

Figure 9-9 Effect of Plume Rise on Model Comparison with Observations for Concorde Aircraft

707028

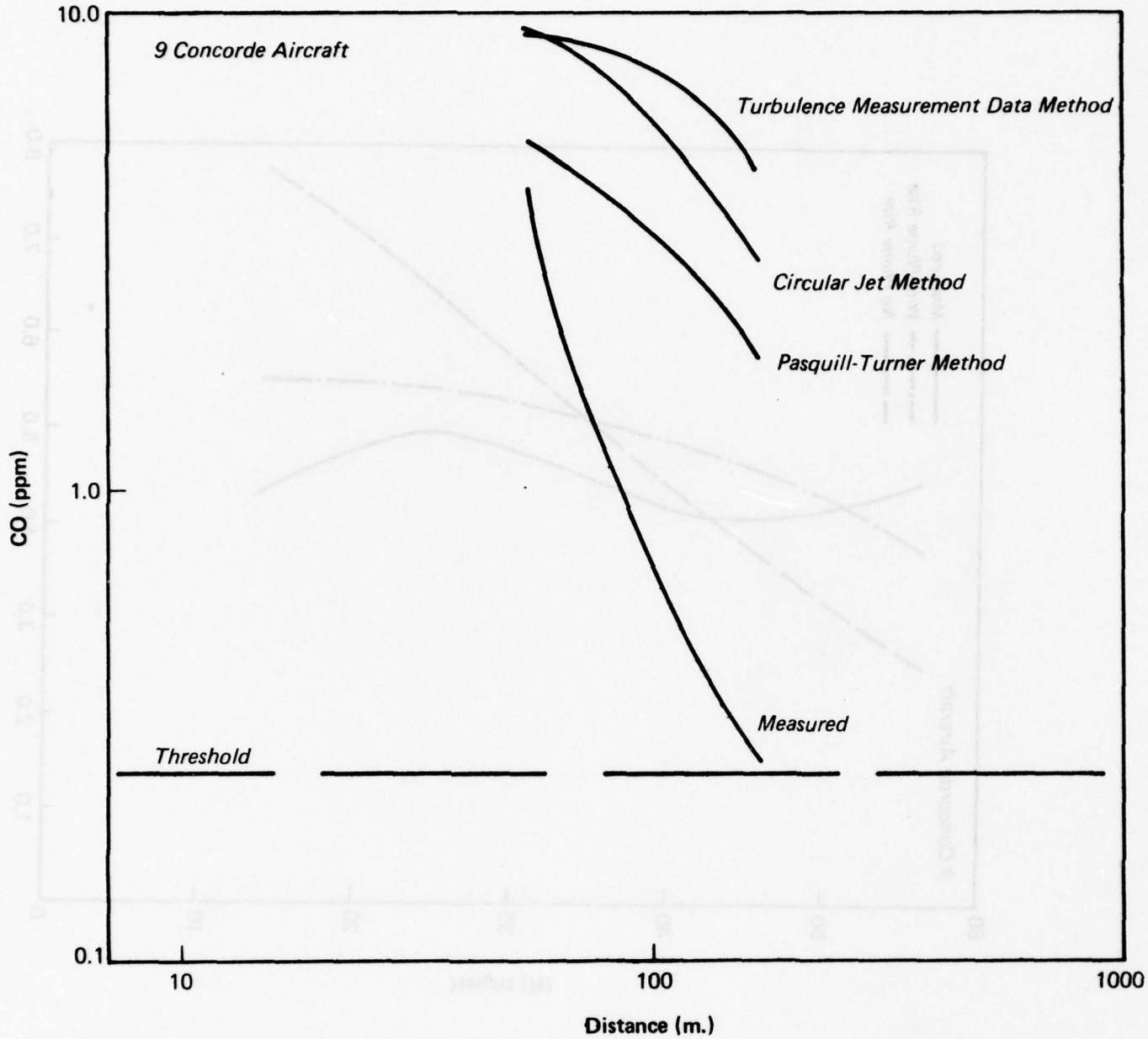

Figure 9-10 Comparison of Model Variants with Observations for Concorde Aircraft

The Pasquill-Turner variant of the quasi-instantaneous model was also a slightly more successful prediction tool than the circular jet model for the Concorde and B727 airplanes. However, the prediction quality of either method is nearly the same for B707 aircraft. It appears that this discrepancy can be traced to the difference in the choice of the initial source volume for each method.

The multi-parameter fit for the two-tower data also indicates that the Concorde exhaust plume is more buoyant and, therefore, continues to rise higher than the plumes from other aircraft as it passes the second tower. To date, the only information available to indicate plume rise for Concordes as a function of distance is a single case (event #63) from the two-tower tests. Analysis for mean plume height for this event yields 60 ft at the first tower, and 130 ft for the second tower and beyond. Comparative analysis has shown that although use of H = 60 ft yields great improvement in the prediction at the second tower and beyond, the 14 ft level concentrations predicted at the first tower are then much smaller than those measured.

An important preliminary result of the analyses in this section involves the determination of the distances for three aircraft types where diffusion has resulted in the lowering of CO concentrations to below a certain threshold value. This calculation is of particular concern at airports where it is necessary to know if people in or around the airport terminal are likely to be exposed to a harmful level of pollutant concentrations. Using the predicted and observed CO concentration curves (Figures 6-6 through 6-8) as a function of distance, previously presented in the curves were extrapolated to the point where the instantaneous peak CO concentration falls to 0.25 ppm. Table 9-1 is a compilation of the distance at which the 0.25 ppm concentration is reached at the 14 ft height level for the measured and predicted curves for all three aircraft types mentioned above. This table shows that all of the models overpredict the distance indicated by measurement data. These distances greatly exceed those determined in Section 9.3 for the point at which the hourly average contribution predicted by ALSM (for a single Concorde) equals 0.25 ppm. Site-specific calibration factors for each model could be derived from these comparisons with measurements.

TABLE 9-1

DISTANCE FROM THE TAXIWAY WHERE THE CO CONCENTRATION FALLS TO 0.25 ppm FOR THREE AIRCRAFT TYPES

Prediction Method or Measurement	Aircraft Type		
	B707	B727	Concorde
Measured	300m	82m	180m
Circular jet method	340m	140m	475m
Pasquill-Turner method	360m	180m	475m
Turbulence measurement data method	410m	210m	680m

9.3 Results of ALSM Quasi-Continuous Model Application

Two principal factors were involved in the modification of the continuous line source model ALSM (and AVAP). The first was the specification of the atmospheric dispersion rates appropriate for modeling a short period release, instead of a continuous release over a time period as long as an hour as conventionally assumed. The AVAP/ALSM model used in the original EIS analysis assumed dispersion rates appropriate for an hourly average concentration calculation. That analysis also assumed that emissions for an average number of aircraft per hour were distributed uniformly over the entire hour. The present quasi-continuous versions of the ALSM model uses dispersion parameters appropriate for a three-minute averaging time* for predicting near field concentrations.

The second factor that differs is the interpretation placed upon the resulting concentration profiles. For a quasi-continuous model approximate to a short duration release, the dosage rather than the concentration is the quantity conserved by the calculation. That is, to evaluate the dose of pollutant material reaching a sensor, the predicted concentration is multiplied by the minimum of the source release time or the duration (in seconds) of the concentration pulse, i.e., the full width time at half of the maximum concentration. Measured dose is evaluated in these comparisons by multiplying the peak concentration value by the pulse duration.

Figure 9-11 illustrates the resulting area of influence for CO predicted by ALSM for a single Concorde aircraft modified to incorporate mean observed (Table 7-2) plume rise and three minute dispersion parameters. The areas have been derived from composite dose calculations representing this sequence of operations leading to a takeoff into a south wind. A five minute engine start and idle period has been assumed. This is followed by three minutes of taxiing and an immediate takeoff. It is apparent that the location of idling operations is most important in determining potential effects of CO upon the public at the terminal. For CO, the buildup of concentrations at the north end of the north-south taxiway and runway, during a 5 mph south wind neutral stability period, is exceeded by that due to a start/idle operation. For NO_x,

*See Appendix B.

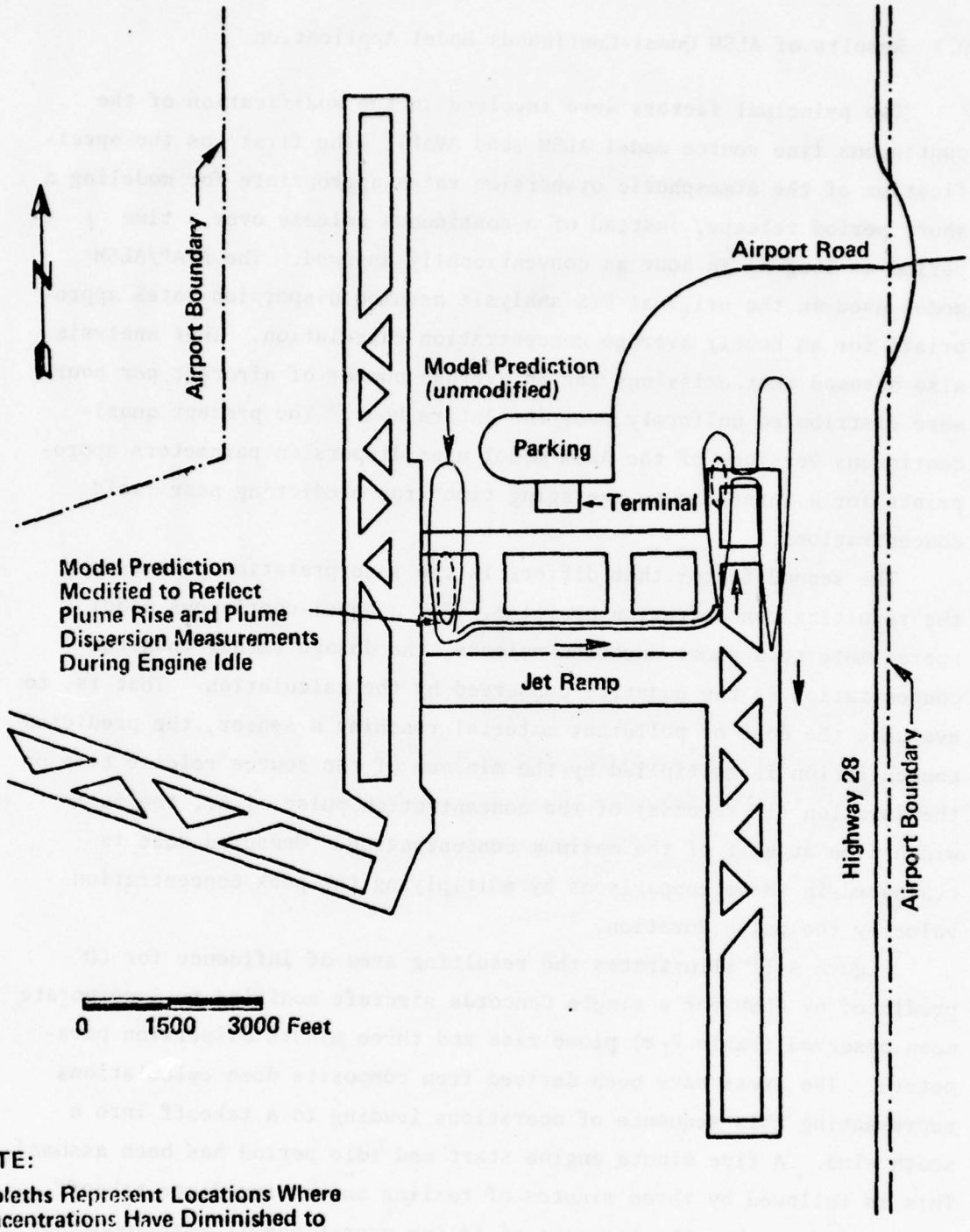

NOTE:

Isopleths Represent Locations Where Concentrations Have Diminished to 0.25 ppm Above Background.

Figure 9-11. Area of Concorde Influence for CO at Dulles for South Wind.

the buildup at the northern end of the takeoff runway is more important, as would be expected with the higher emission rates during takeoff. However, in all cases the areas of influence (defined as the location at which the concentrations predicted just exceed background by a detectable amount) are restricted to areas near the aircraft pathway, well within the airport boundaries. Though detectable concentrations at the terminal may be possible with starting and idling operations of the Concorde, for some wind conditions, the 0.25 ppm hourly average CO concentration predicted is quite insignificant in comparison with a 35 ppm hourly or a 9 ppm 8-hour ambient air quality standard.

10. COMPARISON OF RESULTS WITH FEIS CONCORDE (1975)

The original EIS analysis of the impact of Concorde operation on air quality at Dulles International Airport was made using the AVAP model. The Concorde FEIS contained a number of drawings illustrating the expected influence of operations at Dulles Airport on the air quality in its vicinity. Cases characterized by several different sets of assumptions regarding the operation of Concorde aircraft were evaluated. For 1978, subsonic emission factors were the same as those listed by EPA, and Concorde emission levels were the present day level. Constant passenger flow was assumed for comparison with and without Concorde for a given period. For 1978, one B747 or DC10 replaced two Concordes. Only aircraft operations were considered for analysis; indirect sources, such as access vehicles, were not.

In each instance the projected impacts of the maximum hourly airport activities for each pollutant species governed by ambient air quality standards were evaluated. Plots were prepared for each averaging period appropriate for comparison with each particular ambient air quality standard. Worst-case meteorological conditions were originally selected for the EIS analysis: summertime (high air traffic), low ventilation (approximately 2 knots wind speed) and stable conditions (stability 5). For each case evaluated the worst-case meteorological conditions were assumed to concur and persist with the period of maximum activity to yield conservatively high concentration estimates. Due to the north-south orientation of the two major runways used for most Concorde take-offs and landings at Dulles, either a north or a south wind was generally assumed to yield the maximum downwind concentrations. In the comparisons between the updated and refined sample calculations presented below, the south wind case is the one evaluated.

Note that although the refined calculations have the advantage that their methodology has been tested against direct measurements of CO concentrations, the range of meteorological conditions occurring during the measurement program did not include stable atmospheric conditions

and rarely included wind orientation angles that were less than 20° away from the axis of the taxiway or runway. Thus, the model accuracy under these more extreme conditions has been assumed on the basis of the realistic nature of the calculation method and the success of the Pasquill-Turner stability method for cases in which appropriate comparative measurement data were available.

10.1 AVAP Comparisons

The original AVAP code used Pasquill-Gifford and modified Turner time-dependent dispersion coefficients, which depend upon the Pasquill-Turner stability class. The stability category was chosen by relating it to observed wind speed, cloud cover and insolation conditions, with the incoming solar radiation classified in terms of solar elevation angle, cloud cover and cloud ceiling. The values for these coefficients were increased from the original reference (according to a 1/5 power law dependence on averaging time) so that they would reflect a one-hour average.

In the current analysis, a plume rise formulation obtained from actual observations at Dulles was used, in contrast to the 10 ft release height assumed for all aircraft in the EIS analysis, since that height was much lower than indicated by the multi-parameter fit results in Section 9.2. Due to the uncertainty about local wake building effects noted earlier, the AVAP code was not modified to use actual measurements of wind fluctuation data to determine dispersion coefficients. However, the vertical plume spread was augmented by the plume rise turbulence:

$$\sigma_z = \sqrt{\sigma_z^2 + \left(\frac{\Delta H}{10}\right)^2} \qquad (10\text{-}1)$$

as recommended by Pasquill (1976). The critical parameters in the Gaussian plume model are the source strength, the effective source height, and dispersion parameters, which are functions of the atmospheric stability at the airport. The modification of plume height and

source strength alone represented a small improvement in modeling air pollution from aircraft operation. Use of dispersion rates appropriate for typical meteorological conditions during Concorde operations had more substantial effect. The accuracy of concentration estimates would be most notably improved in the immediate source vicinity, on the airport property.

The approach of the FEIS was conservative in that "worst-case" meteorological conditions were selected that would result in the largest impact of the Concorde. As reported above, these worst-case conditions are given by low wind speeds and mixing heights, a stable atmosphere and high temperatures. The actual hourly mean temperature during the February-April 1977 monitoring period at Dulles varied from 45°F to 63°F; hourly mean wind speed varied from 9 to 21 miles per hour and hourly mean σ_θ ranging from 8 to 18°. The hours of sampling during this monitoring period were 9 A.M. to 5 P.M. Typical hourly meteorological conditions for the day representative of this monitoring period were used for predicting pollutant concentrations by means of the modified AVAP code. These typical meteorological conditions consist of moderate winds of 8 to 10 miles per hour, a temperature ranging from 40°F at 5 A.M. to 61°F at 2 P.M., and wind direction fluctuation of 5 to 15°.

Other assumptions used in this modified study were identical to those used in the FEIS. Each isopleth represents a one-hour average concentration (9 to 10 A.M.) for a southerly wind, the condition most likely to affect the terminal and the nearby community. Results of this modification were compared with the predictions presented in the FEIS for CO, THC and NO_x in Figures 10-1 through 10-3.

Figures 10-4 through 10-6 present the hourly longitudinal cross sections of concentration isopleths to the north of the 1R/19L taxiway and runway (which runs north to south) for a two-Concorde per hour operation schedule. These isopleths show the comparison between the FEIS AVAP predictions and those of the modified AVAP code, using meteorological conditions typical of late winter and early spring for the area.

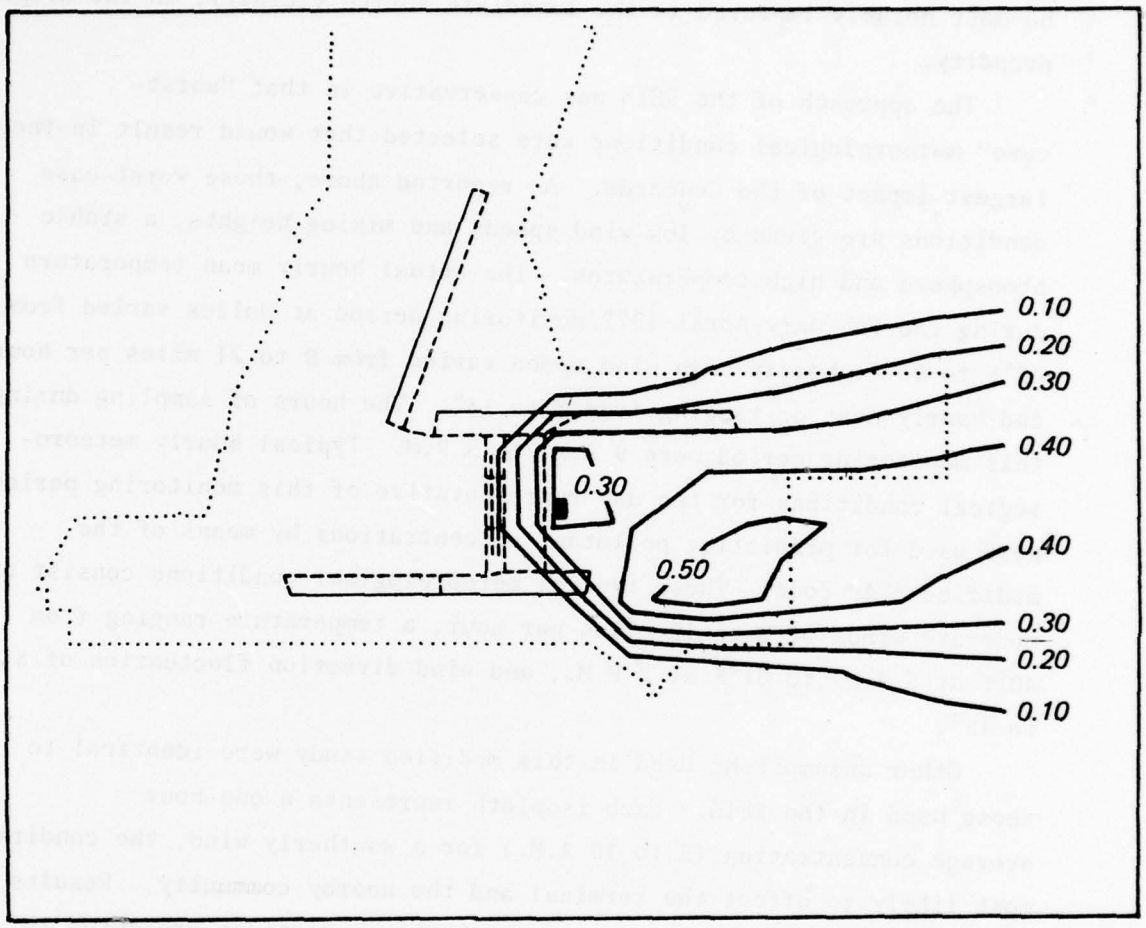

Figure 10-1a Dulles 1978 with Concorde Original AVAP Prediction (EIS) Carbon Monoxide (CO) (ppm) 1-Hour Average (9 AM to 10 AM) Wind from South

712057

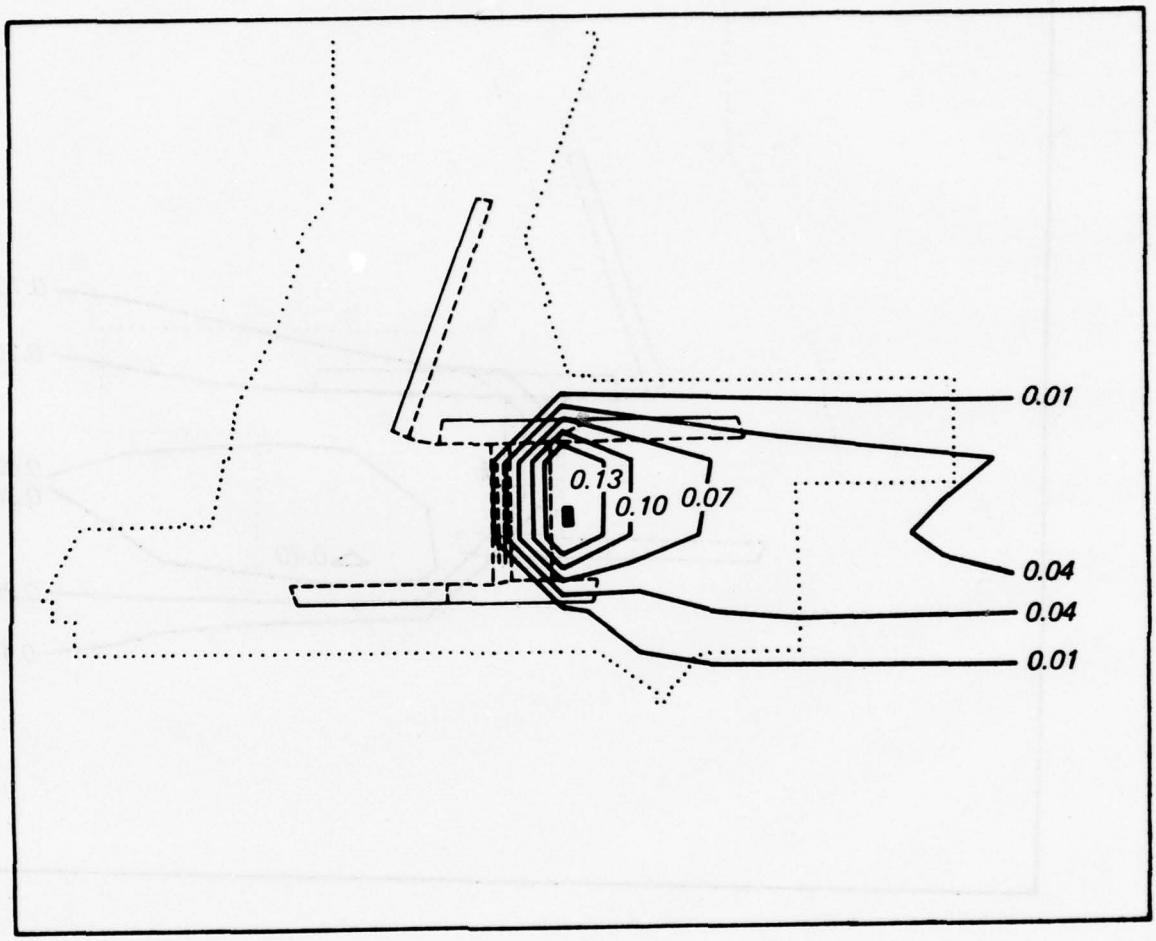

Figure 10-1b Dulles 1978 with Concorde Modified AVAP Prediction (EIS) Carbon Monoxide (CO) (ppm) 1-Hour Average (9 AM to 10 AM) Wind from South

712058

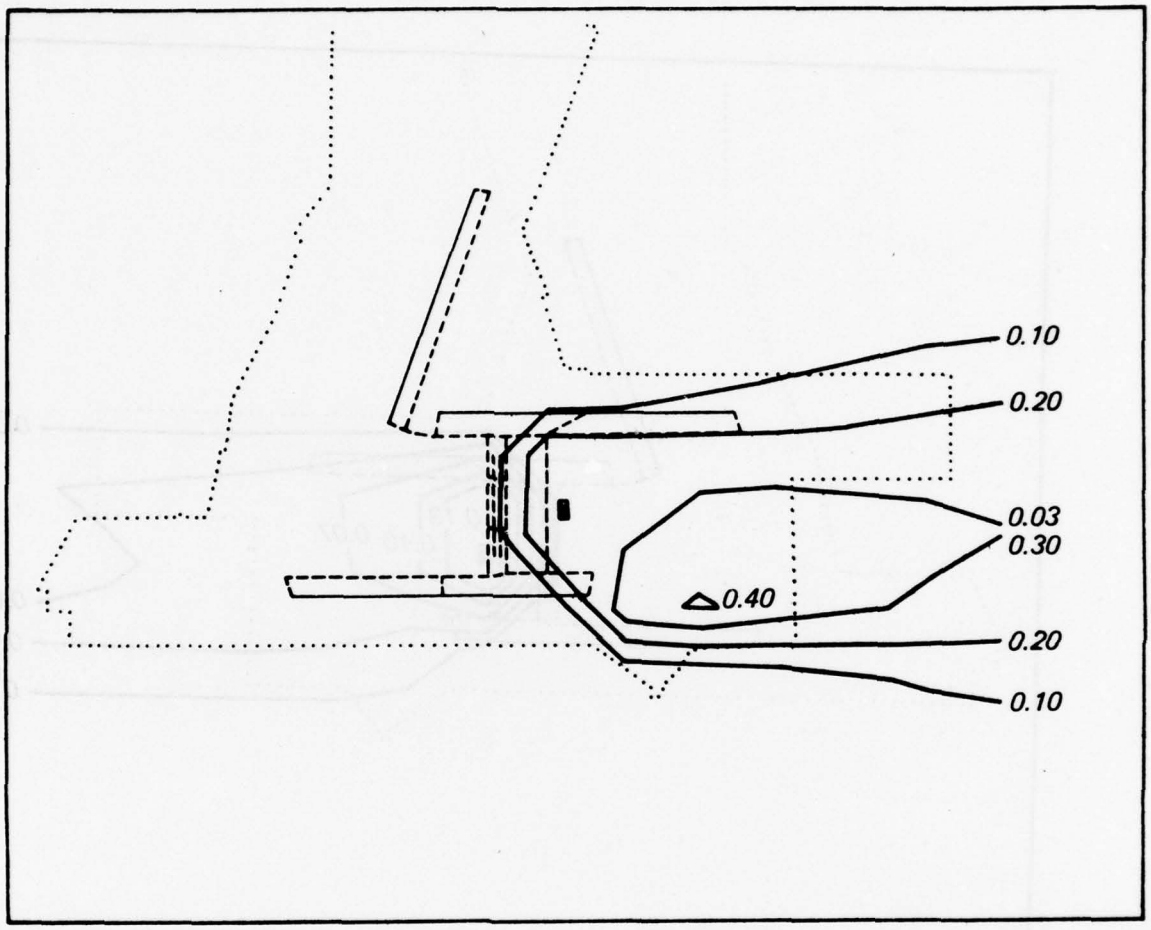

Figure 10-2a Dulles 1978 with Concorde Original AVAP Prediction (EIS) Hydrocarbon (THC) (ppm) 1-Hour Average (9 AM to 10 AM) Wind from South

712059

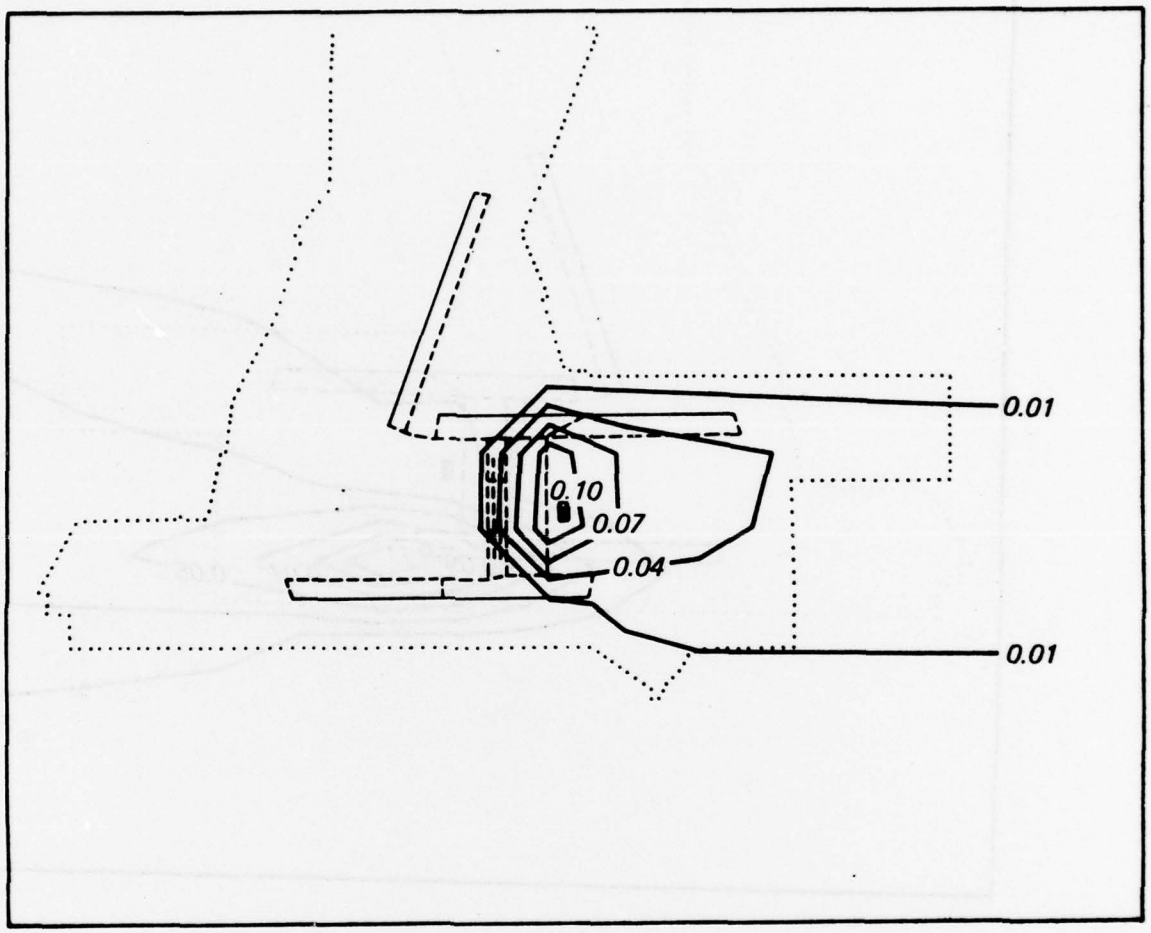

Figure 10-2b Dulles 1978 with Concorde Modified AVAP Prediction (EIS) Hydrocarbon (THC) (ppm) 1-Hour Average (9 AM to 10PM) Wind from South

712060

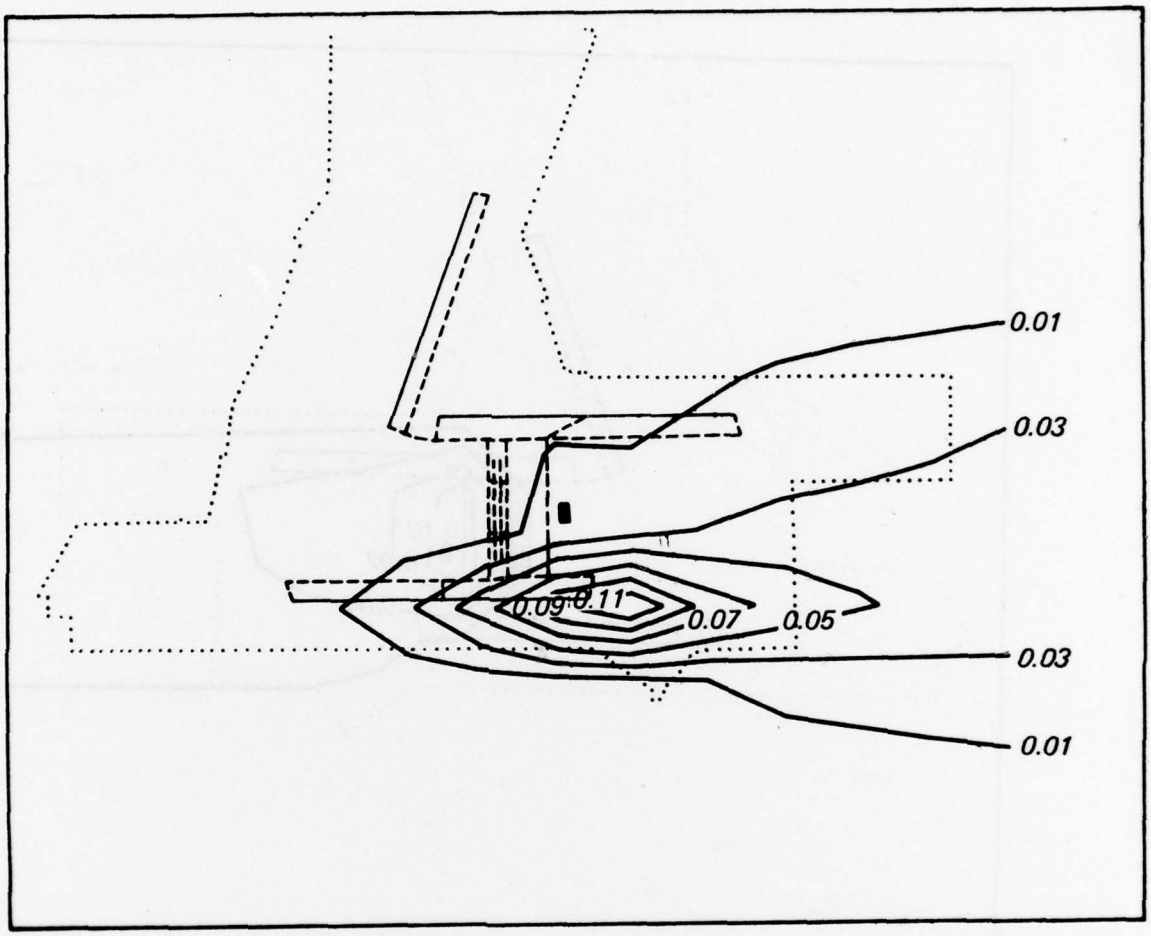

Figure 10-3a Dulles 1978 with Concorde Original AVAP Prediction (EIS) Nitrogen Oxides (NO_x) (ppm) 1-Hour Average (9 AM to 10 AM) Wind from South

712061

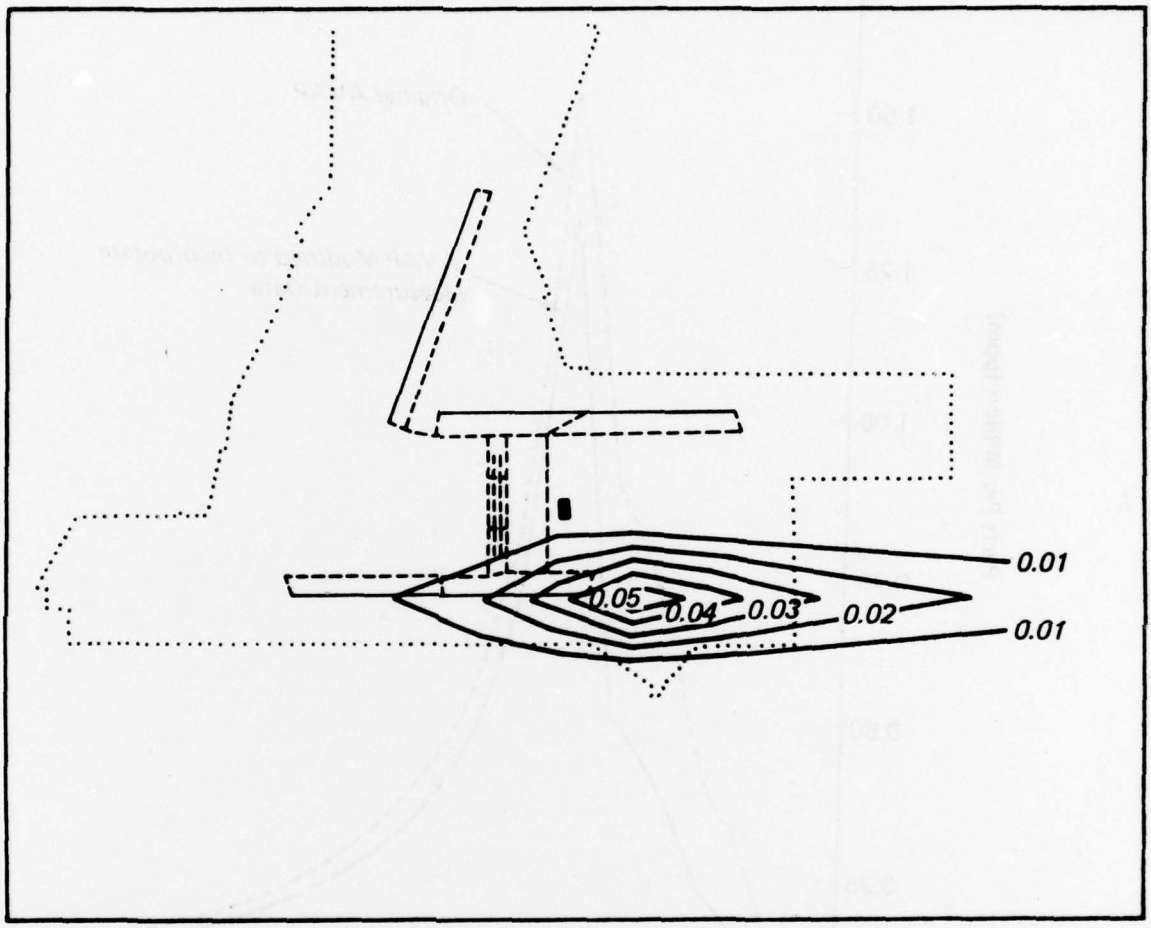

Figure 10-3b Dulles 1978 with Concorde Modified AVAP Prediction (EIS) Nitrogen Oxides (NO_x) (ppm) 1-Hour Average (9 AM to 10 AM) Wind from South

712062

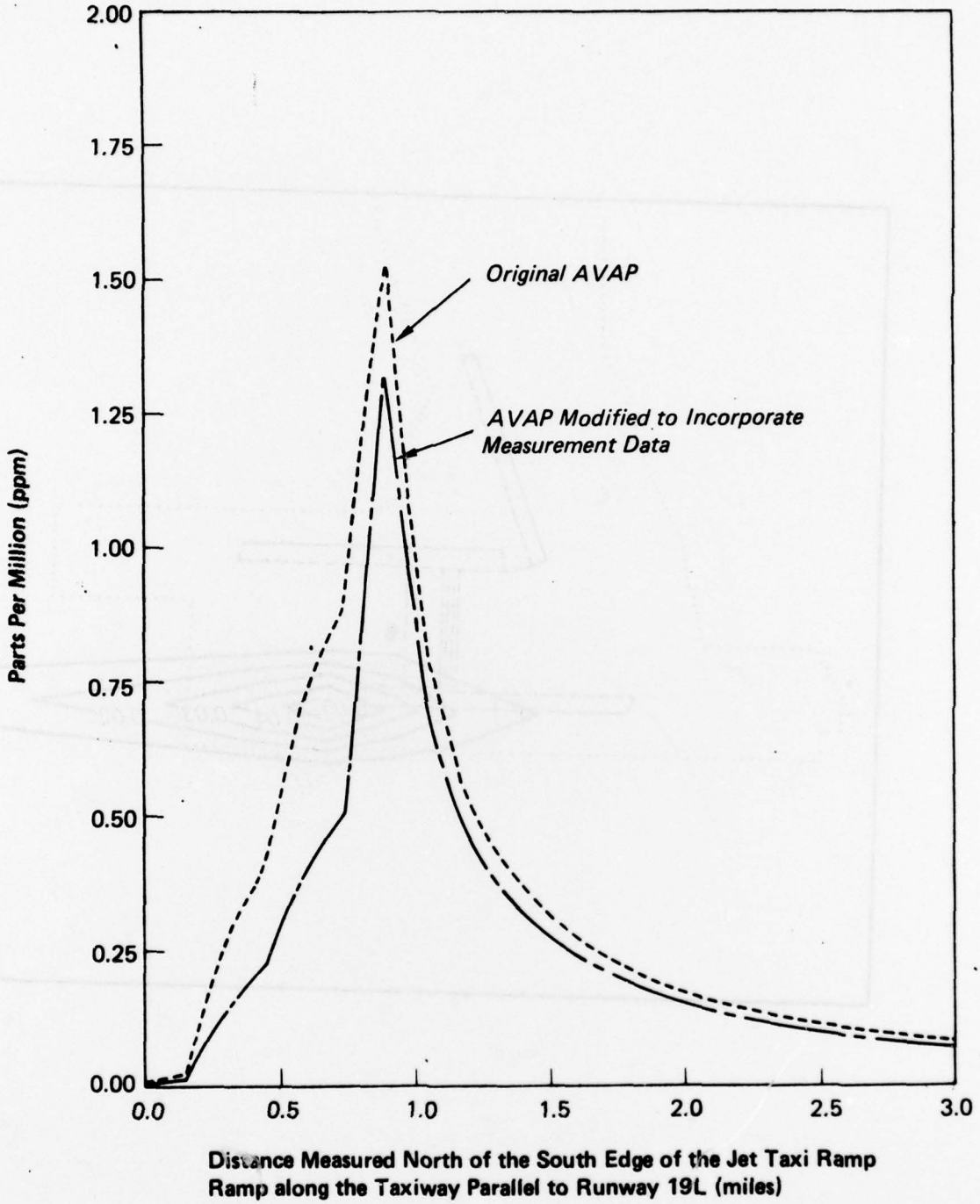

Figure 10-4 Hourly CO Concentrations Vs. Distance (10 AM to 11 AM) with Concorde

712065

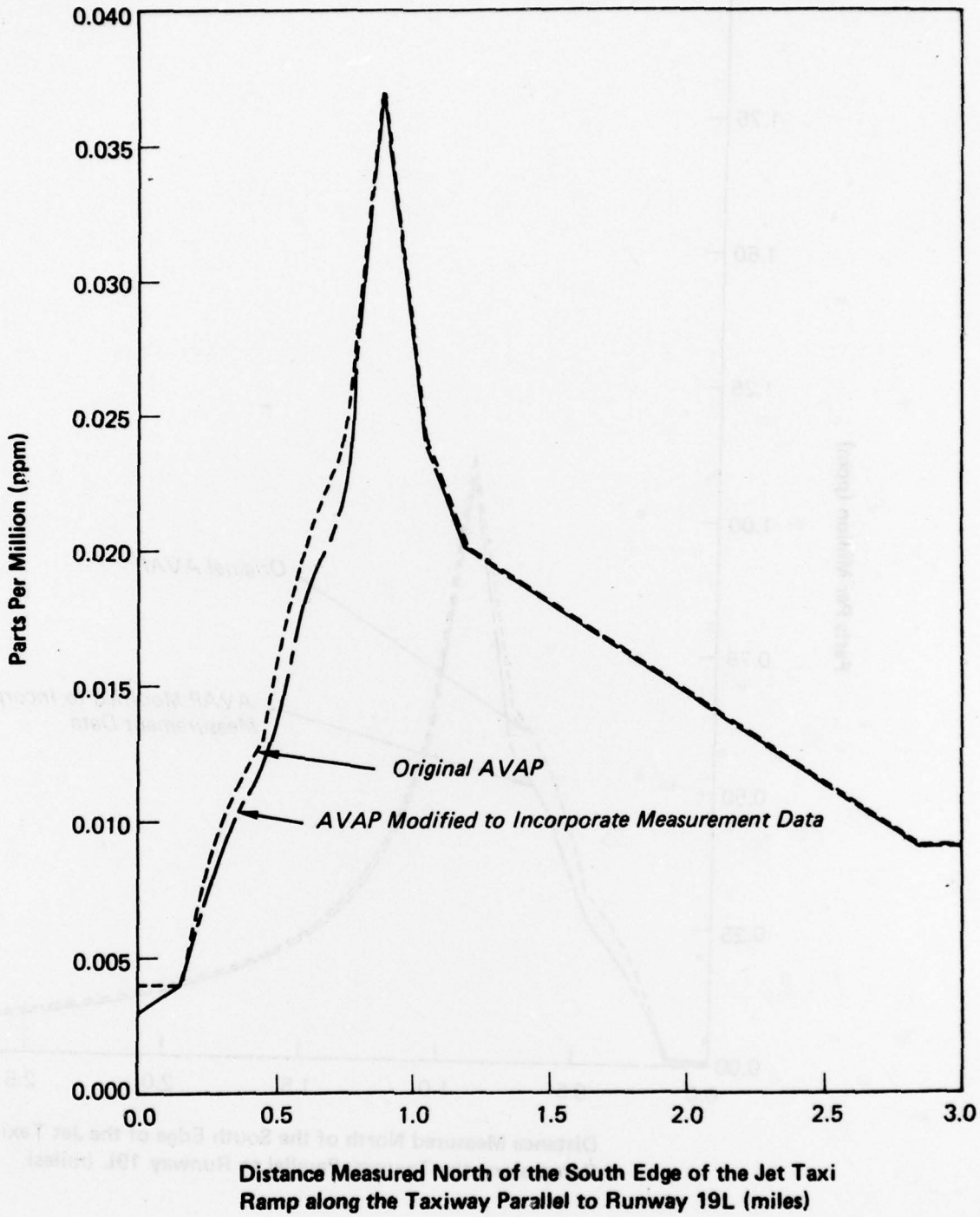

Figure 10-5 Hourly Nitrogen Oxide Concentration vs. Distance (10 AM to 11 AM) with Concorde

712063

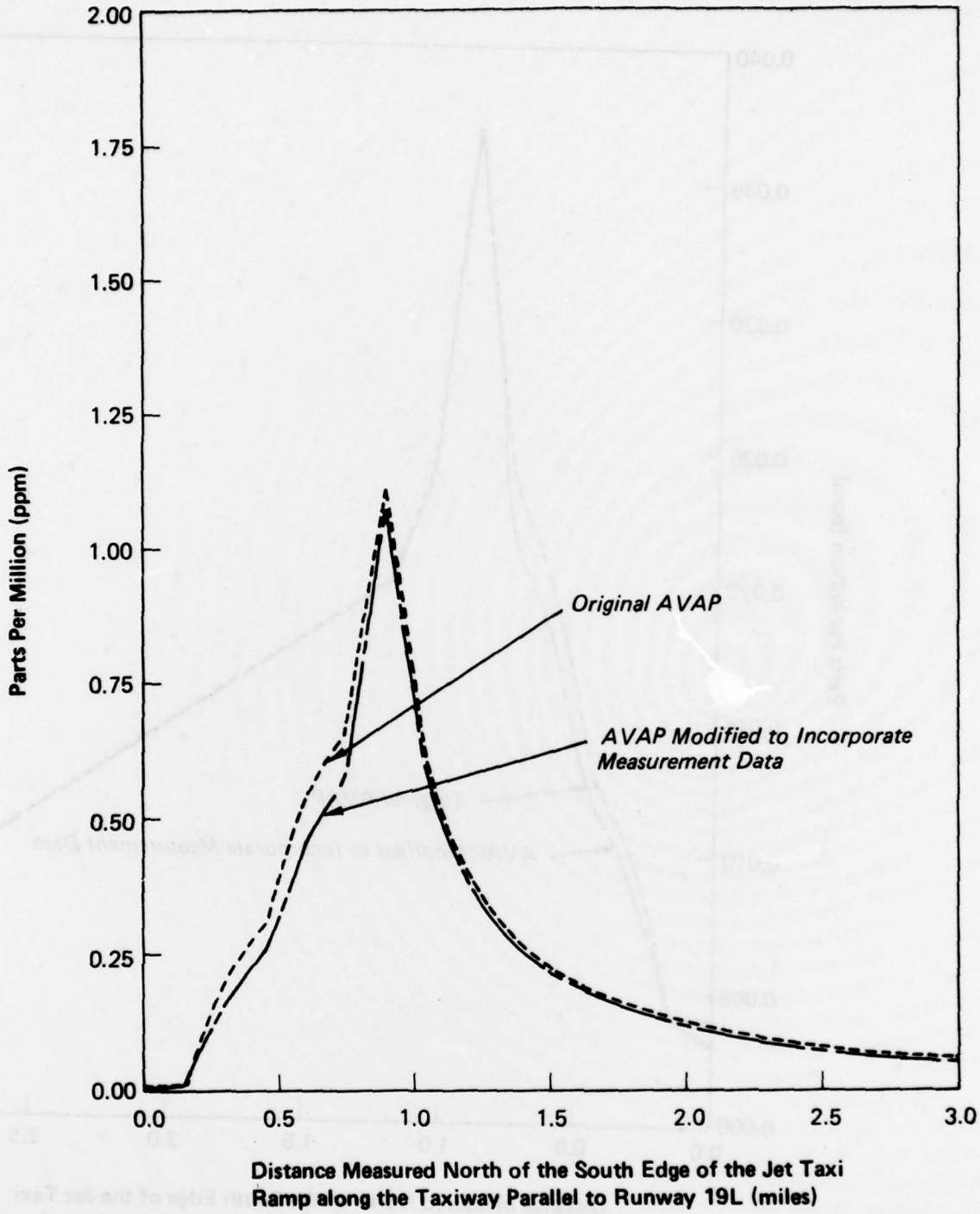

Figure 10-6 Total Hydrocarbon Concentration Vs. Distance (10 AM to 11 AM) with Concorde

712064

A noticeable decrease in concentrations, particularly in the near-field, resulted in comparison with the original predictions in the FEIS. This is because more unstable and dispersive atmospheric conditions were observed and used for simulation and a larger plume rise was assumed for the buoyant exhaust plumes.

Figures 10-4 to 10-6 thus represent a simple way of displaying this isopleth information under the most severe pollution conditions (wind blowing up the runway from the south). These figures show that model calculations utilizing the modifications of the Concorde measurement program lead to lower concentration than the calculations based upon the original unmodified AVAP model. The measurement program has thus shown that the impact of Concorde emissions on ambient air quality is even less than was concluded in the FEIS.

10.2 Single Event Area of Influence

Using the ALSM predictions of dose as a basis, the air quality area of influence for CO has been derived, as previously presented, in Figures 9-11. As indicated in the legend, the area is defined by a concentration threshold that is marginally detectable above an hourly background for that pollutant. This area is smaller than those predicted for the EIS using AVAP. Some of the differences noted can be ascribed to the differences in assumptions about plume rise and atmospheric stability, and the isolation of the influence area due to a single event by the ALSM method.

It is expected that realistic estimates of the impact of specific mixes of individual aircraft operations can be derived from judicious use of the ALSM model and the area of influence plots given here. The more complex calculations of AVAP are also useful for assessing overall impacts at larger distances, such as beyond the airport boundaries; but the simplicity and superior resolution of the ALSM model gives it several significant advantages in the analysis of potential pollution problems on the airport property and in its immediate vicinity.

10.3 Aircraft Emission and Wake Characteristics

The emission geometries and rates given in Section 5.5 have been used in the present analyses, but the effective initial concentration and geometry of the exhaust plume from an aircraft a few seconds after it leaves the jet engines are factors that are, as yet, not at all well known. The difficulties inherent in measuring a jet's exhaust and its fuel use rates precisely to derive an emission index (EI) are only part of the problem. The continuous updating of engine designs with new series having slightly different combustion characteristics results in the assumption of a single EI value that is probably somewhat obsolete by the time it is published. Also, each pilot's method of operating each aircraft can markedly affect the emission rate in any of the LTO cycle modes. Consequently, the use of models calibrated against averages of measured concentrations are expected to be a superior basis for assessment of the area of influence for each aircraft type.

The comparisons of the raw measurement data for average concentrations and doses for all three CO experiment series, the comparison of CO dose versus emission indexes (given in Section 6), as well as the results of the multiparameter fitting method, showed that the factor of 3 difference in published CO emissions between Concordes and B707s is not a reliable indication of the ambient concentration impact of the two planes. In fact, the impacts observed were about equal for both aircraft types and the multiparameter fit projected at most a factor of 1.5 difference.

The interactions between jet turbulence, aircraft wake turbulence and ambient atmospheric turbulence are also not very well understood at present. However, the relative success of the quasi-instantaneous model that relied on a rate of plume growth proportional to a measure of ambient turbulence, rather than jet wake turbulence alone, suggests that after a relatively short distance of plume travel (approximately 600 ft) ambient turbulence levels are the most significant. Future analyses of the monitoring data obtained for the Concorde and other aircraft at Dulles will continue to examine these factors. However, It may be noted

that the comparisons of measurements with predictions in Section 9 were relatively successful for the geometries examined in spite of the current lack of detailed information about the interactions of turbulent wake flows.

11. CONCLUSIONS

Extensive measurements of Concorde (and other aircraft) emissions and background air quality have been made at Dulles International Airport and in the nearby community. Measurements made at the airport included data on jet plume rise, atmospheric dispersion parameters, and vertical and horizontal "profiles" of exhaust plume pollutant concentrations for individual aircraft in actual service. Data were obtained to identify the contribution of specific aircraft types to hourly-average pollution levels measured on the airport property. In the community, hourly-average values of ambient air pollution data were obtained for statistical analysis of the possible influence of aircraft emissions on nearby Sterling Park.

Analysis of this extensive air quality measurement data base has led to a number of conclusions regarding the influence of Concorde operations, and other aircraft emissions on air quality at the airport and in the neighborhood. The overall result of the detailed investigation of statistical trends in regional measurements is that airport activities, in total, had no observable effect upon pollutant levels at any of the regional monitoring stations, including the nearest community, Sterling Park. This conclusion was consistently reached in spite of attempts (in the statistical analysis) to isolate specific hours during the monitoring period in which such influence would be most likely, such as when the prevailing wind was from the airport toward the monitoring site during an atmospheric inversion.

This lack of airport influence on Sterling Park or other regional monitoring stations was confirmed by the measurements made on the airport property near taxiways and runways. Measurements in the near-field established that concentrations of all pollutants emitted by the Concorde, as well as by other individual aircraft, rapidly disperse to concentration levels that are small compared with ambient backgrounds.

The detailed measurements of jet plume dispersion characteristics (single event) and a number of meteorological variables were used as dispersion model input parameters. A number of important results were obtained from this analysis.

1) Pollutant concentrations measured at the ground level within 500 ft of a taxiway or runway were significantly reduced by the observed jet exhaust plume rise.

2) Plume rise estimates for Concordes were consistently higher than those for most other aircraft.

3) Initial wake dispersion and buoyant rise of an aircraft's exhaust plume significantly reduces concentrations at all downwind distances, but most importantly in the near-field.

4) Comparison of modeled initial source volumes with concentration measurements indicated that the engine placement is an important factor, but not the only factor determining that volume.

5) Concentrations of CO observed at distances of 500 to 600 ft from taxiing Concordes were only one to one and a half times those associated with B707s, while published CO emission rates for the Concorde (such as those used in the FEIS) are a factor of 3 higher.

6) Comparisons of measured doses (time-integrated concentrations) versus published emission rates indicate that Concordes are not proportionally higher in their impact upon the air quality, even at downwind distances as close as 200 ft.

Given these results, it is possible to conclude that engine emission rate measurements alone may not reflect the true environmental impact of aircraft emissions. Factors contributing to the difference between published engine emission rates and measured air quality concentration include engine-airplane geometry, engine exhaust temperature and wake dynamics. The most direct measure of aircraft emissions impact is the change in nearby ambient air quality. Thus, ambient air measurements such as those obtained in the Dulles Airport program can provide important information, supplemental to engine emission measurements made in test stand experiments.

Comparisons between air quality predictions using several models and field measurements were made. The refined and validated forms of these models were then used to assess the areas of Concorde influence on air quality. The results were examined in terms of the conclusions reached in the original FEIS. The original analyses carried out for the FEIS with the AVAP model were reproduced, and then compared with results obtained with a version of AVAP which was modified to reflect measured meteorological conditions at Dulles during the current program. The conclusions derived from these comparisons indicate:

1) The use of more representative meteorological conditions and measurements of exhaust plume rise as input to AVAP result in lower predicted concentrations.

2) Utilizing modeling assumptions consistent with those employed in the FEIS, but using the data from the Dulles measurement program, result in lower concentrations of CO, NO_x and THC for the total mix of aircraft.

3) The small area of influence predicted for a single Concorde aircraft is further reduced when the model (ALSM) is modified to reflect the rates of dispersion and plume rise measured in this program.

The monitoring and analysis program at Dulles Airport not only permitted the specific evaluation of the impact of Concorde operations at Dulles, but has also provided new insights in the modeling and analysis requirements for the evaluation of air quality impacts of aircraft engine emissions and airport operations at other airports.

12. REFERENCES

Bierly, E. W and E. W. Hewsen 1962. Some Restrictive Meteorological Conditions to be Considered in the Design of Stacks. J. Applied Meteorology 1: 383-390.

Cramer, H. E., G. M. DeSanto, R. K. Dumbauld, P. Morgenstern and R. W. Swanson 1964. Meteorological Prediction Techniques and Data System. Report GCA 64-3-6, Geophysical Corporation of America, Bedford, MA.

Gifford, F. A. 1966. Atmospheric Dispersion Calculations Using the Generalized Gaussian Plume Model. Nuclear Safety, Vol. 2, No. 2, December 1960.

Gifford, F. A. 1968. An Outline of Theories of Diffusion in the Lower Layers of the Atmosphere. Meteorology and Atomic Energy D. H. Slade editor.

Haber, J. M. 1975. A Survey of Computer Models for Predicting Air Pollution from Airports.

Hay, J. S. and F. Pasquill 1959. Diffusion from a Continuous Source in Relation to the Spectrum and Scale of Turbulence. Atmospheric Diffusion and Air Pollution, ed. F. N. Frenkiel and P. A. Sheppard, Advances in Geophysics 6:345, Academic Press.

Pasquill, F. 1974. Atmospheric Diffusion. New York: John Wiley and Sons.

Pasquill, F. 1976. Atmospheric Dispersion Parameters in Gaussian Plume Modeling, Part II. EPA-600/4-76-030b.

Rote, Wang, Wangen, Hecht, Civille, Prataps 1973. Airport Vicinity Air Pollution Study. Department of Transportation. Federal Aviation Administration Systems Research and Development Service.

Rote, D. M. and L. E. Wangen 1975. A Generalized Air Quality Assessment Model for Air Force Operations, Air Force Weapons Lab. Report AFWL-TR-74-304.

Segal, H. 1973. Airport Pollution through the year 2000. Annual Meeting APCA Air Pollution Control Assoc., Pacific N.W. Section, November 1973, Seattle, Washington.

Slade, D. H. (ed.) 1968. Meteorology and Atomic Energy. U.S. Atomic Energy Commission Office of Information Services.

Sutton, O. G. 1932. A Theory of Eddy Diffusion in the Atmosphere. Proc. Royal Society (London), Ser. A 135:143-165.

Taylor, John, W. R. (ed.) 1976. Janes All The World's Aricraft 1976-1977. Watts 1976, ISN 0-531-03260-4.

Turner, D. B. 1964. A Diffusion Model for an Urban Area. J. Applied Meteorology 3:83.

Turner, D. B. 1970. Workbook of Atmospheric Dispersion Estimates. EPA AP-26.

U. S. Environmental Protection Agency, 1975. Compilation of Air Pollutant Emission Factors, AP42.

Wang, I. T. and D. M. Rote 1975. A Finite Line Source Dispersion Model for Mobile Source Air Pollution. Journ. Air Poll. Control Assoc., 25:730.

Wang, I. T. Conley and D. M. Rote 1976. Airport Vicinity Air Pollution Model User Guide, Argonne National Laboratory Contract DOT-FA71W1-223 Report.

ED

78